Development of efficient and chemoselective quasi-heterogeneous catalytic systems for C-C cross-coupling reactions mediated by Pd/Ce based solid-solution catalysts.

By

Philani Perfect Mpungose

January 2018

Development of efficient and chemoselective quasi-heterogeneous catalytic systems for C-C cross-coupling reactions mediated by Pd/Ce based solid-solution catalysts.

By

Philani Perfect Mpungose

Submitted in fulfilment of the academic requirements for the degree of
Doctor of Philosophy
at the
School of Chemistry and Physics,
University of KwaZulu-Natal,
Durban,
South Africa

January 2018

Note: This thesis has been written according to Format 3, as outlined in the guidelines from the Faculty of Science and Agriculture, University of KwaZulu-Natal, which states:

This a thesis in which the chapter are written as a set of discrete research papers, with the overall Introduction and Final Discussion. These papers would not be published yet, but at least one paper would have been submitted for publication. The references are reformed to a uniform standard.

As the candidate's supervisors, we have approved this thesis for submission.

Signed:_____ Name: _____ Date: _____

Signed:_____ Name: _____ Date: _____

Abstract

Construction of carbon-carbon bonds is of pivotal importance in chemistry and their careful assembly can allow complex molecules such as peptides to be created. As a result, the development of carbon-carbon bond forming reactions has turned into an area appreciated by Chemists both in academia and industry. In addition, numerous Nobel prizes in chemistry have been awarded for this area of research. The C-C forming reactions have also facilitated the synthesis of natural products, pharmaceuticals, agrochemicals, conjugated polymers and nanomaterials.

In this study, the intention is to synthesize heterogeneous palladium based catalysts that can efficiently catalyze Heck-Mizoroki, Sonogashira and Suzuki-Miyaura C-C cross-coupling reactions. The heterogenisation of these coupling reactions improves their overall efficiency, since it allows for easy work-up and the reusability of the expensive palladium catalysts. In this direction, we used palladium and ceria based solid-solution oxides, $Pd_xCe_{1-x}O_{2-\delta}$, as heterogeneous nanocrystalline catalysts for the three C-C cross-coupling reactions. The $Pd_xCe_{1-x}O_{2-\delta}$ based solid solution oxides were synthesized in one-step using a urea-assisted solution combustion method. These $Pd_xCe_{1-x}O_{2-\delta}$ solid solution oxides were fully characterized by XRD, ICP-OES, BET, XPS, SEM, EDX, TEM, TGA and Raman spectroscopy. All characterization techniques strongly suggested that Pd^{2+} was successfully incorporated into the lattice structure of ceria.

The effect of reaction conditions on the catalytic properties of the $Pd_xCe_{1-x}O_{2-\delta}$ solid-solution oxide catalysts was studied in detail with the model Heck-Mizoroki, Sonogashira and Suzuki-Miyaura cross-coupling reactions to obtain the optimum reaction conditions for each transformation. Then, a wide range of aryl halides was efficiently coupled to various alkenes or alkynes or boric acids. All the $Pd_xCe_{1-x}O_{2-\delta}$ based solid solution oxide catalysts exhibited high activity and afforded the desired products in good to excellent yields. A careful investigation through a series of suitable tests clearly showed that the C–C cross-coupling is accomplished via a quasi-homogeneous mechanism by leached palladium(0) species. Characterization of the used catalyst suggests that Pd^{2+} in $Pd_xCe_{1-x}O_{2-\delta}$ is reduced *in situ* to Pd^0 when employed in the cross-coupling reactions. However, the $Pd_xCe_{1-x}O_{2-\delta}$ catalysts were found to be both recoverable and recyclable.

Dedicated to

S'thokozi Amahle Mpungose

Preface

The experimental work described in this thesis was carried out at the University of KwaZulu-Natal in the School of Chemistry and Physics. The experimental work was performed from January 2015 to December 2017, under the guidance and supervision from Dr GEM Maguire and Prof HB Friedrich.

The studies presented here represent original work by the author and have not otherwise been submitted in any form for any degree or diploma to any tertiary institution. Where use has been made of the work from others it is duly acknowledged in the text.

Signed: _____

Declaration 1

Plagiarism

I, _____ declare that

1. The research reported in this thesis, except where otherwise indicated is my original research.
2. This thesis has not been submitted for any degree or examination at any other university.
3. This thesis does not contain other persons' data, pictures, graphs or other information, unless specifically acknowledged as being sourced from other person.
4. This thesis does not contain other persons' writing, unless specifically acknowledged as being sourced from other researchers. Where other written sources have been quoted, then:
    a. Their words have been re-written but the general information attributed to them has been referenced.
    b. Where their exact words have been used, then their writing has been placed in italics and inside quotation marks, and referenced.
5. This thesis does not contain text, graphics or tables copied and pasted from the Internet, unless specifically acknowledged, and the source being detailed in the thesis and in the References sections.

Signed: _____

Declaration 2

Publications and conference contributions.

DETAILS OF CONTRIBUTIONS TO PUBLICATIONS that form part and/or include research presented in this thesis.

Publications

Publication 1.

Authors: Philani P. Mpungose, Neo I. Sehloko, Venkat D.B.C. Dasireddy, Narayanappa Mahadevaiah, Glenn E. Maguire and Holger B. Friedrich.

Title: $Pd_{0.09}Ce_{0.91}O_{2-\delta}$: A sustainable ionic solid-solution precatalyst for heterogeneous, ligand free Heck coupling reactions.

Status: Published in Molecular Catalysis, 443 (2017) 60-68.

Contribution: I carried out all the experimental work and manuscript preparation under the guidance and supervision of N.I. Sehloko, V.D.B.C. Dasireddy, N. Mahadevaiah, G.E. Maguire and H.B. Friedrich.

Publication 2.

Authors: Philani P. Mpungose, Neo I. Sehloko, Thandanani Cwele, Glenn E. Maguire and Holger B. Friedrich.

Title: $Pd_{0.02}Ce_{0.98}O_{2-\delta}$: A copper- and ligand-free quasi-heterogeneous catalyst for aquacatalytic Sonogashira cross-coupling reactions.

Status: Published in Journal of the Southern African Institute of Mining and Metallurgy, 117 (2017) 955-962.

Contribution: I carried out all the experimental work and manuscript preparation under the guidance and supervision of N.I. Sehloko, T. Cwele, G.E. Maguire and H.B. Friedrich.

Publication 3.

Authors: Philani P. Mpungose, Neo I. Sehloko, Glenn E. Maguire and Holger B. Friedrich.

Title: PdCuCeO-TPAB: A new catalytic system for quasi-heterogeneous Suzuki-Miyaura cross-coupling reaction under ligand-free conditions in water.

Status: Published in New Journal of Chemistry, 41 (2017) 13560-13566.

Contribution: I carried out all the experimental work and manuscript preparation under the guidance and supervision of N.I. Sehloko, G.E. Maguire and H.B. Friedrich.

Conference contributions

Oral presentations:

- $Pd_{0.02}Ce_{0.98}O_{2-\delta}$: A copper- and ligand-free quasi-heterogeneous catalyst for aquacatalytic Sonogashira cross-coupling reactions, AMI: The Precious Metals Development Network, 2017, Polokwane, South Africa.

Poster presentations:

- $Ce_{0.95}Pd_{0.05}O_{2-\delta}$: An efficient, chemoselective and new heterogeneous catalyst for one-pot double cross coupling reactions under ligand free conditions, NAM25, 2017, Denver, USA.
- $Pd_{0.02}Ce_{0.98}O_{2-\delta}$: A copper- and ligand-free quasi-heterogeneous catalyst for aquacatalytic Sonogashira cross-coupling reactions, CATSA conference, 2016, Drankensburg, South Africa
- PdCuCeO-TPAB: A new catalytic system for heterogeneous Suzuki-Miyaura cross-coupling reaction under ligand-free conditions in water, College of Agriculture, Engineering and Science: Post-graduate Research Day, 2016, Durban, South Africa
- $Pd_{0.09}Ce_{0.91}O_{2-\delta}$: a sustainable ionic solid-solution catalyst for heterogeneous, ligand free Heck coupling reactions, CATSA conference, 2015, Cape Town, South Africa
- $Pd_{0.09}Ce_{0.91}O_{2-\delta}$: a sustainable ionic solid-solution catalyst for heterogeneous, ligand free Heck coupling reactions, SACI conference, 2015, Durban, South Africa

Signed: _____

Acknowledgments

I would like to start with expressing my sincere gratitude to my supervisor Prof. HB Friedrich for allowing me into his group and guiding me throughout my entire postgraduate life. His continuous support and insight have been crucial to both this thesis work and my personal development. My special thanks are also due to my co-supervisor Dr Glenn Maguire for his kind guidance and support throughout my PhD studies. I also wish to acknowledge AMI/Mintek for a generous research grant.

Besides my supervisors, I would like to thank my best friend, mentor and scientific brother, Mr Neo Sehloko for everything he has done for me. Thanks for your undying interest and enthusiasm towards my project. Big thanks also go to Dr Soboo Singh, Dr Mzamo Shozi and Dr Abdul Mohamed for their encouragement, insightful comments, and hard questions during group presentations.

My sincere thanks also go to University of KwaZulu-Natal technical staff for all their help throughout my PhD work. I am thankful to the past and current members of the UKZN Catalysis research group for the stimulating discussions and for all the fun we have had during my studies.

Many thanks to my life coaches, Mrs Khethiwe Mpungose-Ngubane and Wayne Peddie, I owe it all to you. In the same breath, I would also like to thank Mr Bongani Ngubane and his family for the fruitful relationship we have built over the years and for being a positive role model to every aspiring kid in Mpophomeni Township. Umndeni wakwaNgubane has literally become my second family.

Last, but not the least, I would like to thank my family and friends for supporting me emotionally, financially and spiritually throughout my life. *Ngiyabonga, iNkosi inibusise*. Family: Musa (may her soul rest in peace), S'thokozi, Nokuphiwa, Gogo, S'celo, Amenda, Thando, Amahle, Banathi, Mbali and Siyabonga Mpungose. And my friends: Mxolisi Zondi, S'miso Makhaye, Mbuso Mabaso, Roots "Mtaka-Jah" Ngobese, Sphelele Sosibo, Sphamandla Mhlongo, Busa Maphumulo, Lungisani "Naziri" Ziqubu and Bheki "Gambiri" Gumbi.

TABLE OF CONTENTS

List of Figures

(Figure 2.1 and 2.3 were reproduced by permission of The Royal Society of Chemistry; Figure 2.2 and 2.14 were reproduced by permission of John Wiley and Sons; Figure 2.4 and 2.13 were reproduced by permission of Springer Nature; Figure 2.6, 2.7, 2.10, 2.11, 2.12 were reproduced by permission of Elsevier; Figure 2.16 was reproduced by permission of American Chemical Society)

List of Schemes

(Scheme 2.2 was reproduced by permission of The Royal Society of Chemistry; Scheme 2.4 and 2.14 were reproduced by permission of John Wiley and Sons; Scheme 2.5, 2.6 and 2.8 were reproduced by permission of Elsevier)

List of Tables

(Table 2.1 and 2.2 were reproduced by permission of John Wiley and Sons; Table 2.3 was reproduced by permission of Springer Nature)

Abbreviations

BET	Brunauer-Emmett-Teller
β_{hkl}	Peak broadening at half the maximum intensity
D	Average crystallite size
EXAFS	Extended X-ray Absorption Fine Structure
EDX	Energy Dispersion X-ray spetroscopy
FID	Flame Ionisation Detector
GC-FID	Gas Chromatography-Flame Ionisation Detector
GC-MS	Gas Chromatography-Mass Spectrometry
HRTEM	High Resolution Transmission Electron Microscopy
ICP-OES	Inductively Coupled Plasma-Optical Emission Spectrometry
JCPDS	Joint Committee on Powder Diffraction Standards
K	Shape factor (0.891)
Mol	Molar
NMR	Nuclear Magnetic Resonance
ppm	Part Per Million
PZC	Point of Zero Charge
SEM	Scanning Electron Microscopy
STEM	Scanning Transmission Electron Microscopy
TEM	Transmission Electron Microscopy
TGA-DTA	Thermal Gravimetric Analysis-Differential Thermal Analysis
TOF	Turn-Over Frequency
TON	Turn-Over Number
TPAB	Tetrabutylammonium Bromide
µL	Micro (10^{-6}) Litre
XANES	X-ray Absorption Near Edge Structure
XRD	X-Ray Diffraction
XPS	X-ray Photoelectron Spectrometry
@	Denotes a core–shell structure

Chapter 1

A Brief Historical Overview of Palladium Catalysed Cross-Coupling Reactions

The aim of this chapter is to use the available enormous amount of literature to classify, define and give an overview of the palladium catalysed C-C cross-coupling reactions. In addition, the reader is introduced to generally accepted and new knowledge on the catalytic mechanism of homogeneous C-C cross-coupling reactions.

1.1 Introduction to palladium catalysed carbon-carbon cross-coupling reactions

Carbon–carbon (C-C) bond-formation reactions are important processes in chemistry. They provide key steps in the building of complex and bioactive molecules that are developed as medicines and agrochemicals [1, 2]. They are also vital in developing the new generation of organic materials with novel electronic, optical, or mechanical properties that play a significant role in the growing area of nanotechnology [1]. The careful construction of carbon-carbon bonds has continued to receive much attention following the awarding of Nobel prizes in chemistry for this area of research. These include works with the Grignard reaction (1912), the Diels Alder reaction (1950), the Wittig reaction (1979) and olefin metathesis by Y. Chauvin, R. H. Grubbs, and R. R. Schrock (2005). Recently, in 2010, it was awarded to Richard F. Heck, Ei-ichi Negishi and Akira Suzuki for their work on palladium catalyzed cross coupling reaction [3, 4].

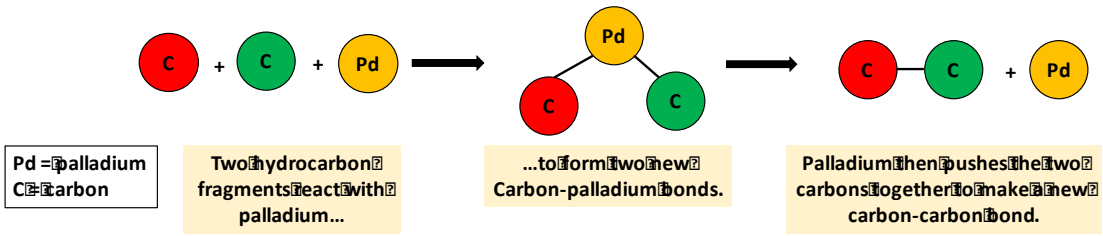

Scheme 1.1: Illustration of a palladium mediated carbon-carbon bond formation.

A coupling reaction in organic chemistry is a general term for a variety of reactions where two hydrocarbon fragments are coupled with the aid of a metal catalyst (Scheme 1.1) [3, 4]. The palladium catalyzed C-C cross coupling reactions are largely divided into two types:

- **Heterocouplings** couple two different hydrocarbon fragments (coupling partners); for example, the Sonogashira reaction of an Alkyne (RC≡CH)

and an aryl halide (R'-X) to give a substituted phenylacetylenes (RC≡CR').

- **Homocouplings** couple two identical hydrocarbon fragments; for example, the Glaser coupling of two acetylides (RC≡CH) to form a dialkyne (RC≡C-C≡CR).

The field of C-C cross-coupling has undoubtedly turned into an area appreciated by all synthetic chemists, both in academia and industry [2, 5]. An advantageous feature of these C-C cross-coupling reactions is substitution with retention of the configuration at the sp^2 carbon, which had not been possible by conventional organic reactions (Scheme 1.2) [6]. These reactions can also selectively couple specific points even in complicated molecules with many reactive sites. These innovations have facilitated the synthesis of pi-conjugated compounds such as natural products, pharmaceuticals, liquid crystals, conjugated polymers, luminescence materials and the organic semiconductors.

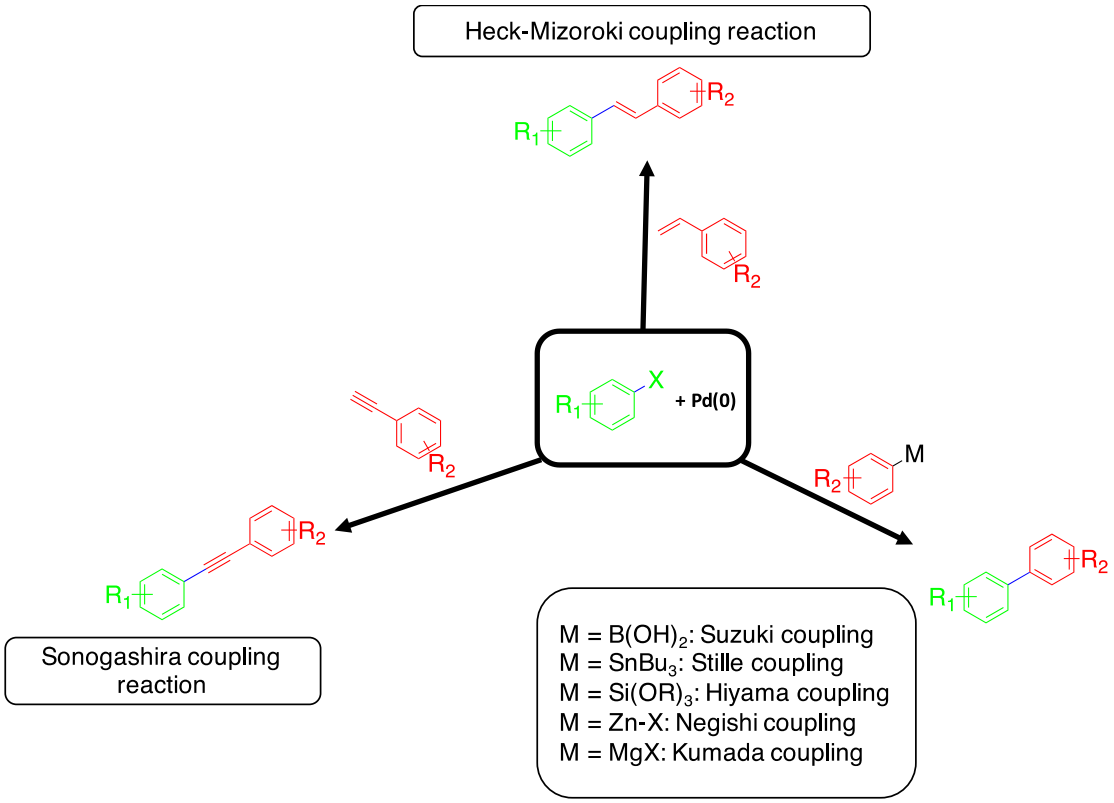

Scheme 1.2: Selected examples of palladium-catalyzed C-C coupling reactions.

The field of C-C coupling reactions has gone through numerous stages of development (Table 1.1). The "first wave" (1965-1980) in the development of C-C cross-coupling reactions was the investigation of metal catalysts that were capable of promoting these transformations in a selective fashion [7-9]. The "second wave" (1980-2000) focused on expanding the scope of coupling partners. The "third wave" (2000-2010) focused on the continuous improvement

and extension of each reaction type through ligand variation, accommodating wider substrates scope, by optimization and fine-tuning reaction conditions [10].

Table 1.1: Selected examples of C-C coupling reactions

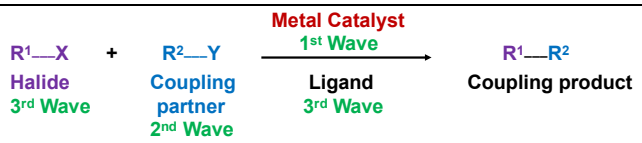

Reaction (year of discovery)	Reactant A		Reactant B		Catalyst	Ref.
Grignard reaction (1900)	R-HC=O or $R(C=O)R_2$		R-MgBr	-	-	[11]
Cadiot-Chodkiewicz coupling (1957)	RC≡CX	sp	RC≡CH	sp	Cu	[12]
Castro-Stephens coupling (1963)	Ar-X	sp^2	RC≡CH	sp	Cu	[13]
Tsuji-Trost reaction (1965)	R(O=C-C-C=O)R	-	R-$PdCl_2$	-	-	[14]
Corey-House synthesis (1967)	R-X	sp^2, sp^3	R_2CuLi or R-MgX	sp^3	Cu	[15]
Kumada coupling (1972)	Ar-X	sp^2	Ar-MgBr	sp^2, sp^3	Pd or Ni or Fe	[16]
Heck reaction (1972)	Ar-X	sp^2	RC=CHR	sp^2	Pd or Ni	[17]
Sonogashira coupling (1975)	R-X	sp^2, sp^3	RC≡CH	sp	Pd or Ni	[18]
Negishi coupling (1977)	R-X	sp^2, sp^3	R-Zn-X	sp^2, sp^3	Pd or Ni	[19]
Stille cross coupling (1978)	R-X	sp^2, sp^3	$R-SnR_3$	sp^2, sp^3	Pd	[20]
Suzuki reaction (1979)	R-X	sp^2, sp^3	$R-B(OR)_2$	sp^2	Pd or Ni	[21]
Hiyama coupling (1988)	R-X	sp^2, sp^3	$R-SiR_3$	sp^2	Pd	[22]
Buchwald-Hartwig reaction (1994)	R-X	sp^2	R_2N-H	sp^3	Pd	[23]
Fukuyama coupling (1998)	R-X	sp^2	R-Zn-I	sp^3	Pd or Ni	[24]
Liebeskind–Srogl coupling (2000)	RCO(Set) Ar-SMe	sp^2	$R-B(OR)_2$	sp^2, sp^3	Pd	[25]

Currently, the development of recoverable and recyclable catalysts through heterogenization of homogeneous catalysts is one of the hottest research topics. Hence, we are currently in the "fourth wave" of development for C-C cross-coupling reactions.

The first example of palladium-mediated carbon–carbon bond forming reactions was reported by Tsuji and co-worker in 1965 when they realized that a mixture of a palladium complex and ethyl malonate under basic conditions successfully generated carbopalladation products [14]. This discovery led to the universal development of palladium mediated coupling reactions. From this point on, throughout the 1970s, further examples of palladium mediated C–C cross-coupling reactions continued to appear in literature (Table 1.1). Researchers worldwide strove to extend, apply and discover new variants of C-C cross coupling reactions; and such efforts still continue at an ever increasing pace today [26, 27]. Mizoroki and Heck independently investigated the palladium-catalyzed reactions of alkenes with aryl or alkenyl halides in the presence of a base to afford the corresponding coupled products through a substitution of hydrogen in the alkenes. The coupling of aryl halides with alkynes instead alkenes was further improved by Sonogashira using copper and Pd catalysts. Makoto Kumada and Ei-ichi Negishi independently explored the coupling of aryl halides with organometallic derivatives of zinc and magnesium. The exploration of tin reagents in coupling chemistry is attributed to John K. Stille. A number of extremely useful transformations can be carried out using this chemistry [28-30].

In the late 1970's, Akira Suzuki and Miyaura employed boric acids as alternative coupling partner to successfully prepare biaryl derivatives. The main advantage of using arylboronic acids as the coupling partner is that they are air-stable and readily accessible. In addition to the generation of new C-C bonds, highly efficient carbon-oxygen (C-O) and carbon-nitrogen (C-N) bond forming reactions are also known nowadays. Stephen Buchwald and John Hartwig developed the most notable C-N bond forming reactions. All these coupling reactions have been developed further and are now applied regularly on an industrial scale [31].

1.1.1 General mechanisms for Pd-catalyzed C-C cross-coupling reactions

The generally accepted mechanisms for palladium catalyzed C-C cross-coupling reactions are summarized in Scheme 1.3. All reactions start with a Pd(0) species preformed or formed *in situ* from Pd(II) catalyst precursors. The first step is common for all reactions, consisting of the **oxidative addition** reaction of aryl or vinyl halide to the Pd(0) species affording the R_1-Pd^{II}-X intermediate [26, 32]. Therefore, the Pd(0) species is a nucleophile and the organohalide is an electrophile [32, 33]. Thus, in general, ligands L having strong electron donating

abilities and organohalides having an R_1–X bond that can be considered as ''electron-poor'' are expected to promote the oxidative addition step [32]. In the case of coupling reactions involving an organometallic partner (R_2-M), the R_1-Pd^{II}-R_2 intermediate is formed by a **transmetalation step** [5]. Finally, **reductive elimination** provides the R_1-R_2 coupling product, and regenerates the Pd(0) species.

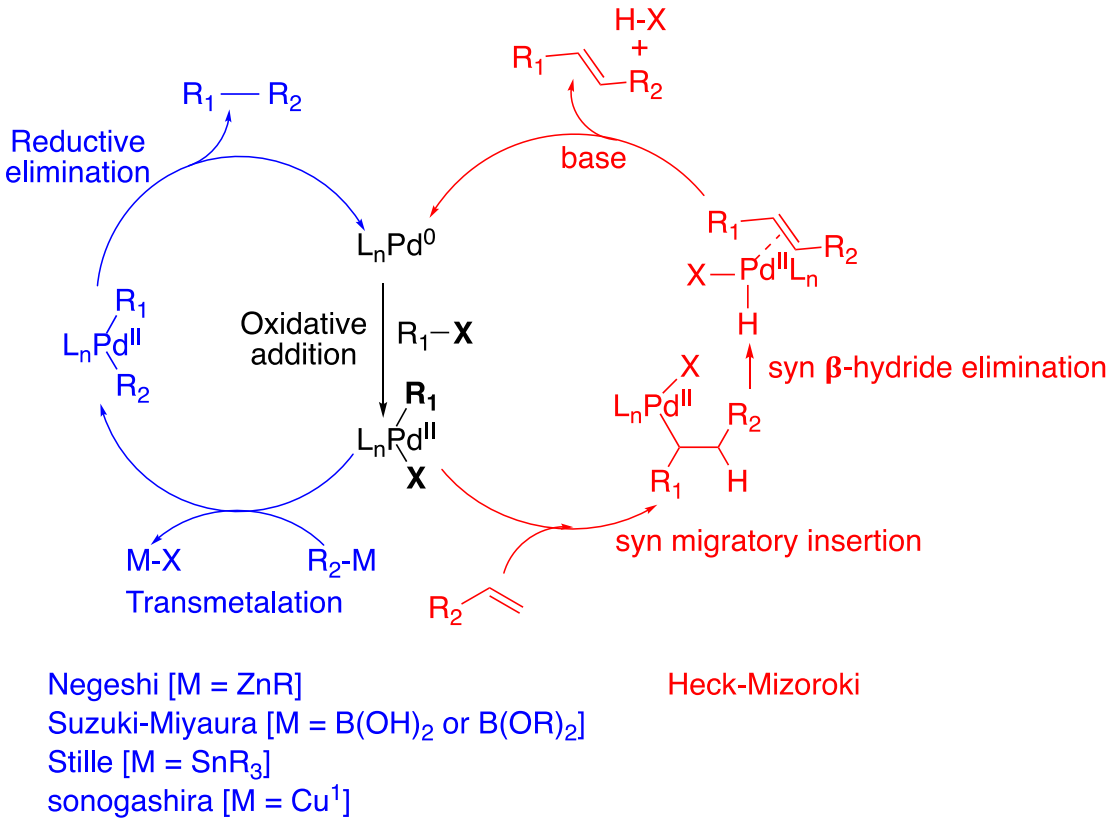

Scheme 1.3: General mechanism of cross-coupling reactions and the Heck–Mizoroki reaction under homogeneous reaction conditions [34].

A different catalytic cycle is involved in the Heck-Mizoroki reaction. In this case, the alkene is coordinated to the common R_1-Pd^{II}-X intermediate. Then, a **syn migratory insertion** occurs and the organopalladium species formed undergoes **β-hydride elimination** to form the alkene product ($R_1C{=}CR_2$). Finally, a base-assisted elimination of H-X regenerates the Pd(0) catalyst [26, 32, 35]. The issue of a possible Pd(II)/(IV) catalytic cycle, and the factors influencing the relative preference of Pd(0)/(II) versus Pd(II)/(IV) catalytic cycles are still not well understood and thus require further experimental and theoretical studies [32].

1.2 The types of palladium catalysed C-C cross-coupling reactions

The following discussion on the palladium catalyzed cross-coupling reaction will be limited to Heck-Mizoroki, Sonogashira and Suzuki-Miyaura cross-coupling reactions. Research on these three coupling reactions has seen rapid growth in

the past several years, as evidenced by the growing total number of publications and patents in the area [2]. Literature search via the browser SciFinder gave the following results: "Heck reaction" = 7730 hits, Sonogashira reaction = 1101 hits, and "Suzuki reaction" = 2050 hits. However, the intent of this discussion is not to provide an exhaustive review of the history on the three chosen type of cross-coupling reactions, but is to identify the most notable milestones and the genesis of the three cross-coupling reaction procedures presented here. There are several comprehensive handbooks and review articles on these and other type of C-C cross coupling reactions that are available in literature [4, 5, 32, 36-41].

1.2.1 Heck-Mizoroki cross-coupling reaction

The father of palladium catalysed C-C cross-coupling chemistry is generally considered to be Professor Richard Heck [31]. Although other reports on organometallic coupling reactions had already been published, it was through his work that the palladium catalysed reactions became widely known and applied [42-53]. In the early 1970s, Richard F. Heck and Tsutomu Mizoroki independently discovered that aryl or alkenyl halides react with alkenes at elevated temperatures in the presence of a catalytic amount of a Pd(0) catalyst and a base to form substituted alkenes (Table 1.2) [17, 54]. Heck's first publication of palladium catalysed cross-coupling reaction of alkenes with aryl halides appeared in 1972, the year following the publication of the same conversion, though under different conditions, by Mizoroki. Heck's initial choice of catalyst was Pd(II) acetate, while Mizoroki used $PdCl_2$ as a catalyst. However, Mizoroki didn't follow up on his reaction and passed away in 1980 due to cancer [55]. Afterwards, the Pd-catalysed reactions were aggressively researched by Heck [43-46, 56-59] and in 1982 he wrote an Organic Reactions chapter that covered all the known instances on "palladium-catalyzed vinylation of organic halides" [44]. Through Heck's work, the palladium catalyzed coupling reactions became widely known and applied [55]. Today, the palladium-catalyzed arylation of alkenes is most commonly referred to as the "Heck cross-coupling reaction".

Table 1.2: The original reports of Pd-catalysed coupling of alkenes with aryl iodides by Heck and Mizoroki.

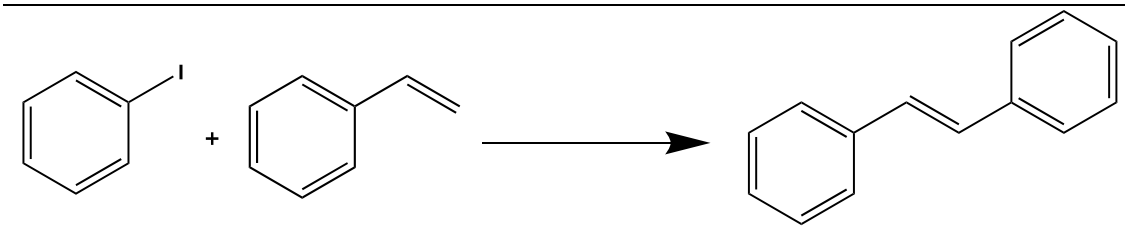

	Reaction conditions	%Yield	Ref.
Mizoroki et al. 1971	1 mol% $PdCl_2$, KOAc, MeOH, 120 °C, autoclave.	90	[54]
Heck et al. 1972	1 mol% $Pd(OAc)_2$, tri-*n*-butylamine, 100 °C.	75	[17]

The Heck cross-coupling reaction nowadays is known as the chemical reaction that forms substituted alkenes through reaction of unsaturated halides (or triflate) with an alkene in the presence of a base and a palladium catalyst (or Pd nanomaterial based catalyst) (Scheme 1.4) [42, 60-62]. In addition, the Heck reaction enables the functionalization of various molecules with different substituents, which otherwise take multiple steps to produce. Thus, an impressive list of synthetically useful transformations is possible via the Heck reaction. Nevertheless, intensive research efforts have been continuing because simpler, "greener," and more efficient catalytic systems beyond the traditionally used organopalladium-based catalysts and phosphine ligands are needed for many existing and other possible new Heck cross-coupling reactions.

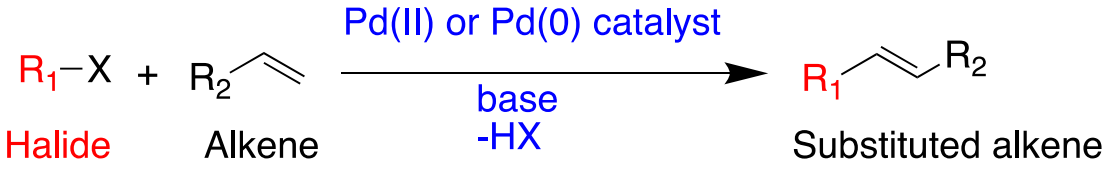

Scheme 1.4: General schematic showing of the Heck reaction between an unsaturated halide or triflate and an alkene that contains at least one hydrogen atom (R_1 = aryl, benzyl or vinyl; and R_2 = aryl, acrylate ester, etc).

1.2.1.1 Reaction mechanism of Heck-Mizoroki cross-coupling reaction

The accepted Heck-Mizoroki cross-coupling reaction mechanism can be simplified into six distinct steps (Scheme 1.5). Initially, the palladium(II) precatalyst is reduced *in situ* by the reaction component (ligand, base and solvent) to form Pd(0) species (**1**). The catalytic cycle is initiated by the oxidative addition of the aryl halide (R_1-X) to Pd(0) (**2**). Then, the olefin coordinates to palladium via π-bond formation to give a Pd-π complex (**5**).

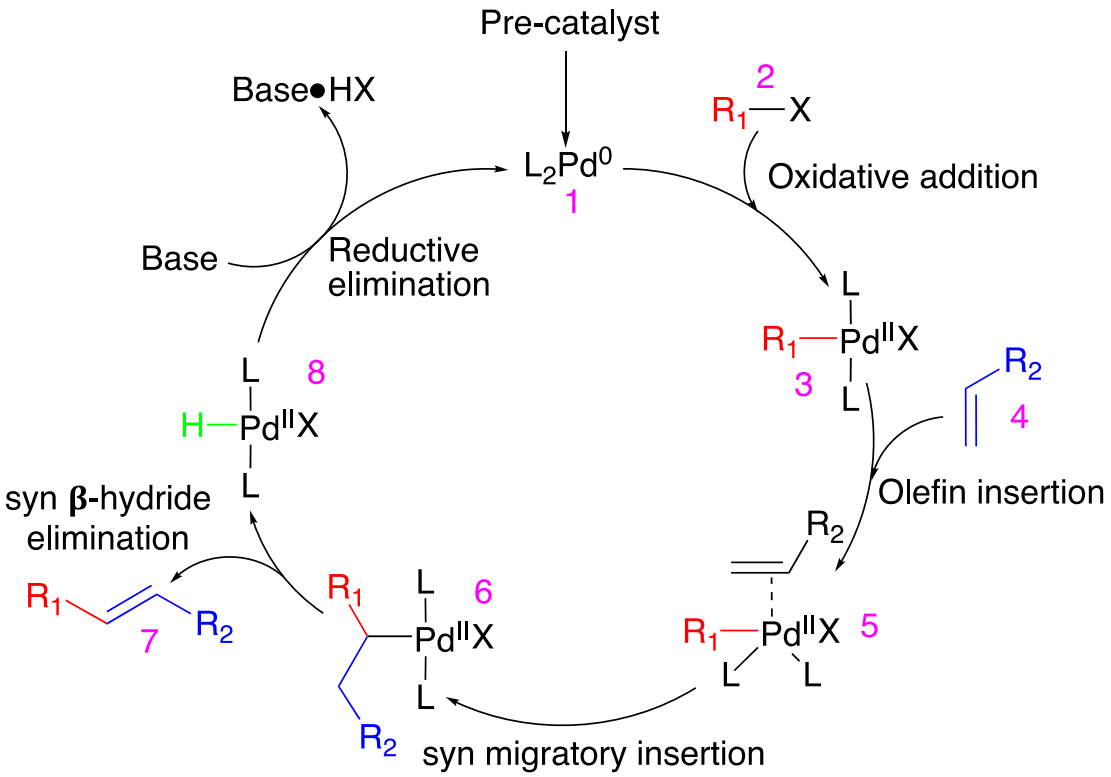

Scheme 1.5: General reaction mechanism for the Heck cross coupling reaction.

In the *syn*-migratory step, the organopalladium group (R_1) migrates to the adjacent carbon (less hindered) of the palladium-olefin species and effects syn addition of palladium and R_1 groups to alkene (**6**). The resulting intermediate undergoes β-hydride elimination to produce a C-C cross-coupled olefin product. In the final step, a stoichiometric amount of base reacts with the palladium complex (**8**) to regenerate the initial Pd(0) species via reductive elimination.

1.2.1.2 The general features of Heck-Mizoroki cross coupling reactions

In the traditional homogeneous Heck reaction, the active palladium catalyst is generally generated *in situ* from suitable precatalysts. The reaction conditions (base, temperature and solvent) controls the formation of the true active catalyst [55, 63]. The optimized reaction conditions usually tolerate a wide range of functional groups (esters, ethers, carboxylic acids, nitriles, phenols, dienes, etc.) on the aryl halide and the olefin components. The degree of substitution and the nature of the aryl halide have a large effect on the rate of the reaction. Usually, the alkene with a higher degree of substitution on the olefinic carbon undergoes a slower Heck-Mizoroki cross-coupling reaction; and substitution predominantly occurs at the least substituted olefinic carbon [63]. With regards to the aryl halide (R_1-X), the nature of the X group on the aryl halide influences the reaction rates in the following order: I > Br >> Cl. Hence, under similar conditions,

iodoarenes are more reactive than bromo- and chloroarenes. The Heck-Mizoroki cross-coupling reaction rates are also influenced by the electronic nature (electron-donating or electron-withdrawing) of the substituents on the aryl halide and the olefin component. Usually, the electron deficient olefins are more reactive and give higher yields. Lastly, the migratory insertion of the palladium complex into the olefin and the β-hydride elimination both proceed with *syn*-stereochemistry; hence, the Heck-Mizoroki cross-coupling reactions are stereospecific [55, 63].

1.2.1.1 Industrial application of Heck-Mizoroki cross-coupling reaction

The Heck-Mizoroki coupling reaction has become one of the most studied and frequently applied palladium catalyzed cross-coupling reactions in the pharmaceutical, agrochemical and fine chemical industry [64]. The application of Heck-Mizoroki coupling reactions in the fine chemical industries offer several advantages such as total cost reduction, tolerance to many functional group (no waste-producing protection/deprotection steps), and mild reaction conditions [65]. The industrial application of Heck-Mizoroki coupling reactions includes the large-scale (250 Kg) synthesis of Rilpivirine, which is a pharmaceutical drug for the treatment of HIV infection by Johnson & Johnson (Scheme 1.6) [66]. Their optimized method involves the Heck-Mizoroki coupling of iodoanaline and acrylonitrile to form an intermediate for the synthesis of Rilpivirine.

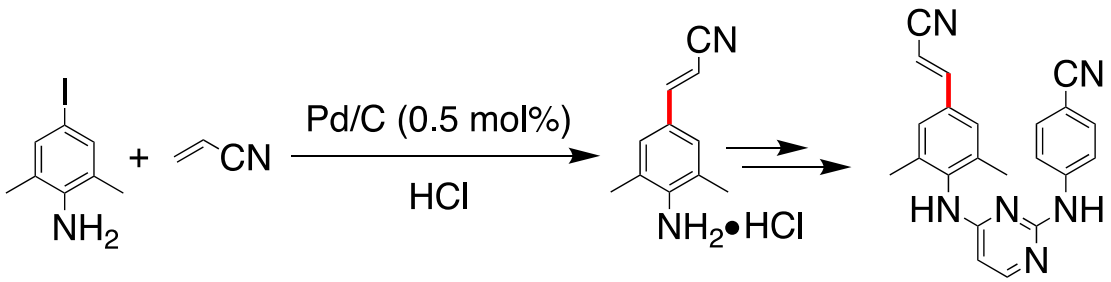

Scheme 1.6: The use of the Heck reaction in the synthesis of rilpivirine [66].

The industrial application of Heck-Mizoroki coupling reactions includes the large-scale production of the herbicide prosulfuron (Figure 1.1) by Syngeta AG and Novartis [40, 65]. Another example is the production of naproxen by Albemarle with a scale of about 500 tons per year. Other selected examples of fine chemicals that are produced industrially using the Heck reaction are shown in Figure 1.1. These include the synthesis of montelukast (anti-asthma agent) by Merck and cinacalcet (calcium regulator) by Teva [40, 66].

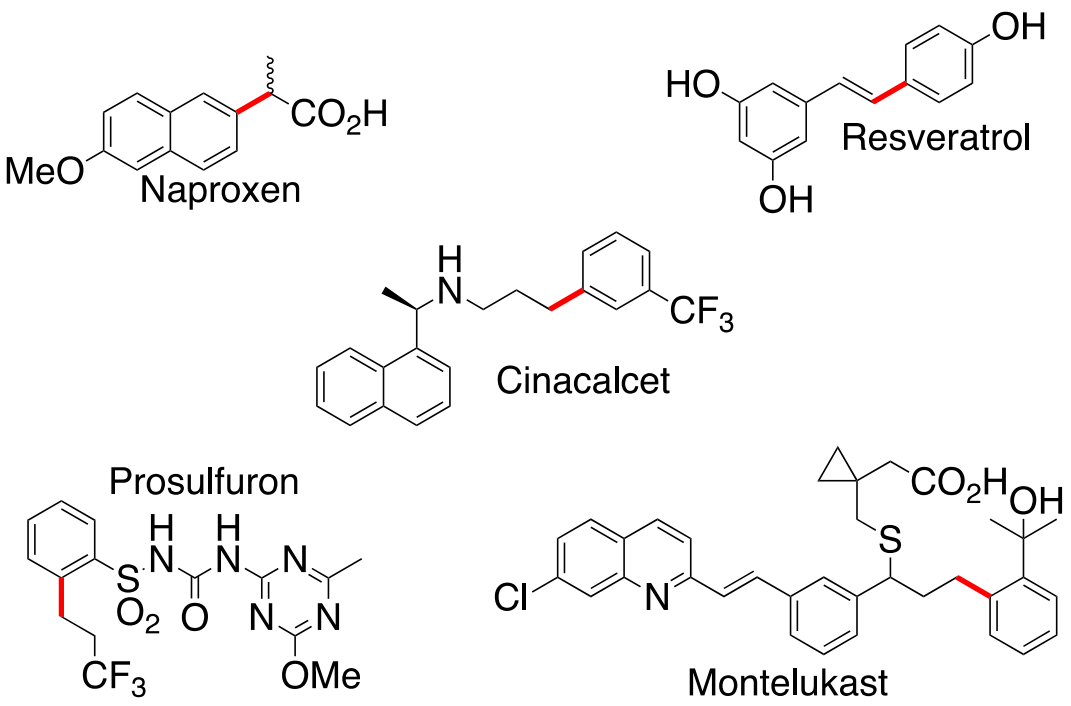

Figure 1.1: Representative examples of the application of the Heck reaction in the synthesis of pharmaceutical (bonds which are formed are highlighted in red) [40, 64, 65].

1.2.2 Sonogashira cross-coupling reactions

In 1975, Kenkichi Sonogashira and co-workers reported on the cross-coupling reactions of aryl halides with alkynes in the presence of a palladium catalyst and copper(I) salts to prepare substituted alkynes (Scheme 1.7) [18]. Although, similar reactions that used palladium only had been reported earlier by Cassar et al. [67] and Heck et al. [56], Sonogashira et al. demonstrated that their catalytic system improved the yields of the products under milder conditions by using the copper(I) salts as co-catalysts. The Sonogashira cross-coupling reaction has become one of the most important and widely used sp^2–sp carbon–carbon bond formation reactions in organic synthesis [37, 68-74]. This reaction has the advantage that the desired products can be obtained in excellent yields under comparatively milder reaction conditions [73-75]. It is frequently employed in the synthesis of natural products, biologically active molecules, heterocycles, molecular electronics, dendrimers and conjugated polymers or nanostructures [36, 37, 76].

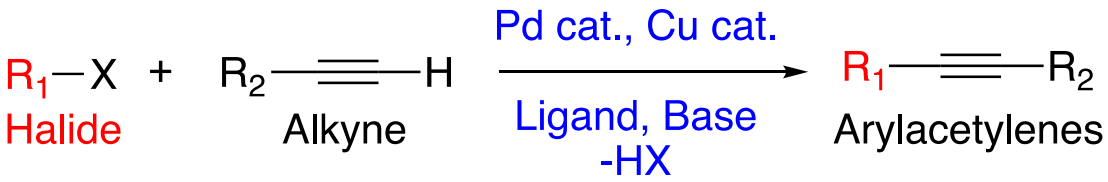

Scheme 1.7: General equation of the Sonogashira cross-coupling reaction [18].

1.2.2.1 Reaction mechanism of Sonogashira cross-coupling reaction

The mechanism of the Sonogashira cross-coupling reactions follows the expected oxidative addition-reductive elimination pathway. However, the structure of the catalytically active species and the precise role of the copper(I) salt co-catalyst are unknown [73]. The reaction begins with the generation of the Pd(0) species (**1**) from a Pd(II) precatalyst by reduction with the alkyne substrate (or base or ligand). The Pd(0) then undergoes oxidative addition (**2**) with the aryl halide followed by transmetallation by the copper(I)-acetylide (**7**). It is suggested that the presence of base results in the formation of a pi-alkyne Cu-complex (**6**) which makes the terminal proton on the alkyne more acidic, leading to the formation of the copper acetylide (**7**) [73]. This copper acetylide complex continues to react with the palladium intermediate (**3**), with regeneration of the copper(I) salt (**4**). Reductive elimination affords the coupled product (**10**) and the regeneration of the catalyst completes the catalytic cycle [73].

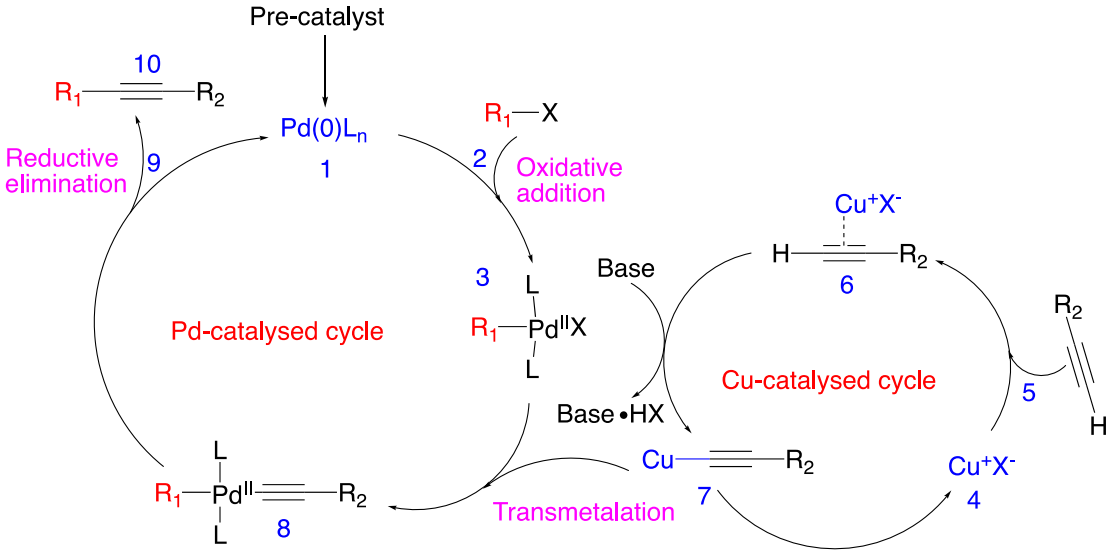

Scheme 1.8: General reaction mechanism of the Sonogashira cross-coupling reaction.

1.2.2.2 The general features of the Sonogashira cross-coupling reactions

The beneficial features of the Sonogashira cross-coupling reaction are that it can be conducted under mild reaction conditions, it tolerates almost all functional groups and the copper(I) salts are commercially available [36, 71, 75]. Thus, it can be performed at lower temperatures and the reagents don't need to be thoroughly dried. Depending on the desired outcome of the reaction, the reactions can be simplified even further by using the base as a solvent without the need of the co-solvent [71]. In addition, the reactions are very scalable; it works well on both very small and large scale without the product losing its stereochemical information. Hence, it is possible to use the Sonogashira coupling reaction for complex substrates in the late stages of a total synthesis [36].

1.2.2.3 Industrial and synthetic application of the Sonogashira reaction

The Sonogashira cross-coupling reaction is widely used for total synthesis because of its broad applicability and convenience [38, 77-79]. Recently, researcher at Wyeth reported a method for a multi-kilogram synthesis of GRN-529 (Scheme 1.7), which is a negative allosteric modulator of the metabotropic glutamate receptor 5 (mGluR5) [65]. This drug was found to be efficient in reducing repetitive behaviours (autism) without sedation and is generally therapeutic.

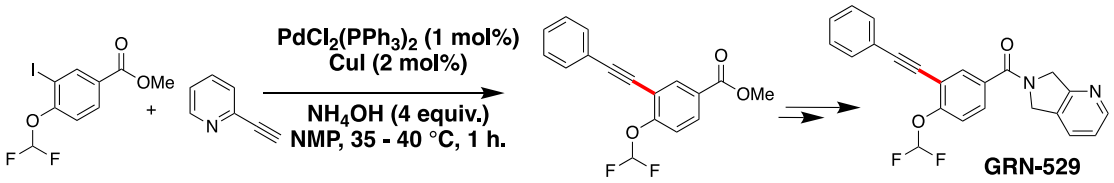

Scheme 1.9: Application of the Sonogashira cross-coupling reaction in the synthesis of the GRN-529 drug [26, 65].

Other examples of the use of the Sonogashira cross-coupling reactions at the industrial scale include the synthesis of an ammunomudula drug (fingolimod) for treating multiple sclerosis by Novartis (Figure 1.2) [26, 65]. Another example is the synthesis of terbinafin, which is an active agent of the antimyotic lamisil by Sandoz [65]. Lastly, there are currently two different companies, Medichem and Dipharma Francis, that hold patents for synthetic routes to cinacalcet using Pd/C or $PdCl_2$ catalysed Sonogashira cross coupling reactions [26, 65].

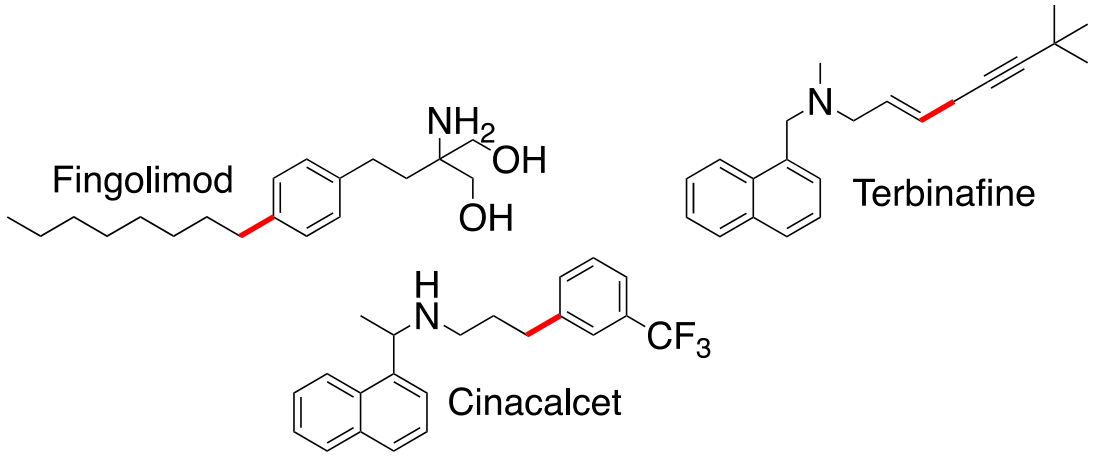

Figure 1.2: Examples of fine chemicals industrially produced using the palladium catalysed Sonogashira reaction (creation of the bold red bond) [65].

1.2.3 Suzuki-Miyaura cross-coupling reactions

The Suzuki-Miyaura reaction is a palladium catalyzed C-C cross-coupling reaction between different types of organoboron compounds and various organohalides or triflates in the presence of base to form poly-olefins, styrenes

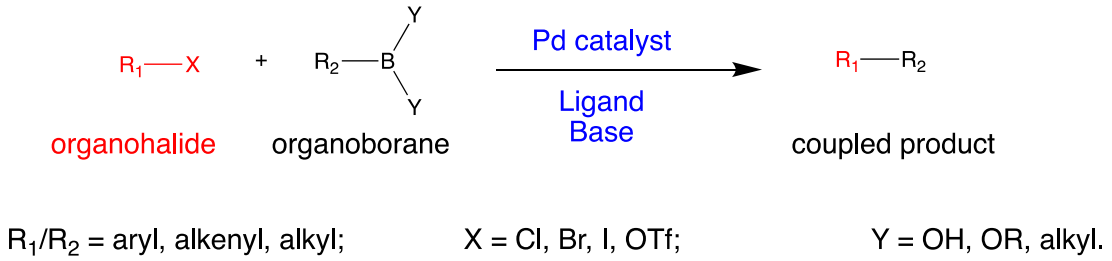

Scheme 1.10: Suzuki-Miyaura cross-coupling reactions

and substituted biphenyls (Scheme 1.10) [1, 21, 80-83]. The Suzuki-Miyaura cross coupling reaction has been recognized as a powerful tool for the construction of new organic compounds. Akiri Suzuki and Norio Miyaura discovered it in 1979 [21, 81].

Table 1.3: The representative examples of Suzuki-Miyaura cross-coupling reactions.

Cross-coupling reaction	Year	Ref.
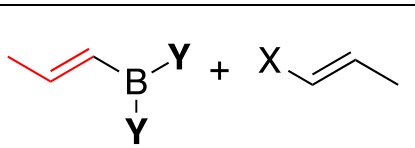	1979	[81]
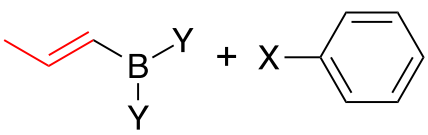	1979	[21]
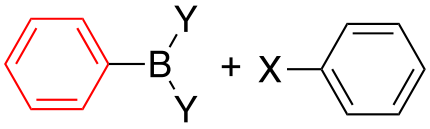	1981	[84]
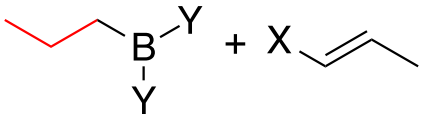	1985	[86]
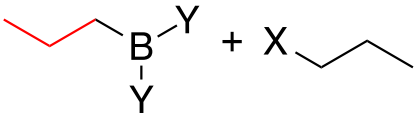	1992	[87]
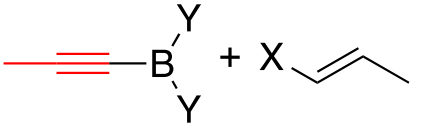	1995	[80]

A further significant development came in 1981 when they realized that arylboronic acids were able to participate efficiently as coupling partners; this allowed for efficient synthesis of substituted biaryls [84]. The importance of biaryl units as components in many kinds of compounds, such as pharmaceuticals, herbicides, natural products, polymers, molecular wires and

liquid crystals has attracted enormous interest from the chemical community [1, 80, 85]. The stability and weak nucleophilic nature of organoboron compounds makes this reaction very practical. It tolerates a wide range of functional groups and it is highly chemoselective. Furthermore, boron compounds are generally non-toxic and the reaction can be run under very mild conditions. Hence, the Suzuki-Miyaura cross-coupling reaction is very popular in the pharmaceutical industry [83]. Some of representative reactions between various organoboranes and a number of organic electrophiles are shown in Table 1.3.

1.2.3.1 Reaction mechanism of Suzuki-Miyaura cross-coupling reactions

The Suzuki-Miyaura cross-coupling reaction mechanism is similar to the catalytic cycle for the Heck and Sonogashira cross-coupling reactions (Scheme 1.9).

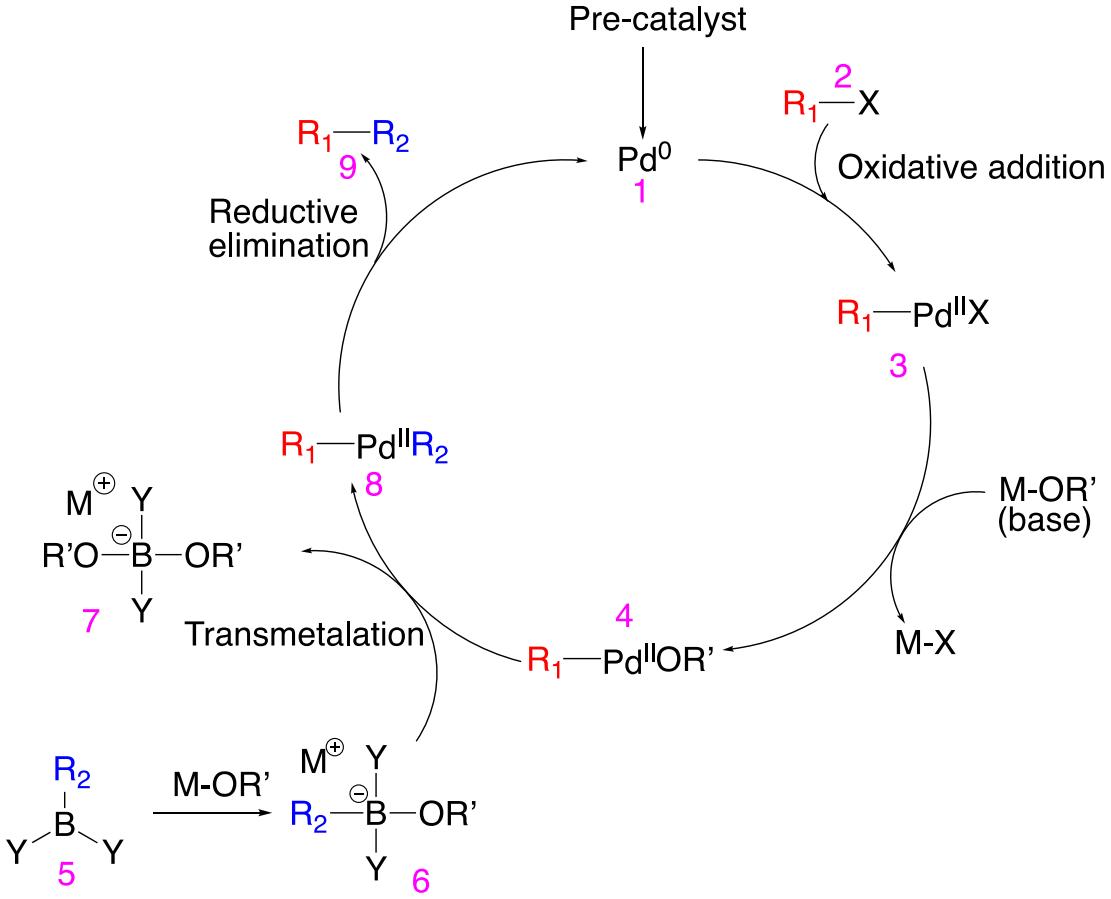

Scheme 1.11: Generally accepted reaction mechanism for Suzuki-Miyaura cross-coupling reactions.

The mechanistic difference being that the organopalladium intermediate (**3**) formed from the oxidative addition of the aryl halide (**2**) to the Pd(0) species goes through a metathesis process to give another organopalladium species (**4**). This metathesis step is the exchange of the halide anion (e.g. I^-) attached to the palladium for the anion of the base (e.g. CO_3^{2-}). The quaternization of the boric acid (**5**) through its reaction with the base forms a highly nucleophilic alkylborate complex (**6**) that readily undergoes a transmetallation step with the

Pd(II) complex (**4**). Finally, the C-C coupled product (**9**) is formed through the reductive elimination step and the active Pd(0) species (**1**) is regenerated in the process [1, 82, 83].

1.2.3.2 The general features of the Suzuki-Miyaura cross-coupling reactions

The Suzuki-Miyaura cross-coupling reaction has numerous beneficial features because the reactions can be conducted under mild reaction conditions and it tolerates a wide variety of functional groups [83, 88-91]. In addition, the boric acids are stable or unaffected by water. Boronic acids are environmentally safer and their inorganic by-products are easily removed from the reaction mixture. Lastly, the stereochemistry of the reactants in preserved in the coupled products. Hence, these reactions are highly suitable for industrial processes [1].

1.2.3.3 Industrial application of Suzuki-Miyaura coupling reactions

Suzuku-Miyaura cross-coupling reactions are heavily used in the synthesis of natural products, pharmaceuticals, agrochemicals, and new electronic materials because substituted biaryls are key substructures of these compounds [2, 26, 64]. The largest industrial process that uses Suzuki cross-coupling reactions is operated by BASF in their production of the fungicide boscalid (1000 tons per year) (Scheme 1.12) [64, 65]. The fungicide boscalid is used on a large number of crops, especially vegetables and fruit growing in open air [26, 65].

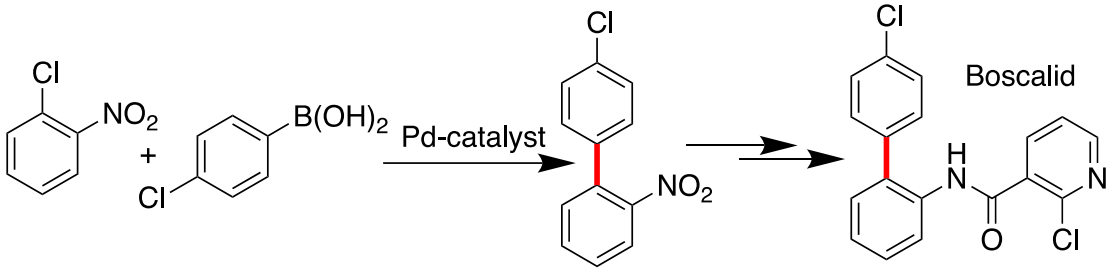

Scheme 1.12: Application of the Suzuki cross-coupling reaction in the synthesis of fungicide boscalid.

Another important example involves the production of *o*-tolylbenzonitrile (Figure 1.3) on a multiton scale by Clariant AG. The *o*-tolylbenzonitrile serves as a common intermediate for the production of an entire family of Sartan derivatives as blood pressure lowering agents [2, 26, 64, 65]. Some additional examples of the use of the Suzuki reaction in industrial processes include the synthesis of crizotinib (Figure 1.3), an anticancer drug marketed by Pfizer; the synthesis of ruxolitinib (Figure 1.3), a drug for treatment of myelofibrosis, marketed by incyte; and the synthesis of an anticancer drug, abiraterone acetate (Figure 1.3) that is manufactured by Hoffmann-La Roche and Janssen Pharmaceuticals [26, 65].

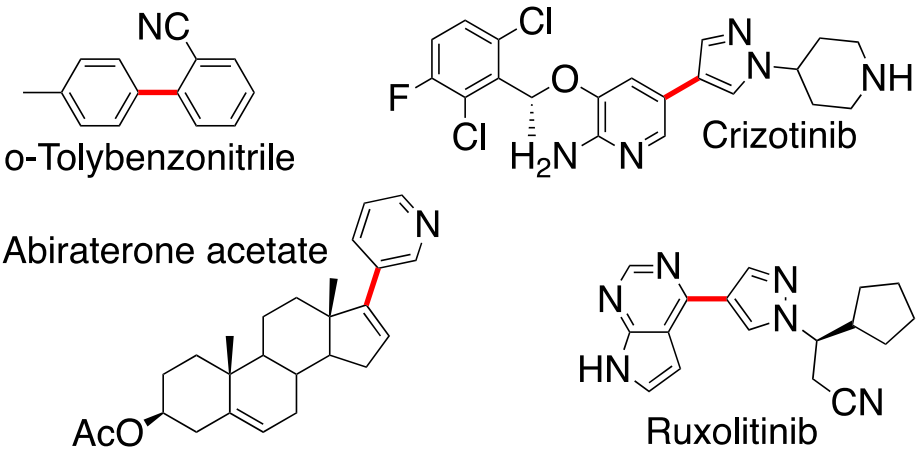

Figure 1.3: Examples of fine chemicals industrially produced using the palladium catalysed Suzuki reaction (creation of the bold red bond) [26, 65].

1.3 The palladium catalysts

Palladium based catalyst are the most robust and most frequently used catalysts for C-C cross-coupling reactions. This is due to their high functional group tolerance and the low sensitivity of their organopalladium intermediates towards water and air [2]. The properties of a palladium catalyst can be easily fine-tuned to enhance its catalytic activity through appropriate ligand design [92]. Furthermore, the oxidation-reduction processes required in C-C cross-coupling reaction are easily attainable with palladium, since the 0 and +2 (and +4) oxidation states prevail [93]. Hence, palladium catalysts tend to react without the involvement of radical intermediates; thus, the formation of side products is limited. Other metals in catalysts that have been used for C-C cross coupling reactions include copper [94, 95], nickel [93, 96], cobalt [97, 98] and iron [99, 100]. However, these catalysts are more likely to undergo one electron redox processes and are not well understood mechanistically [93]. Furthermore, they require higher catalyst loadings and elevated reaction temperatures. Hence, palladium based catalysts continue to be the catalysts of choice for most C-C cross-coupling reactions.

Most C-C cross-coupling reactions are carried out under homogenous conditions using organopalladium complexes. This is because homogeneous systems have higher reactivity, hence, high turnover numbers can be obtained under milder reaction conditions [101]. However, the efficient separation and subsequent recycling of homogenous palladium catalysts remains a challenge and an aspect of economic relevance [88, 102-104]. Herein, we will look very briefly at the most prominent homogeneous based palladium catalytic systems, and the development of heterogeneous based catalytic systems will be discussed in detail later, in Chapter two.

1.3.1 Prominent types of organopalladium complexes as catalysts

The past three decades have seen important advances in the development of highly active organopalladium complexes as catalysts for a variety of C-C cross-coupling reactions [92, 105]. However, there is no universal catalytic system for the palladium catalysed cross-coupling reactions that has been developed so far. Many of the methods varying in ligand, solvent and ancillary reagents, effectively perform specific subtasks.

A diverse range of organopalladium complexes can be used as homogeneous catalyst because palladium can form strong and weak metal–ligand complexes with a wide variety of ligands containing donor atoms such as phosphorus, nitrogen, and oxygen [62, 105-107]. The synthesis of these organopalladium complexes typically involves the complexation of Pd(II) salts with organic ligands containing phosphines, phosphites, carbenes, thioethers, or pincer functional groups [106]. The roles of ligands can be categorized into three major divisions: (i) Tuning the reactivity and selectivity of catalytic species by increasing the rate of oxidative addition. (ii) Binding palladium into a relatively stable complex, which slowly releases active palladium species during the reaction by means of thermal decomposition or reaction with components of the reaction system. (iii) Support of zero-valent palladium as reactive monomeric complexes and prevention of cluster formation that eventually leads to catalyst deactivation [106]. The three most prominent organopalladium complexes that are used as catalysts in C-C cross-coupling reaction are discussed below.

1.3.1.1 Phosphorous ligands based palladium complexes

The phosphine ligand can be regarded as a classical ligand; most of the earliest palladium precatalyst relied on phosphine ligands ($Pd(PPh_3)_4$, $PdCl_2(PPh_3)_2$ and [1,1'-bis(diphenylphosphino)ferrocene]palladium(II) dichloride) [4, 31, 108]. Several groups have established that the combination of bulky and electron-rich phosphines with different sources of palladium generate species that show high catalytic activity in cross-coupling reactions (Figure 1.4) [39, 93, 103]. The use of strong σ-donating ligands, such as trialkylphosphines, increases electron density around the palladium metal center, thus, accelerates the oxidative addition step [105]. In addition, bulky phosphine ligands have been found to accelerate the elimination step in the reaction mechanism [93].

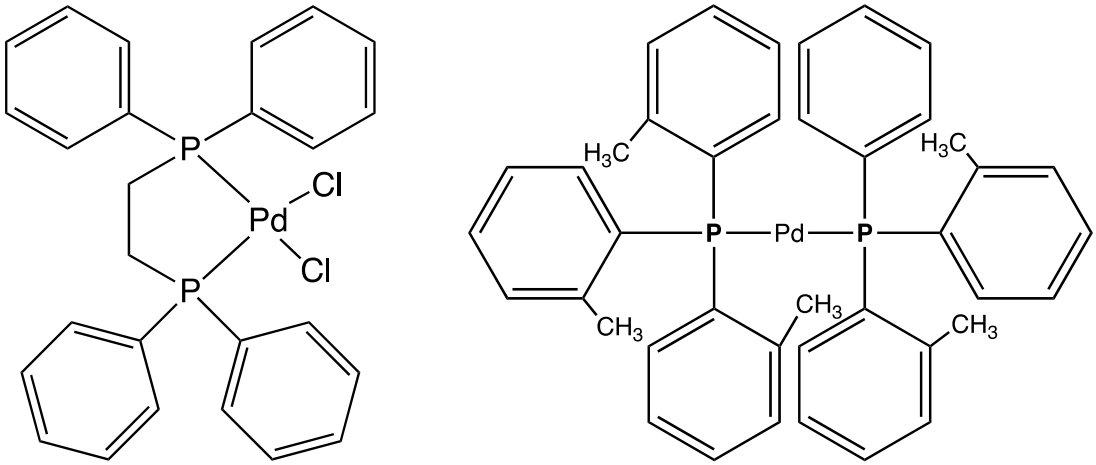

Figure 1.4: Depiction of common phosphine based palladium complexes.

1.3.1.2 N-heterocyclic carbene palladium complexes

Palladium complexes bearing N-heterocyclic carbene (NHC) ligands have emerged as the system of choice for cross-coupling reactions due to their stable metal–ligand framework (Figure 1.5) [39, 92, 93, 109]. NHCs can offer very high catalytic activity combined with stability and longevity in comparison with phosphine ligands [109].

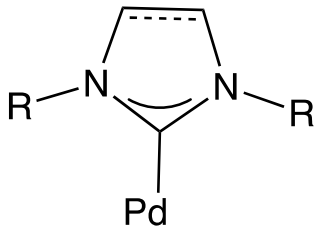

Figure 1.5: General structure of palladium complexes bearing N-heterocyclic carbene ligands.

The two-electron donor NHC ligands combine strong sigma-donating properties with a shielding steric pattern that allows for both stabilization of the metal center and enhancement of its catalytic activity (Figure 1.6) [39]. As a result, the number of well-defined NHC-containing palladium(II) complexes is growing, and their use in coupling reactions is witnessing increasing interest [92, 93, 109]. The palladium complexes with sterically demanding and electron-rich NHC ligands are one of the most active cross-coupling catalysts [92, 93, 109, 110].

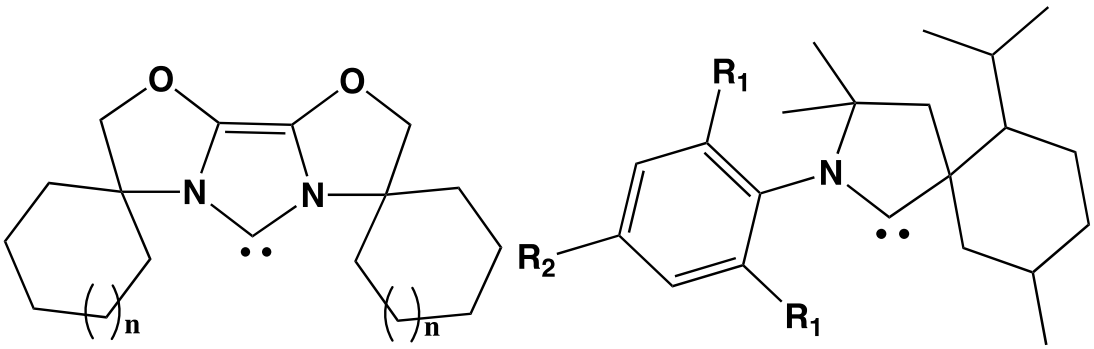

Figure 1.6: Depiction of common NHCs ligands used for the synthesis of NHC based palladium complexes.

In general, most palladium NHC complexes are believed to be disassembled or decomposed *in situ*, during the pre-activation stage to liberate highly active palladium(0) species. Hence, most organopalladium complexes serve as precursors for the active palladium catalyst. Astakhov et al. [62] recently did a study on the catalytic activity of a broad range of Pd-NHC catalytic systems. They discovered that the Pd-NHC's activity is predominantly determined by the cleavage of the metal–NHC bond, and the catalyst performance is strongly affected by the stabilization of the metal clusters that are formed *in situ* (Scheme 1.13).

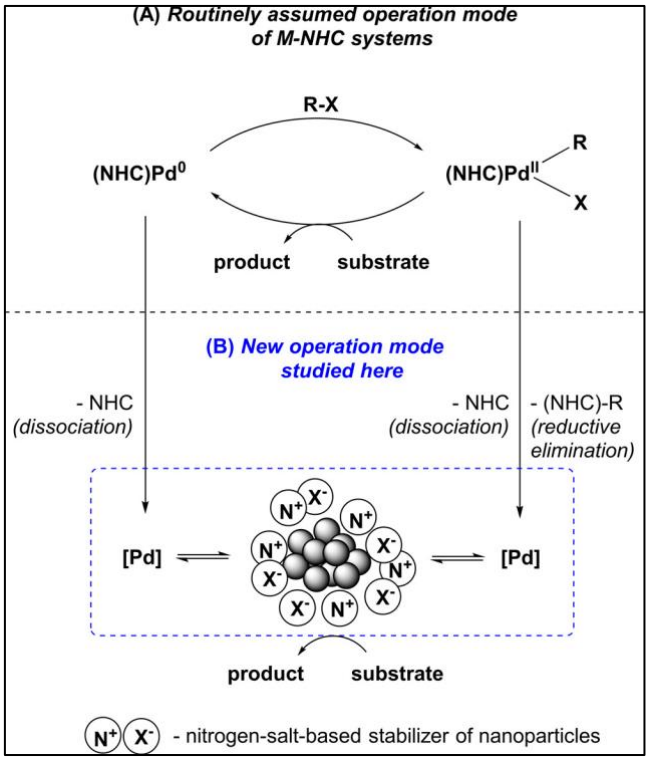

Scheme 1.13: Routinely assumed (A) and new (B) operation modes for palladium-NHC catalytic systems [62].

In their study, the formation of Pd nanoparticles was observed from a broad range of metal complexes with NHC ligands under standard Heck-Mizoroki reaction conditions (Scheme 1.13). A mechanistic analysis revealed two different pathways to connect palladium-NHC complexes to "cocktail" type catalysis: (i) Reductive elimination from a Pd(II) intermediate and the release of NHC-containing byproducts and (ii) dissociation of NHC ligands from palladium intermediates. Hence, the operational mode of most organopalladium complexes is still not clear, however, a combinational mode of operation (molecular and cocktail-type) might have to be assumed as an intrinsic feature for homogeneous systems that are catalysed by organopalladium complexes.

1.3.1.3 Palladacycles complexes

Palladacycles were introduced as new air and moisture stable precatalyst for Heck and Suzuki cross-coupling reactions by Beller et al. in 1995 [111]. Since then, palladacycles have been extensively used for a wide variety of cross coupling reactions [39, 71, 111-114]. The palladacycles appeared as long-sought structurally defined catalysts, promising a conservation of coordination shell during the catalytic action (Figure 1.8).

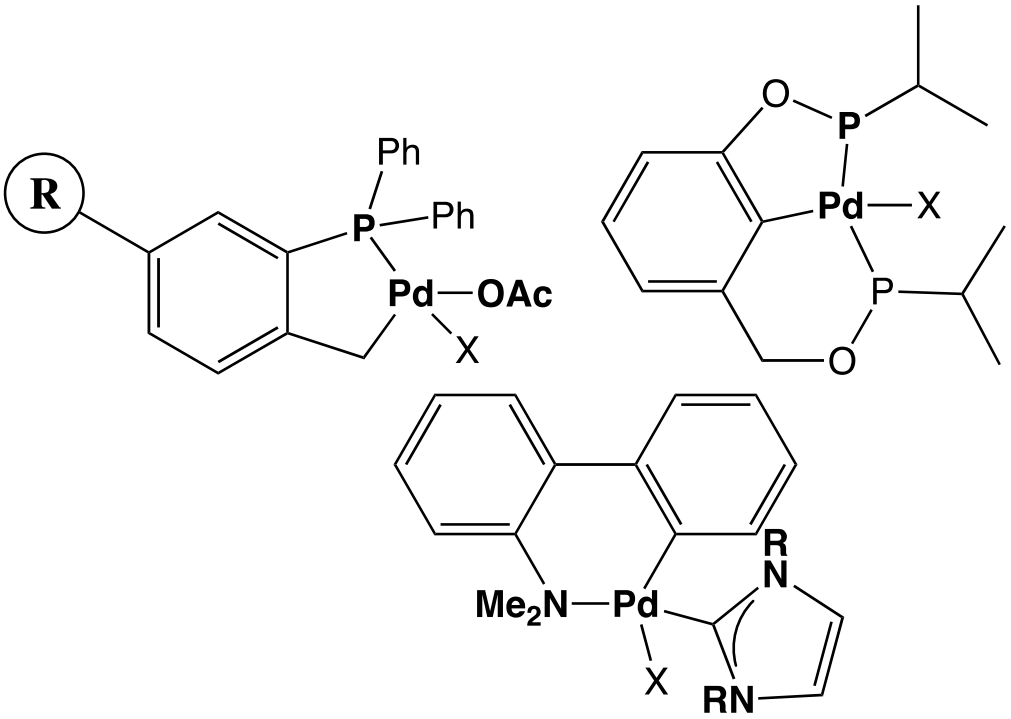

Figure 1.7: Depiction of common classes of palladacycles that are used in cross coupling reactions [114].

However, recent findings have demonstrated that palladacycles actually are not structurally robust catalysts, but are disassembled during the pre-activation stage and release either mono-phosphine or phosphine-free low-ligated Pd(0)

complexes [112]. Thus, there is a strong possibility that palladacycles also form part of a large class of Pd catalyst precursors, which loose their structural identity in the catalytic cycle.

1.4 Factors influencing the catalytic activity: Operating conditions

1.4.1 Reaction media

The palladium catalyzed C-C cross-coupling reactions can be carried out in wide variety of solvents, even though the reactions are media sensitive. Some cross-coupling reactions prefer solvents of low polarity and low Lewis basicity, while others prefer media of high polarity and high coordination capability [105]. Common solvents are N,N-dimethylformamide (DMF), dimethylacetamide (DMA), N-methylpyrrolidone (NMP), dimethylsulfoxide (DMSO), toluene, acetonitrile, tetrahydrofuran (THF), dioxane and ionic liquids [71]. More recently, a lot of attention has been paid to environmentally benign media, which include supercritical carbon dioxide, fluorous systems, solvent-free systems, water and aqueous systems. However, in most cases, the "solvent-free" conditions are actually not literally such, but are performed in media composed of substrates and often liquid amine base.

1.4.2 Reaction temperature

Temperature is a very important parameter in palladium catalyzed cross-coupling reactions; it controls the operation mode of catalytic systems. There are contradicting views on the role of temperature in literature [105]. In general, the reactivity of the catalyst is improved at elevated temperatures; at room temperature, the reaction may take days or weeks to go to completion. This is important since a lower rate of oxidative addition would result in the build-up of unsupported palladium(0) that leads to deactivation [71, 105]. In addition, high catalyst loadings are required in most cases if the reactions are performed at room temperature. However, in some cases the selectivity of the catalyst is suppressed at elevated temperature. Thus, the choice of the reaction temperature depends a lot on (i) the type of coupling reaction performed, (ii) and the desired outcomes of the reaction [71].

1.4.3 Substrate dependence

The limiting stage for the most cross-coupling catalytic cycles is the oxidative addition step. The nature of the halide group on the aryl halide influences the reaction rates in the following order: I > Br >> Cl [71, 105]. Thus, the aryl halides can be subdivided into very reactive (aryl iodides and electron-deficient aryl bromides), less reactive (all other aryl bromides and electron-deficient aryl chlorides) and very unreactive (all other aryl chlorides). Another type of

substrate dependence is a largely seen in Heck coupling reaction, where the degree of substitution and steric effect around the olefinic carbon determine the net results (yield and selectivity) [71, 105].

1.4.4 Bases

The palladium catalyzed C-C cross-coupling reactions doesn't take place in the absence of a base [35, 71]. The role of the base is not entirely clear, however, it is believed to play multiple roles in the coupling reactions. The base is believed to play a role in preactivation and reduction of palladium(II) precatalysts to form the active Pd(0) species. The base also stabilizes and prevents deactivation of palladium(0) in the form of weak labile ligands. It is also responsible for the regeneration of palladium(0) from the palladium(II) hydride intermediate through the reductive elimination step. The common bases that are used in C-C cross-coupling reactions include tertiary amines (triethylamine), and inorganic bases (acetates, carbonates, bicarbonates and phosphates) [35].

1.4.5 Additives

Additives are commonly used to stabilize the small clusters of palladium(0) that are formed *in situ*, and prevent their growth to palladium metal particles (deactivation by nucleation) [71, 105]. They do this by allocating palladium(0) species more time to enter the catalytic cycle through balancing the rate of palladium(0) formation, the rate of oxidative addition and the rate of nucleation of palladium particles. Common additives are tetraalkylammonium salts (*n*-Bu_4NBr, *n*-Bu_4NCl, Et_4NCl, $BnEt_3NBr$) [71, 105].

1.5 References

1. A. Suzuki, *Angewandte Chemie International Edition*, 50 (2011) 6722-6737.
2. C.C.C. Johansson Seechurn, A. DeAngelis, T.J. Colacot, *Introduction to New Trends in Cross-Coupling: New Trends in Cross-Coupling: Theory and Applications, The Royal Society of Chemistry*, 2015, pp. 1-19.
3. R. Bates, *Organic Synthesis Using Transition Metals, 2nd ed., John Wiley & Sons, Ltd, Chichester, United Kingdom*, 2012, pp. 1-455.
4. C.C.C. Johansson Seechurn, M.O. Kitching, T.J. Colacot, V. Snieckus, *Angewandte Chemie International Edition*, 51 (2012) 5062-5085.
5. J.P. Corbet, G. Mignani, *Chemical Reviews*, 106 (2006) 2651-2710.
6. T. Kohei, N. Miyaura, *Introduction to Cross-Coupling Reactions: Cross-Coupling Reactions: A Practical Guide, Springer Berlin Heidelberg, Berlin, Heidelberg*, 2002, pp. 1-9.
7. R. Jana, T.P. Pathak, M.S. Sigman, *Chemical Reviews*, 111 (2011) 1417-1492.
8. B.M. Rosen, K.W. Quasdorf, D.A. Wilson, N. Zhang, A.M. Resmerita, N.K. Garg, V. Percec, *Chemical Reviews*, 111 (2011) 1346-1416.

9. G. Evano, N. Blanchard, M. Toumi, *Chemical Reviews*, 108 (2008) 3054-3131.
10. A. Roglans, A. Pla-Quintana, M. Moreno-Mañas, *Chemical Reviews*, 106 (2006) 4622-4643.
11. D. Seyferth, *Organometallics*, 28 (2009) 1598-1605.
12. W. Chodkiewicz, *Annali Di Chimica*, 2 (1957) 69-819.
13. R.D. Stephens, C.E. Castro, *The Journal of Organic Chemistry*, 28 (1963) 3313-3315.
14. J. Tsuji, H. Takahashi, M. Morikawa, *Tetrahedron Letters*, 6 (1965) 4387-4388.
15. E.J. Corey, G.H. Posner, *Journal of the American Chemical Society*, 89 (1967) 3911-3912.
16. K. Tamao, K. Sumitani, M. Kumada, *Journal of the American Chemical Society*, 94 (1972) 4374-4376.
17. R.F. Heck, J.P. Nolley, *The Journal of Organic Chemistry*, 37 (1972) 2320-2322.
18. K. Sonogashira, Y. Tohda, N. Hagihara, *Tetrahedron Letters*, 16 (1975) 4467-4470.
19. A.O. King, N. Okukado, E. Negishi, *Journal of the Chemical Society*, *Chemical Communications*, (1977) 683-684.
20. D. Milstein, J.K. Stille, *Journal of the American Chemical Society*, 100 (1978) 3636-3638.
21. N. Miyaura, K. Yamada, A. Suzuki, *Tetrahedron Letters*, 20 (1979) 3437-3440.
22. Y. Hatanaka, T. Hiyama, *The Journal of Organic Chemistry*, 53 (1988) 918-920.
23. F. Paul, J. Patt, J.F. Hartwig, *Journal of the American Chemical Society*, 116 (1994) 5969-5970.
24. H. Tokuyama, S. Yokoshima, T. Yamashita, T. Fukuyama, *Tetrahedron Letters*, 39 (1998) 3189-3192.
25. L.S. Liebeskind, J. Srogl, *Journal of the American Chemical Society*, 122 (2000) 11260-11261.
26. A.F.P. Biajoli, C.S. Schwalm, J. Limberger, T.S. Claudino, A.L. Monteiro, *Journal of the Brazilian Chemical Society*, 25 (2014) 2186-2214.
27. H. Wan, X. Bai, *Huaxue Yu Nianhe*, 34 (2012) 48-54.
28. B.S. Kumar, R. Anbarasan, A.J. Amali, K. Pitchumani, *Tetrahedron Letters*, 58 (2017) 3276-3282.
29. S. Ghasemi, F. Farjadian, B. Tamami, *Applied Organometallic Chemistry*, 30 (2016) 818-822.
30. J.K. Stille, K.S.Y. Lau, *Accounts of Chemical Research,* 10 (1977) 434-442.
31. B.C. Barnard, *Platinum Metals Review*, 52 (2008) 38-45.
32. L. Xue, Z. Lin, *Chemical Society Reviews*, 39 (2010) 1692-1705.
33. C. Amatore, A. Jutand, *Accounts of Chemical Research*, 33 (2000) 314-321.
34. A. Jutand, *Mechanisms of the Mizoroki–Heck Reaction: The Mizoroki–Heck Reaction, John Wiley & Sons, Ltd, Chichester, United Kingdom*, 2009, pp. 1-45.
35. A. Tougerti, S. Negri, A. Jutand, *Chemistry – A European Journal*, 13 (2007) 666-676.
36. R. Chinchilla, C. Najera, *Chemical Society Reviews*, 40 (2011) 5084-5121.

37. R. Chinchilla, C. Nájera, *Chemical Reviews*, 107 (2007) 874-922.
38. K.C. Nicolaou, P.G. Bulger, D. Sarlah, *Angewandte Chemie International Edition*, 44 (2005) 4442-4489.
39. N.T.S. Phan, M. Van Der Sluys, C.W. Jones, *Advanced Synthesis & Catalysis*, 348 (2006) 609-679.
40. C. Torborg, M. Beller, *Advanced Synthesis & Catalysis*, 351 (2009) 3027-3043.
41. L. Yin, J. Liebscher, *Chemical Reviews*, 107 (2007) 133-173.
42. R.F. Heck, *Journal of the American Chemical Society*, 91 (1969) 6707-6714.
43. R.F. Heck, *Palladium-Catalyzed Vinylation of Organic Halides: Organic Reactions, John Wiley & Sons, Inc.*, 2004, pp. 345-390.
44. R.F. Heck, *Organic Reactions*, 27 (1982) 345-390.
45. R.F. Heck, *Journal of the American Chemical Society*, 85 (1963) 3383-3387.
46. R.F. Heck, Synlett, (2006) 2855-2860.
47. R.F. Heck, *Journal of the American Chemical Society*, 90 (1968) 5546-5548.
48. R.F. Heck, *Journal of the American Chemical Society*, 90 (1968) 5542-5546.
49. R.F. Heck, *Journal of the American Chemical Society*, 90 (1968) 5538-5542.
50. R.F. Heck, *Journal of the American Chemical Society*, 90 (1968) 5535-5538.
51. R.F. Heck, *Journal of the American Chemical Society*, 90 (1968) 5531-5534.
52. R.F. Heck, *Journal of the American Chemical Society*, 90 (1968) 5526-5531.
53. R.F. Heck, *Journal of the American Chemical Society*, 90 (1968) 5518-5526.
54. T. Mizoroki, K. Mori, A. Ozaki, *Bulletin of the Chemical Society of Japan*, 44 (1971) 581-581.
55. X.F. Wu, P. Anbarasan, H. Neumann, M. Beller, *Angewandte Chemie International Edition*, 49 (2010) 9047-9050.
56. H.A. Dieck, R.F. Heck, *The Journal of Organic Chemistry*, 40 (1975) 1083-1090.
57. P.E. Garrou, R.F. Heck, *Journal of the American Chemical Society*, 98 (1976) 4115-4127.
58. R.F. Heck, *Accounts of Chemical Research*, 12 (1979) 146-151.
59. J.B. Melpolder, R.F. Heck, *The Journal of Organic Chemistry*, 41 (1976) 265-272.
60. Y. Fujiwara, I. Moritani, S. Danno, R. Asano, S. Teranishi, *Journal of the American Chemical Society*, 91 (1969) 7166-7169.
61. I. Moritanl, Y. Fujiwara, *Tetrahedron Letters*, 8 (1967) 1119-1122.
62. A.V. Astakhov, O.V. Khazipov, A.Y. Chernenko, D.V. Pasyukov, A.S. Kashin, E.G. Gordeev, V.N. Khrustalev, V.M. Chernyshev, V.P. Ananikov, *Organometallics*, 36 (2017) 1981-1992.
63. I.P. Beletskaya, A.V. Cheprakov, *Modern Heck Reactions: New Trends in Cross-Coupling: Theory and Applications, The Royal Society of Chemistry*, 2015, pp. 355-478.
64. J. Magano, J.R. Dunetz, *Recent Large-Scale Applications of Transition Metal-Catalyzed Couplings for the Synthesis of Pharmaceuticals: New Trends in Cross-Coupling: Theory and Applications, The Royal Society of Chemistry*, 2015, pp. 697-778.
65. M. Picquet, *Platinum Metals Review*, 57 (2013) 272-280.
66. G. V. M. Sharma, P. R. Krishna, V. R. Doddi, S. Kashyap, P.S. Reddy, *Catalytic Organic Synthesis: A New Paradigm in Industrial Process Intensification:*

Industrial Catalysis and separations: Innovations for Process Intensification, Apple Academic Press, Boca Raton, Florida, 2015, pp. 329-375.
67. L. Cassar, *Journal of Organometallic Chemistry*, 93 (1975) 253-257.
68. Z. Dehbanipour, M. Moghadam, S. Tangestaninejad, V. Mirkhani, I. Mohammadpoor–Baltork, *Journal of Organometallic Chemistry*, 853 (2017) 5-12.
69. P. Veerakumar, P. Thanasekaran, K.L. Lu, K.C. Lin, S. Rajagopal, *ACS Sustainable Chemistry and Engineering*, 5 (2017) 8475-8490.
70. V.N. Mikhaylov, V.N. Sorokoumov, K.A. Korvinson, A.S. Novikov, I.A. Balova, *Organometallics*, 35 (2016) 1684-1697.
71. D.S. Rosa, F. Antelo, T.J. Lopes, N.F.d. Moura, G.R. Rosa, *Química Nova*, 38 (2015) 605-608.
72. D.D. Dolliver, B.T. Bhattarai, A. Pandey, M.L. Lanier, A.S. Bordelon, S. Adhikari, J.A. Dinser, P.F. Flowers, V.S. Wills, C.L. Schneider, K.H. Shaughnessy, J.N. Moore, S.M. Raders, T.S. Snowden, A.S. McKim, F.R. Fronczek, *The Journal of Organic Chemistry*, 78 (2013) 3676-3687.
73. K. Sonogashira, *Journal of Organometallic Chemistry*, 653 (2002) 46-49.
74. K. Sonogashira, *Palladium-Catalyzed Alkynylation: Sonogashira Alkyne Synthesis: Handbook of Organopalladium Chemistry for Organic Synthesis, John Wiley & Sons, Inc.*, 2002, pp. 493-529.
75. K. Sonogashira, *Cross-Coupling Reactions to sp Carbon Atoms: Metal-Catalyzed Cross-Coupling Reactions, Wiley-VCH Verlag GmbH*, 1998, pp. 203-229.
76. A. Bino, M. Ardon, E. Shirman, *Science*, 308 (2005) 234.
77. D. Mujahidin, S. Doye, *European Journal of Organic Chemistry*, 2005 (2005) 2689-2693.
78. D.X. Wang, H. Booth, N. Lerner-Marmarosh, T.S. Osdene, L.G. Abood, *Drug Development Research*, 45 (1998) 10-16.
79. S. Frigoli, C. Fuganti, L. Malpezzi, S. Serra, *Organic Process Research & Development*, 9 (2005) 646-650.
80. N. Miyaura, A. Suzuki, *Chemical Reviews*, 95 (1995) 2457-2483.
81. N. Miyaura, A. Suzuki, *Journal of the Chemical Society, Chemical Communications*, (1979) 866-867.
82. A. Suzuki, *Pure and Applied Chemistry*, 63 (1991) 419-422.
83. A. Suzuki, *Journal of Organometallic Chemistry*, 576 (1999) 147-168.
84. N. Miyaura, T. Yanagi, A. Suzuki, *Synthetic Communications*, 11 (1981) 513-519.
85. S.R. Chemler, D. Trauner, S.J. Danishefsky, *Angewandte Chemie International Edition*, 40 (2001) 4544-4568.
86. N. Miyaura, K. Yamada, H. Suginome, A. Suzuki, *Journal of the American Chemical Society*, 107 (1985) 972-980.
87. T. Ishiyama, S. Abe, N. Miyaura, A. Suzuki, *Chemistry Letters*, 21 (1992) 691-694.
88. M. Manuel, J.S. César, R. José Rafael, *Current Organic Chemistry*, 16 (2012) 1128-1150.
89. C. Amatore, A. Jutand, G. Le Duc, *Chemistry – A European Journal*, 17 (2011) 2492-2503.
90. B.H. Lipshutz, T.B. Petersen, A.R. Abela, *Organic Letters*, 10 (2008) 1333-1336.

91. G.B. Smith, G.C. Dezeny, D.L. Hughes, A.O. King, T.R. Verhoeven, *The Journal of Organic Chemistry*, 59 (1994) 8151-8156.
92. G.C. Fortman, S.P. Nolan, *Chemical Society Reviews*, 40 (2011) 5151-5169.
93. N. Hazari, P.R. Melvin, M.M. Beromi, *Nature Reviews Chemistry*, 1 (2017) 0025.
94. S. Thapa, B. Shrestha, S.K. Gurung, R. Giri, *Organic & Biomolecular Chemistry*, 13 (2015) 4816-4827.
95. F. Zhou, Q. Cai, *Beilstein Journal of Organic Chemistry*, 11 (2015) 2600-2615.
96. S.Z. Tasker, E.A. Standley, T.F. Jamison, *Nature*, 509 (2014) 299-309.
97. G. Cahiez, A. Moyeux, *Chemical Reviews*, 110 (2010) 1435-1462.
98. C. Gosmini, J.M. Begouin, A. Moncomble, *Chemical Communications*, 0 (2008) 3221-3233.
99. T.L. Mako, J.A. Byers, *Inorganic Chemistry Frontiers*, 3 (2016) 766-790.
100. A. Guérinot, J. Cossy, *Topics in Current Chemistry*, 374 (2016) 49.
101. Z. Gonda, G.L. Tolnai, Z. Novák, *Chemistry – A European Journal*, 16 (2010) 11822-11826.
102. A. Del Zotto, D. Zuccaccia, *Catalysis Science & Technology*, 7 (2017) 3934-3951.
103. M. Pagliaro, V. Pandarus, R. Ciriminna, F. Béland, P. Demma Carà, *ChemCatChem*, 4 (2012) 432-445.
104. A. Corma, H. Garcia, *Topics in Catalysis*, 48 (2008) 8-31.
105. Irina P. Beletskaya, A.V. Cheprakov, *Focus on Catalyst Development and Ligand Design: The Mizoroki–Heck Reaction, John Wiley & Sons, Ltd, Chichester, United Kingdom,* 2009, pp. 51-118.
106. U. Christmann, R. Vilar, *Angewandte Chemie International Edition*, 44 (2005) 366-374.
107. V.P. Ananikov, D.G. Musaev, K. Morokuma, *Organometallics*, 24 (2005) 715-723.
108. C. Baillie, L. Zhang, J. Xiao, *The Journal of Organic Chemistry*, 69 (2004) 7779-7782.
109. S. Würtz, F. Glorius, *Accounts of Chemical Research*, 41 (2008) 1523-1533.
110. J.M. Collinson, J.D.E.T. Wilton-Ely, S. Diez-Gonzalez, *Catalysis Communications*, 87 (2016) 78-81.
111. M. Beller, H. Fischer, W.A. Herrmann, K. Öfele, C. Brossmer, *Angewandte Chemie International Edition*, 34 (1995) 1848-1849.
112. V. Sable, K. Maindan, A.R. Kapdi, P.S. Shejwalkar, K. Hara, *ACS Omega*, 2 (2017) 204-217.
113. F.T. Luo, C. Xue, S.L. Ko, Y.D. Shao, C.J. Wu, Y.M. Kuo, *Tetrahedron*, 61 (2005) 6040-6045.
114. I.P. Beletskaya, A.V. Cheprakov, *Journal of Organometallic Chemistry*, 689 (2004) 4055-4082.

Chapter 2

Recent developments in palladium catalysed heterogeneous C-C cross-coupling reactions

The aim of this chapter is to give an overview of recent developments in heterogeneous palladium catalysed C-C cross-coupling reactions. Selected examples of palladium immobilised on various classes of supports and their application in C-C cross-coupling reactions are reviewed.

2.1 Introduction: Towards heterogeneous catalysis

Homogeneous and heterogeneous catalyses are usually studied separately, with minor intersections between the researchers from each field [1]. The popularity of heterogeneous catalysis is motivated by cost-efficient industrial applications, while the high selectivity needed in organic synthesis facilitated the evolution of homogeneous catalysts [1]. Despite the high activity and selectivity of homogeneous catalysts, the use of heterogeneous catalytic systems has been favoured, and this is chiefly because of the practical advantages of heterogeneous systems, which include easy separation of the catalyst from the products and reusability of the catalyst in successive reactions (Scheme 2.1) [2]. However, on the basis of sustainable development and the unprecedented complexity of the molecules required for new materials in pharmaceutical research, the only conclusion is that neither homogeneous nor heterogeneous catalysis alone can achieve the aim of developing a highly active, selective and recyclable catalyst [1-3]. Thus, the search or development of a "superior catalyst" requires convergence of both catalysis in order to combine the stability and easy recyclability of the heterogeneous catalysts with the high activity and selectivity of the homogeneous catalysts.

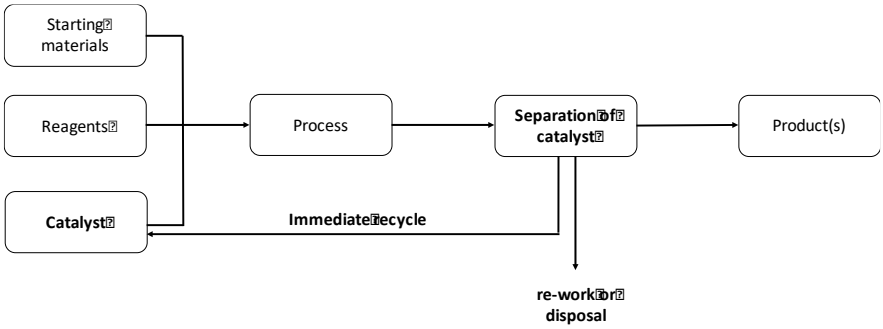

Scheme 2.1: A general flow diagram of a catalytic process.

The challenge of using a homogeneous catalyst is that it requires costly and relatively lengthy multistep procedures to separate it from the reaction mixtures, and usually the catalyst is deactivated during work-up. In addition, homogeneous catalysts have a greater chance of contaminating the desired products with the residual metal. These are significant drawbacks, since they pose a severe problem for large-scale synthesis, especially in the pharmaceutical industry where the palladium contamination levels have to be below 5 ppm (Table 2.1) [2, 4]. There are generally two alternative approaches to homogeneous catalysis; the first one includes the development of ultra-low catalyst loading systems that make recovery of the metal unnecessary for many purposes. This minimizes both the cost and contamination problems. The second approach involves the heterogenization of homogeneous catalysts to take advantage of the easy recovery of the palladium catalyst from the reaction mixture by simple decantation or filtration. The development of recoverable and recyclable catalysts that minimize metal contamination of the products is a crucial issue in view of a hypothetical scale-up of the catalytic process at industrial level [5].

Table 2.1: Maximum acceptable concentration limits for the residues of metal catalysts that can be present in a pharmaceutical products [2]. [Reproduced with permission from John Wiley and Sons]

Metal	Concentration (ppm)	
	Oral	Parenteral
Pd, Pt, Ir, Rh, Ru, Os	**5**	**0.5**
Mo, V, Ni, Cr	10	1.0
Cu, Mn	15	1.5
Zn, Fe	20	2.0

This chapter briefly reviews recent developments in palladium based heterogeneous catalytic systems that catalyse C-C cross-coupling reactions. The common heterogeneous cross coupling reactions mainly differ in (i) chemical nature (organic, inorganic, or hybrid organic-inorganic) of the solid matrix entrapping the Pd catalyst, and (ii) the nature of the catalyst attachment (chemical or physical entrapment). There are also examples of efficient catalysts for cross coupling reactions based on colloidal palladium particles. The usefulness of the developed catalytic system is usually determined by its activity, selectivity and the life-time of the catalyst [6]. The catalytic activity is essentially a measure of percentage of reactants that are converted to product(s); while, the catalytic selectivity is a measure of the percentage of the reactants that are converted to useful or desired product(s). The life-time of a catalyst is the time that the catalyst will maintain the required level of activity and selectivity [6]. The life-time of the catalyst can also be estimated by the number of times it can be recovered and reused. Lastly, the efficiency of a catalytic process is measured in turnover number (TON) and turnover frequency (TOF). The TON indicates the

number of turns or cycles a catalyst does within the catalytic cycle before it is deactivated (Eq 1.1); while, the TOF is simply the TON per unit time (Eq 1.2).

$$TON = \frac{moles\ of\ product}{moles\ of\ catalyst} \tag{1.1}$$

$$TOF = \frac{TON}{time} \tag{1.2}$$

In the following discussion, the catalytic properties discussed above will be used to judge the efficiency of the selected examples of most common palladium catalysed heterogeneous catalytic systems for cross-coupling reactions. The aim of the discussion is not to be exhaustive but rather to report on recent and intersting research progress aimed at developing heterogeneous palladium based catalytic systems.

2.2 Classes of heterogeneous palladium catalysts employed in cross-coupling reactions

The heterogenization of homogeneous catalysts by incorporation into an inorganic support or an organic polymer is currently one of the hottest research topics [7]. However, the "true nature" of the active catalyst is still unclear and debatable [2]. The following discussion will look at recent successes in the development of heterogeneous catalytic systems for C-C cross-coupling reactions. To provide a consistent view, the examples in the discussion below are based on Suzuki and Heck cross coupling reactions only.

2.2.1 "Naked" palladium nanoparticles as precatalysts.

Palladium nanoparticles have become one of the most interesting forms of heterogeneous catalysts because of their size- and shape-dependence, as well as their efficient catalytic activities in cross-coupling reactions (Scheme 2.2) [1, 8]. The "naked" palladium nanoparticles are the simplest form of heterogenoues catalyst for C-C cross-coupling reactions, and they can be separated from the reaction mixture (with varying success) by filtration or centrifugation and reused several times [8, 9]. Despite their great contributions though, it is still relatively hard to recover and recycle them, while preventing their deactivation during work-up. The "naked" palladium nanoparticles can also agglomerate or sinter upon heating, leading to formation of insoluble non-catalytic palladium black [8]. Hence, their use is still limited.

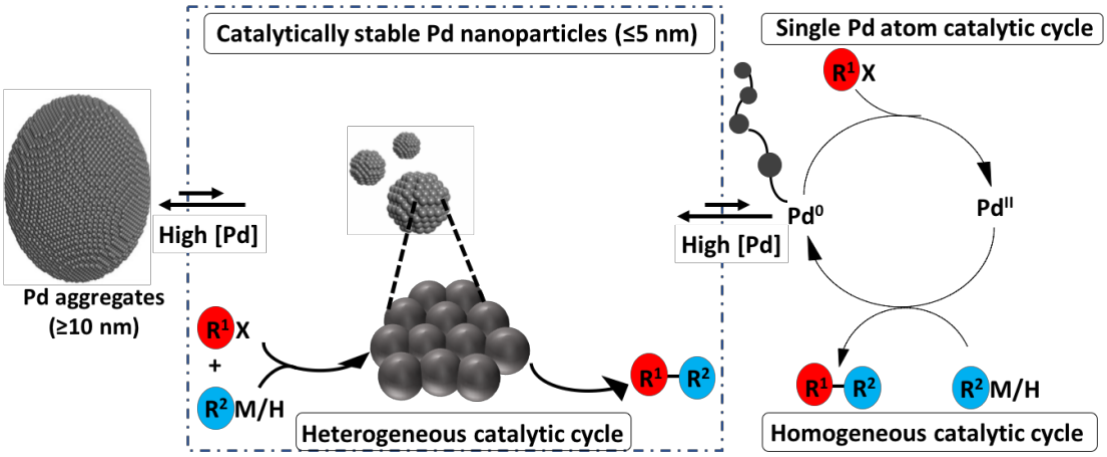

Scheme 2.2: Possible reaction pathways operating in Pd nanoparticle catalysed Suzuki and Heck cross-couplings [1]. [Adapted from reference [1]].

Consequently, supported palladium nanoparticles as catalyst for C-C cross-coupling reactions are being developed. Most often, palladium nanoparticle become less catalytically active upon immobilisation on a solid support. Therefore, there is still a gap between "naked" and immobilized palladium nanoparticle catalysts; thus, an improved catalytic system with desirable aspects of both systems (high activity and easy recovery) is needed. It is envisaged that better understanding of the reactivity of palladium nanoparticle can lead to design of more efficient heterogenoues catalyst for C-C cross-coupling reactions. Hence, the study of "naked" palladium nanoparticle is still relevent.

2.2.2 Palladium nanoparticles supported on carbonaceous supports

Palladium supported on activated carbon and carbon nanotubes has been widely applied in C-C cross-coupling reactions (Scheme 2.3). Palladium on activated carbon (Pd/C) is by far the most often used catalyst in heterogeneous Pd-catalyzed coupling reactions because of its efficiency and commercial availability [4]. It can be purchased in various quantities with a palladium content ranging from 1-20%. Generally, the Pd/C catalyst can convert a large variety of substrates with good to excellent yields, and it is recoverable and recyclable over many cycles [4].

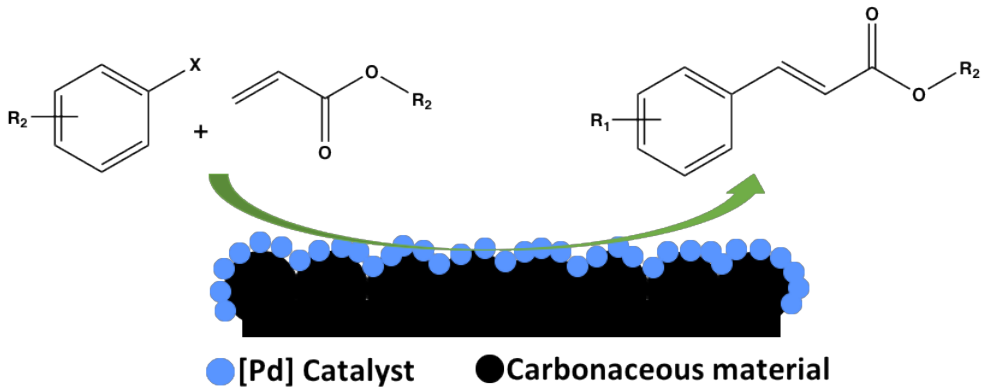

Scheme 2.3: Schematic illustration of palladium nanoparticles supported on carbonaceous material as efficient catalyst for C-C cross-coupling reactions [10]. [Adapted from reference [10]]

Jadhav et al. recently (2016) developed a greener, cost effective and operationally convenient Pd/C based catalytic system for Suzuki and Heck cross-coupling reactions [11]. In their setup, the Pd/C catalyst was dispersed in an aqueous hydrotropic medium (sodium xylene sulphonate solution) that had surfactant like properties and thus stabilised the Pd/C catalyst (Figure 2.1).

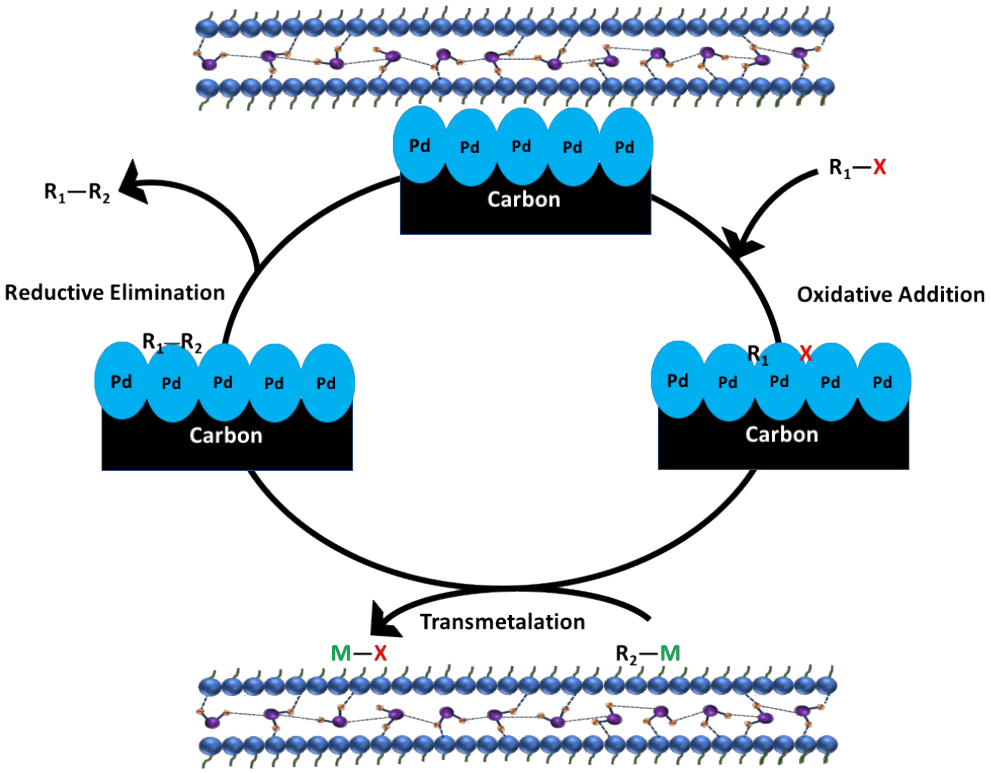

Figure 2.1: Plausible mechanism of the C-C bond forming reactions in the presence of a hydrotrope (sodium xylene sulphonate solution) [11]. [Adapted from reference [11]]

The hydrotropism allows for easy solubility of several types of organic functionalities in water, without the need for toxic and volatile organic co-solvent. In addition, good to excellent yields of the desired product were

obtained and the catalytic system was recycled three times without any significant loss in activity. Lastly, they reported that the palladium metal was "not leached" out into the product solution. Hence, this system is highly desirable from economical as well as environmental points of view.

Carbon nanotubes (CNTs) have emerged as highly efficient supports for palladium and they have been extensively used as alternatives to activated carbon supports [10, 12-14]. The CNTs can be evenly distributed in solution due to their small size, thus increasing interaction between the reactants and the catalyst. In most cases, the activity of CNTs in C-C cross-coupling reactions depends on their preparation method [14]. In a recent review by Labulo et al., a wide range of surface functionalization techniques for carbon nanotubes that improve their properties as catalyst supports was reported (Scheme 2.4) [13]. The resulting CNTs catalysts displayed superior catalytic performance and better recyclability in C-C cross-coupling reactions.

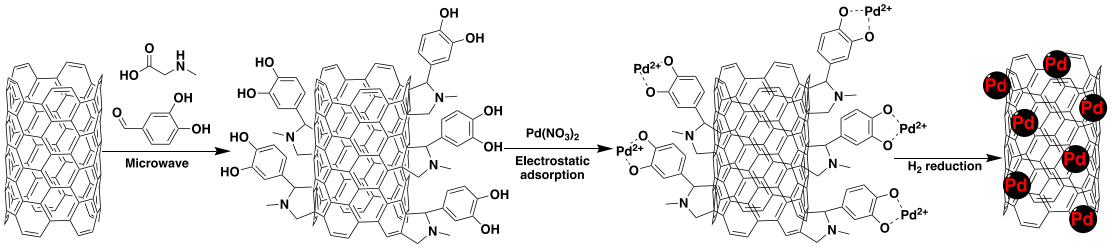

Scheme 2.4: Graphical representation of Pd nanoparticles supported on carbon nanotubes [13]. [Adapted from reference [13]]

Lakshminarayana et al. [10] extended the study by investigating the influence of various carbonaceous materials as supports in C-C cross-coupling reactions. They prepared and studied palladium oxide (PdO) nanoparticles impregnated on nanocarbon supports, such as single walled carbon nanotubes (SWCNT), multiwalled carbon nanotubes (MWCNT), carbon nanofiber (CNF), graphene oxide (GO) and reduced graphene oxide (RGO) [10]. The prepared catalysts were characterized fully and then explored in Heck cross-coupling reactions to assess their catalytic activity. Graphene oxide (GO) was found to be the best support for PdO (Table 2.2). The enhanced catalytic activity of PdO/GO was believed to be due to the combined effect of a high degree of surface-bound oxygenated moieties, high surface area, electron conductivity and the mesoporous nature of graphene oxide.

Table 2.2: Performance of PdO supported carbon materials on Heck coupling reaction [10]. [Reproduced with permission from John Wiley and Sons]

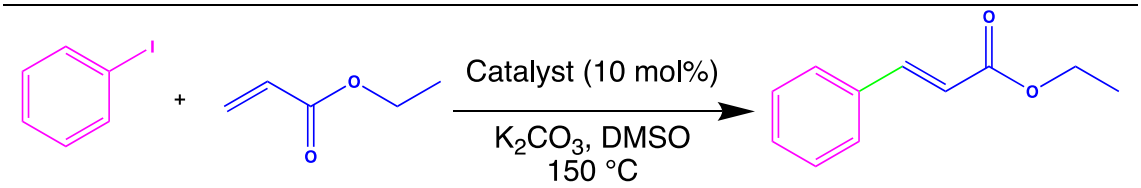

Catalyst	Reaction time (min)	Yield (%)	TOF (h^{-1})
PdO/SWCNT	20	72	939
PdO/MWCNT	15	63	1080
PdO/CNF	40	38	274
PdO/GO	5	80	4144
PdO/RGO	90	68	194

2.2.3 Palladium nanoparticles supported on metal oxides

A significant number of researchers have devoted themselves to finding a new and a more efficient Pd/M_xO_y based heterogeneous catalyst for C-C cross-coupling reactions [15, 16]. In this direction, Köhler and co-worker prepared and comparatively studied the catalytic activity of Pd/Al_2O_3, Pd/TiO_2, Pd/NaY and Pd/CeO_2 [17]. The catalysts were able to efficiently catalyse Suzuki cross-coupling reactions and the obtained TOFs for each catalyst were: Pd/Al_2O_3 = 9600 h^{-1}, Pd/TiO_2 = 9700 h^{-1}, Pd/NaY =4100 and Pd/CeO_2 = 4100 h^{-1}. The Pd/Al_2O_3 and Pd/TiO_2 catalysts showed very similar and high catalytic activities, while the activities of Pd/NaY and Pd/CeO_2 were much lower. The TOF values of Pd/NaY and Pd/CeO_2 catalysts are almost half of those obtained with Pd/Al_2O_3 and Pd/TiO_2. These results clearly suggest that the nature of the support has a great influence on the activity of the catalyst.

In addition, Köhler et al. stated that the Pd concentration in solution during the reaction correlated clearly with the progress of the reaction (Figure 2.2). Thus, this clearly suggests that the dissolved molecular palladium represents the "true" catalytically active species, and the prepared Pd/M_xO_y solids are simply precursors to the "true catalyst". Furthermore, they found that the dissolved "Pd is deposited back" onto the support at the end of the reaction. This phenomenon is commonly referred to as the palladium "release-capture or dissolution-redeposition" mechanism [18].

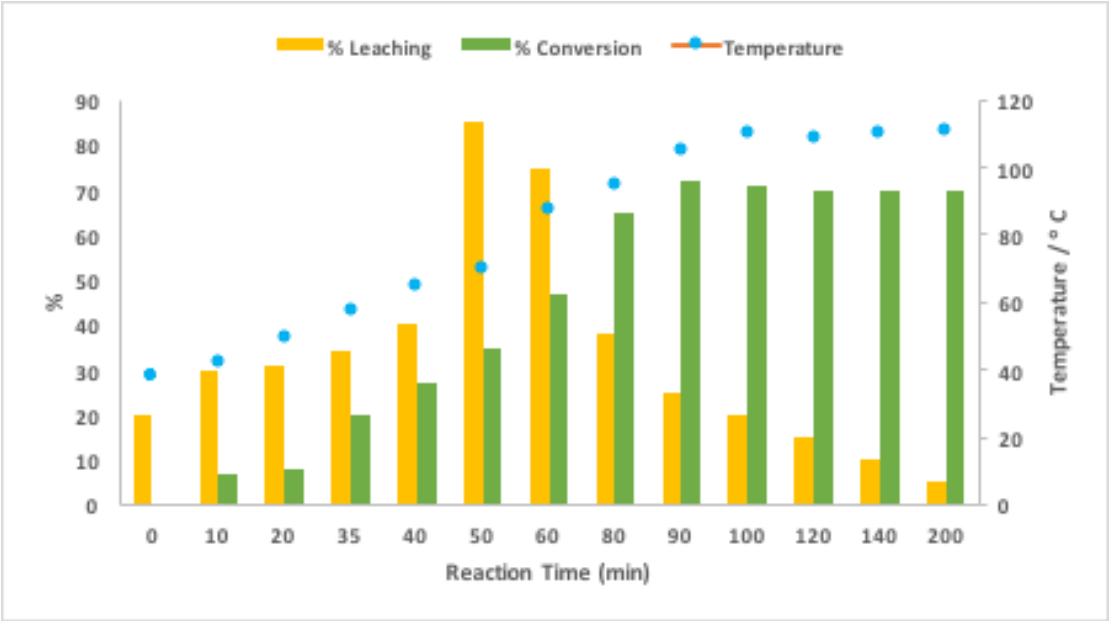

Figure 2.2: Time-dependent correlation of palladium leaching with the progress of the reaction [17]. [Adapted from reference [17]].

In 2013, Amoroso et al. [19] extended the study of Köhler and co-workers [17] to examine the catalytic activity of Pd/M_xO_y type catalysts in more detail. More specifically, they wanted to investigate the influence of the "point of zero charge" on the catalytic activity of the Pd/M_xO_y type catalysts. The point of zero charge (PZC) is commonly used in surface science to determine the ability of a given solid material to adsorb ions. This concept describes the condition when the electrical charge density on a surface of a solid is zero [20].

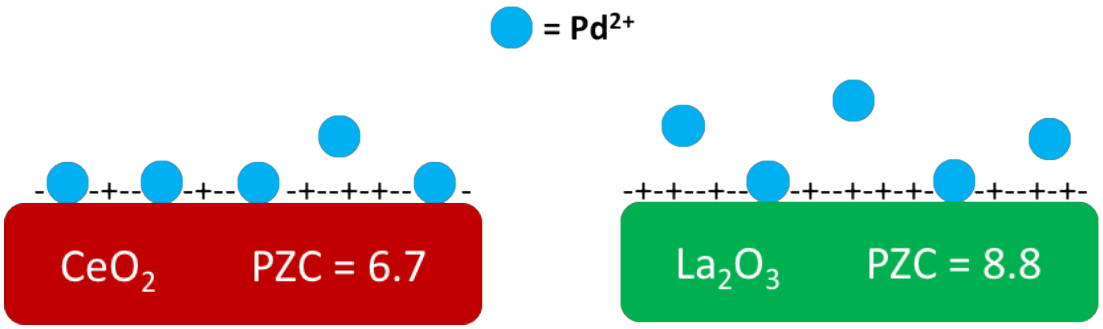

Figure 2.3: Representation of adhesion and release of Pd^{2+} from CeO_2 and La_2O_3 surfaces under catalytic conditions (pH ~10.5) [22]. [Adapted from reference [22]]

Generally, the PZC is represented as the pH value at which a solid submerged in an electrolyte exhibits zero net electrical charge on the surface [20, 21]. A given metal oxide (M_xO_y) surface will have a "positive charge" at solution pH values less than the PZC value and thus be a surface on which anions may adsorb. On the other hand, *the metal oxide surface will have a negative charge at solution pH values greater than the PZC value and thus be a surface on which cations may*

adsorb [20, 21]. The later statement is more relevant to the current discussion since the pH of the reaction mixture in most cross-coupling reactions is around 10, thus it is above the PZC values of the investigated metal oxide supports (Figure 2.3). This allows one to investigate the degree of adhesion of palladium onto the support, which in turn speaks to the observed catalytic activity and the degree of palladium leaching.

Table 2.3: The physicochemical properties of the synthesised Pd/M_xO_y based catalysts and their catalytic activity results [19]. [Reproduced with permission from Springer Nature]

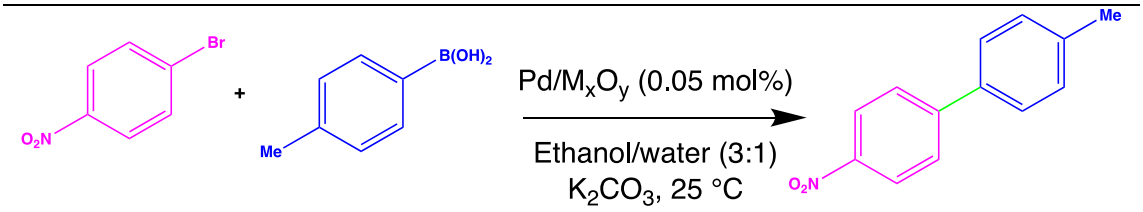

Compound (Pd/M_xO_y)	Pd loading (wt%)	Surface area (m^2/g)	Pore volume (cm^3/g)	PZC (pH)	Time (min)	TOF (h^{-1})
Pd/La_2O_3	1.76	16.6	0.24	8.8	13	9130
Pd/CeO_2	1.93	31.5	0.18	6.7	260	450
Pd/Pr_6O_{11}	1.93	22.4	0.36	7.8	17	6980
Pd/Sm_2O_3	1.84	11.9	0.21	7.4	21	5650
Pd/Gd_2O_3	1.99	10.2	0.09	7.5	20	5940

Hence, Amoroso et al. [19] used the PZC values of each support to investigate the role it plays in the adhesion of the palladium nanoparticle onto the surface of the support (Figure 2.3). Thus, they prepared and investigated the catalytic activity of Pd/La_2O_3, Pd/Pr_6O_{11}, Pd/Gd_2O_3, Pd/Sm_2O_3 and Pd/CeO_2 catalysts. The physicochemical properties of these materials are tabulated in Table 2.3. The study revealed that under basic reaction conditions (pH~10.5), the surfaces of metal oxides with high PZC values are less negatively charged than the surfaces of metal oxides with low PZC values. Thus, the La_2O_3 support has the lowest density of negatively charged sites on the surface since it has the highest PZC value. Hence, the higher reactivity of Pd/La_2O_3 is correlated to a marked degree of Pd^{2+} leaching from the surface of La_2O_3, favoured by its less negatively charged surface. On the contrary, the lowest activity observed with Pd/CeO_2 is correlated to the higher degree of negatively charged surface that helps in keeping Pd^{2+} ions anchored onto the support (Figure 2.3).

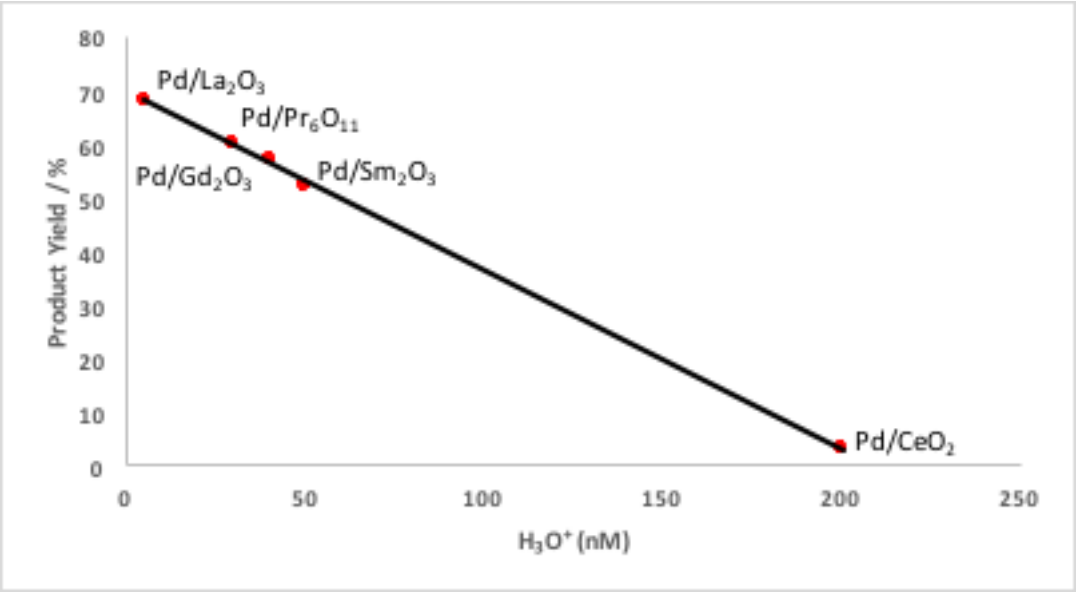

Figure 2.4: Cross-coupling reaction yield (after 2 min of reaction) vs. proton molar concentration (10^{-PZC}) for Pd/M_xO_y [19]. [Adapted from reference [19]]

Figure 2.4 further shows that there is a linear correlation between the yield of the coupling product and the PZC ($[H_3O^+] = 10^{-PZC}$) value of the metal oxide support. Thus, the observed reactivity trend over the M_xO_y support is related to the tendency of each Pd/M_xO_y system to deliver different amounts of palladium into the solution. In summary, the above discussion shows that there is a close relation between the "surface charge" (correlated to the PZC value) and the extent of palladium leaching at the pH of catalysis (determined by reaction conditions). Thus, the more positively charged is the surface (this is the case of Pd/La_2O_3), the more consistently Pd leaches, and therefore, a higher reaction rate is observed. In addition, a much slower reaction is observed when Pd/CeO_2 is used as the catalyst, which shows the lowest PZC value within the series of Pd/M_xO_y. Consequently, prolonged recycling is possible in the case of Pd/CeO_2 due to minimal palladium leaching. Thus, from the studied series of Pd/M_xO_y type catalysts, Pd/CeO_2 was chosen as superior precatalyst based on the following considerations: (i) It can be recycled several times without a significant decrease of activity (prolonged recyclability), and (ii) the organic product is sparsely contaminated since there is minimal leaching of palladium into the solution.

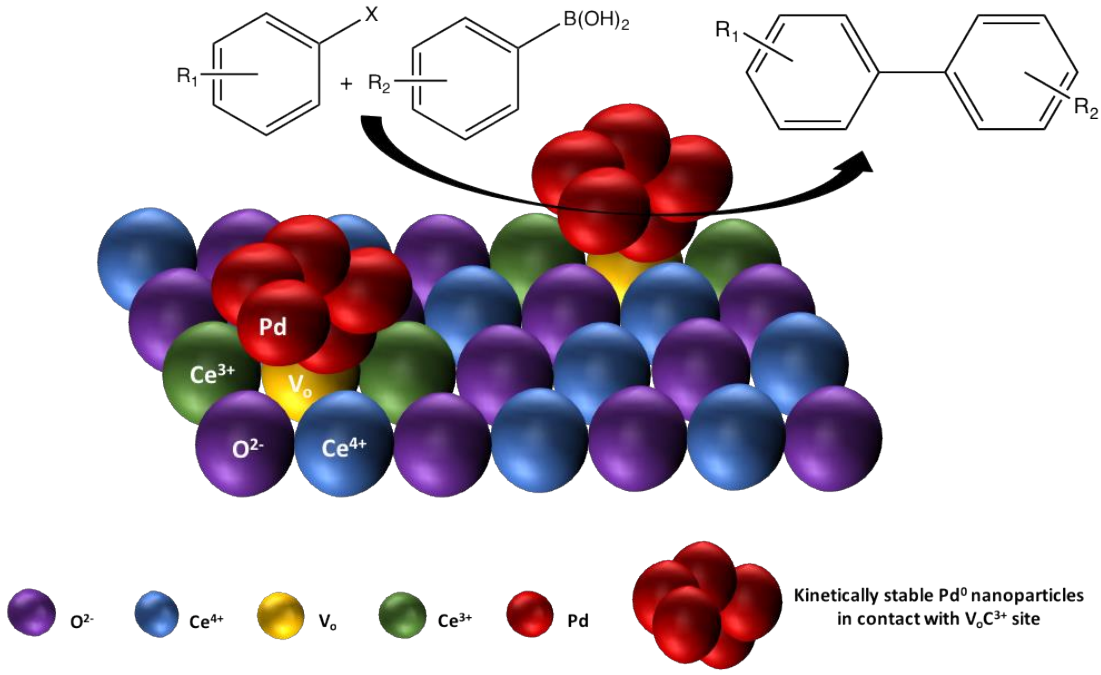

Figure 2.5: Plausible heterogeneous catalytic reaction mechanism suggested for Suzuki cross-coupling over the Pd/$CeZrO_{4-\delta}$ redox catalyst [30]. [Adapted from reference [30]].

Alternatively, the physicochemical properties of the support can be enhanced through substitution of a foreign metal ion in its lattice structure [23]. The substitution of foreign metal ions into the lattice of reducible oxides such as CeO_2 and TiO_2 to form ionic solid-solution oxides ($Ce_{1-x}M_xO_{2-\delta}$ or $Ti_{1-x}M_xO_{2-\delta}$) has given materials which show extraordinarily high activity for a variety of catalytic reactions, especially in gas-phase oxidation reactions [23-29]. However, such catalysts have rarely been applied to C-C cross-coupling reactions. Recently, Burange and co-workers reported that the ionic ceria-zirconia ($CeZrO_{4-\delta}$) solid-solution oxides exhibit high redox properties and thermal stability that make them better catalyst supports than the pure metal oxide counterparts [30]. Hence, $CeZrO_{4-\delta}$ solid-solution oxide was used to immobilise palladium nanoparticles and the resultant catalyst (Pd/$CeZrO_{4-\delta}$) was explored in Suzuki cross-coupling reactions (Figure 2.5). The mechanistic investigation proved that the redox couple (Ce^{4+}/Ce^{3+}) in the $CeZrO_{4-\delta}$ support enhances the catalytic activity through creation of oxygen vacancies. Furthermore, the support displayed strong metal-support (Pd-$CeZrO_{4-\delta}$) interactions and hence, "no leaching" was observed. Thus, it was concluded that the reactions were "truly" heterogeneous [30].

Lichtenegger and co-workers [31] extended Burange et al. [30] study by directly incorporating palladium ions into the lattice of the support (ceria), instead of modifying the properties of the support with a foreign metal. In their study, they used CeO_2 and SnO_2 as supports and prepared a series of corresponding ionic solid-solution oxides: $Ce_{0.99}Pd_{0.01}O_{2-\delta}$, $Ce_{0.79}Sn_{0.2}Pd_{0.01}O_{2-\delta}$, $Ce_{0.495}Sn_{0.495}Pd_{0.01}O_{2-\delta}$,

$Ce_{0.20}Sn_{0.79}Pd_{0.01}O_{2-\delta}$, and $Sn_{0.99}Pd_{0.01}O_{2-\delta}$. These catalysts were thoroughly explored in Suzuki coupling reactions of phenylboric acid with various bromoarenes (Figure 2.6). The $Ce_{0.79}Sn_{0.2}Pd_{0.01}O_{2-\delta}$, $Ce_{0.20}Sn_{0.79}Pd_{0.01}O_{2-\delta}$ and $Sn_{0.99}Pd_{0.01}O_{2-\delta}$ catalysts showed extraordinarily high activities in Suzuki cross-coupling reactions, while the binary solid-solution oxide $Ce_{0.99}Pd_{0.01}O_{2-\delta}$ proved to be the least active catalyst. Thus, the Sn containing catalysts were shown to be more active; however, the results do not show a clear correlation between Sn loadings and the catalytic activity. Furthermore, complete conversion was achieved in five subsequent reactions for all catalysts, except when $Ce_{0.99}Pd_{0.01}O_{2-\delta}$ and $Ce_{0.495}Sn_{0.495}Pd_{0.01}O_{2-\delta}$ were used.

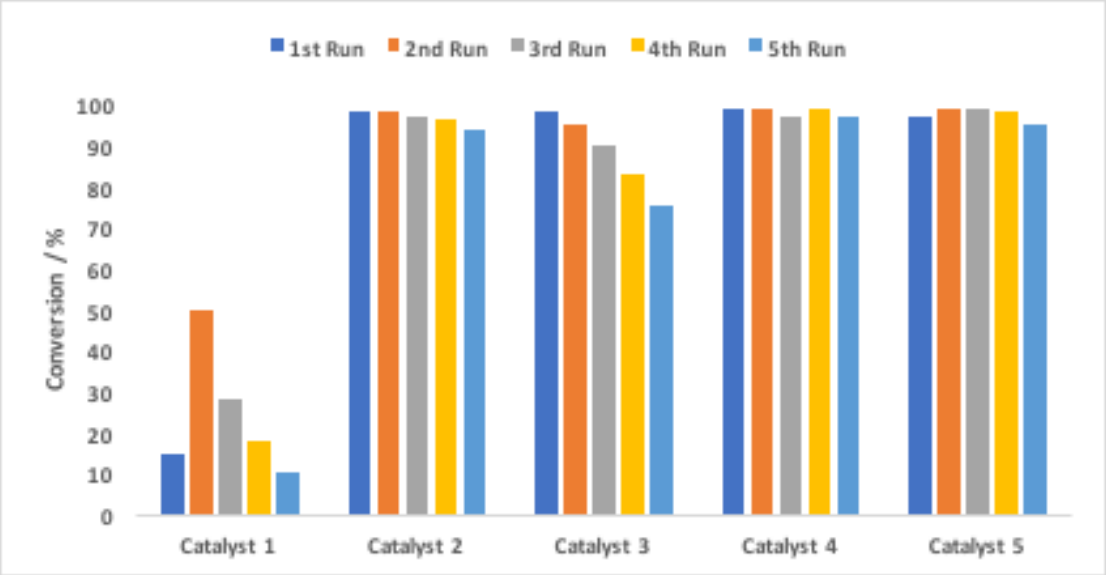

Figure 2.6: The Suzuki coupling of 4-bromotoluene with phenylboronic acid (after 30 minutes) using 0.5 mol% Pd. Cat 1: $Ce_{0.99}Pd_{0.01}O_{2-\delta}$**, Cat 2:** $Ce_{0.79}Sn_{0.2}Pd_{0.01}O_{2-\delta}$**, Cat 3:** $Ce_{0.495}Sn_{0.495}Pd_{0.01}O_{2-\delta}$**, Cat 4:** $Ce_{0.20}Sn_{0.79}Pd_{0.01}O_{2-\delta}$**, Cat 5:** $Sn_{0.99}Pd_{0.01}O_{2-\delta}$ **[31]. [Adapted from reference [31]].**

Thorough catalyst leaching, recovery and recyclability studies were conducted and the results demonstrate a clear correlation between reactivity and amount of leached palladium (Figure 2.7). Hence, these findings also support the hypothesis that the coupling reaction is actually catalyzed by small amounts of leached palladium via a homogeneous reaction mechanism. Thus, the synthesised catalysts are simply precatalysts that act as a palladium reservoir for the active palladium species. Hence, it was concluded that the observed high recyclability of the catalysts could be attributed to a Pd release-capture mechanism, as discussed earlier.

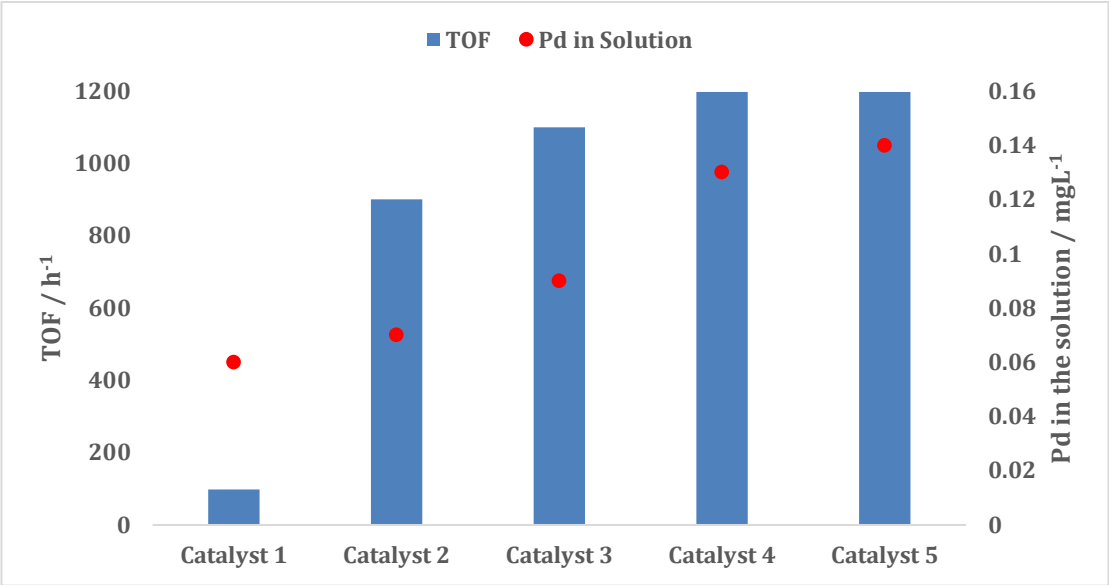

Figure 2.7: TOF vs. Pd-concentration in the solution (Pd leached). Cat 1: $Ce_{0.99}Pd_{0.01}O_{2-\delta}$**, Cat 2:** $Ce_{0.79}Sn_{0.2}Pd_{0.01}O_{2-\delta}$**, Cat 3:** $Ce_{0.495}Sn_{0.495}Pd_{0.01}O_{2-\delta}$**, Cat 4:** $Ce_{0.20}Sn_{0.79}Pd_{0.01}O_{2-\delta}$**, Cat 5:** $Sn_{0.99}Pd_{0.01}O_{2-\delta}$ **[31]. [Adapted from reference [31]].**

2.2.4 Palladium nanoparticle immobilised on magnetic supports

Recent studies show that magnetic nanoparticles are excellent supports for various catalysts [32-39]. There are four different categories for magnetic nanoparticles, namely: metals (Fe, Co, Ni), alloys (FePt, FePd), metal oxides (FeO, Fe_2O_3, Fe_3O_4), and ferrites ($CoFe_2O_4$, $CuFe_2O_4$). Amongst the four categories of magnetic nanoparticles, iron oxides have attracted the most attention because they have stronger magnetic properties and they can be synthesized easily by co-precipitation methods [40]. Supported palladium magnetic catalysts have the benefits of easy recovery and reuse after the completion of the reactions; because the catalyst can be easily separated from the reaction media by application of an external magnetic field [35]. Magnetic separation obviates the requirement of catalyst filtration or centrifugation after the completion of reactions, and provides a practical technique for recycling the magnetized catalysts (Figure 2.8) [34, 35].

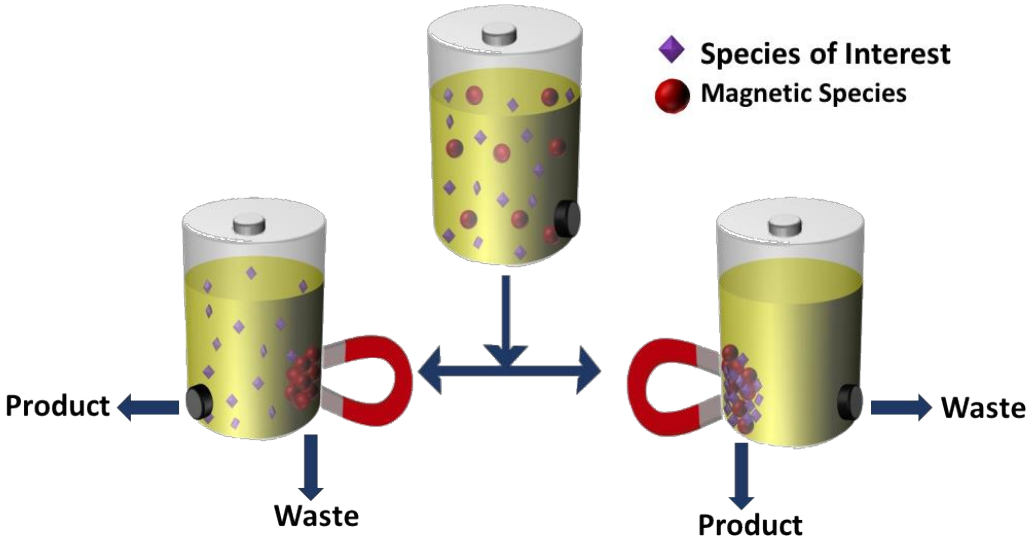

Figure 2.8: Examples of the use of magnetic separation through the application of an external magnetic field [41]. [Adapted from reference [41]].

A growing number of these magnetic supports have been applied in the development of magnetically recoverable palladium based heterogeneous catalysts for C-C cross-coupling reactions. Nasrollahzadeh and co-workers have explored the application of Pd/Fe_3O_4 magnetic nanoparticles as an efficient catalyst for C-C cross-coupling reactions [42]. The Pd/Fe_3O_4 magnetic catalyst was found to be stable during the Suzuki coupling reaction and good to excellent yields (83-95%) were obtained over a wide range of substrates. At the end of the Suzuki reaction the catalyst was recovered by the application of an external magnet, and successively reused (five times) without significant loss of activity.

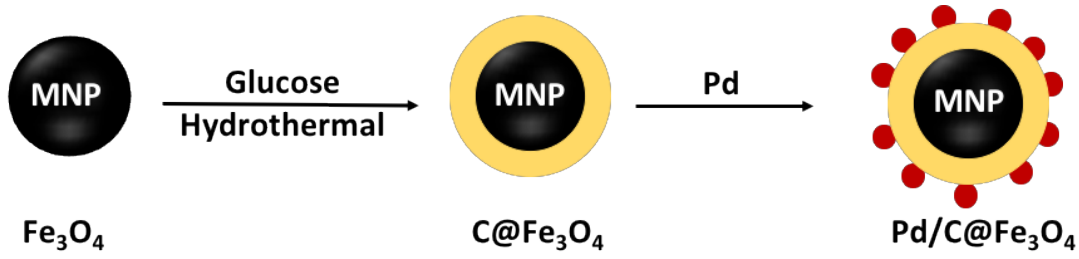

Figure 2.9: Schematic illustration of synthesis steps for $C@Fe_3O_4$ core-shell nano-spheres.

Although the bare or "naked" iron oxide nanoparticles have been shown as efficient supports for cross-coupling reactions, the immobilization of palladium directly on the iron oxide occasionally suffers from aggregation or surface oxidation. The oxidation and agglomeration of magnetic nanoparticles results in the loss of their magnetism, thus it is crucial to develop efficient strategies to strengthen their chemical stability [38]. In this regard, a wide range of stabilizing or coating materials, including organic stabilizers (polymers and surfactants) and inorganic stabilizers (silica and carbon materials), have been used to protect

magnetic nanoparticles (Figure 2.9) [38, 43]. In this direction, Kumar et al. [44] developed efficient C@Fe_3O_4 magnetic core-shell nano-sphere by coating the Fe_3O_4 nanoparticle with a carbon shell to protect them from being corrupted or oxidized under cross-coupling reaction conditions. Palladium was then immobilised on the synthesized C@Fe_3O_4 magnetic core-shell to form a structurally stable Pd/C@Fe_3O_4 catalyst (Figure 2.10). This catalyst was efficiently used as a heterogeneous catalyst for Heck cross-coupling reactions and good to excellent yields were obtained. The catalyst was easily separated from the reaction mixture through application of an external magnet and the catalyst was reused five times without any significant drop in activity. The authors claim that this catalytic system is "truly heterogeneous" even though some leaching was observed. They concluded that their catalytic system is advantageous because of its heterogeneity, high stability, gram scale applicability, magnetic separability and consequent reusability [44].

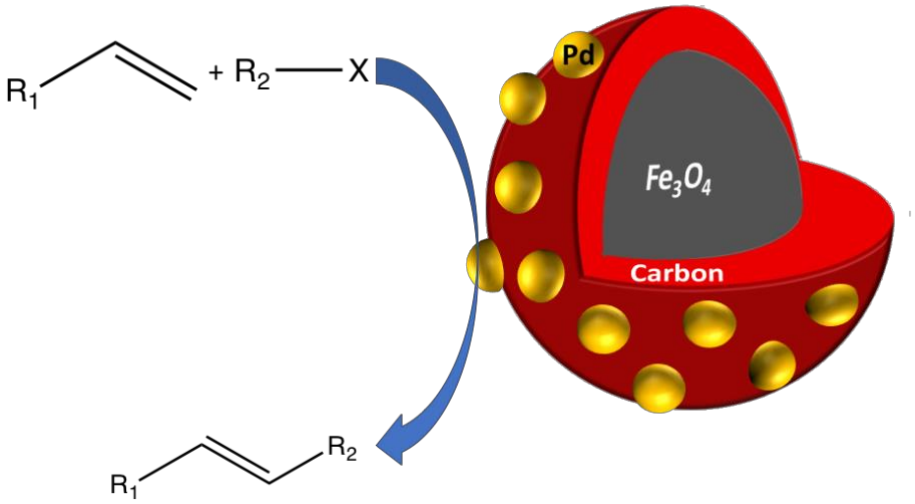

Figure 2.10: Graphical illustration of Pd/C@Fe_3O_4 catalysed cross-coupling reactions [44]. [Adapted from reference [44]].

The coated magnetic nanoparticles can be further modified by functionalising their surface with various functional groups (Figure 2.11). The functionalization of the surface of magnetic nanomaterials is an important step in the design of supported catalysts, because it significantly improves the physical and chemical properties of the magnetic supports [41].

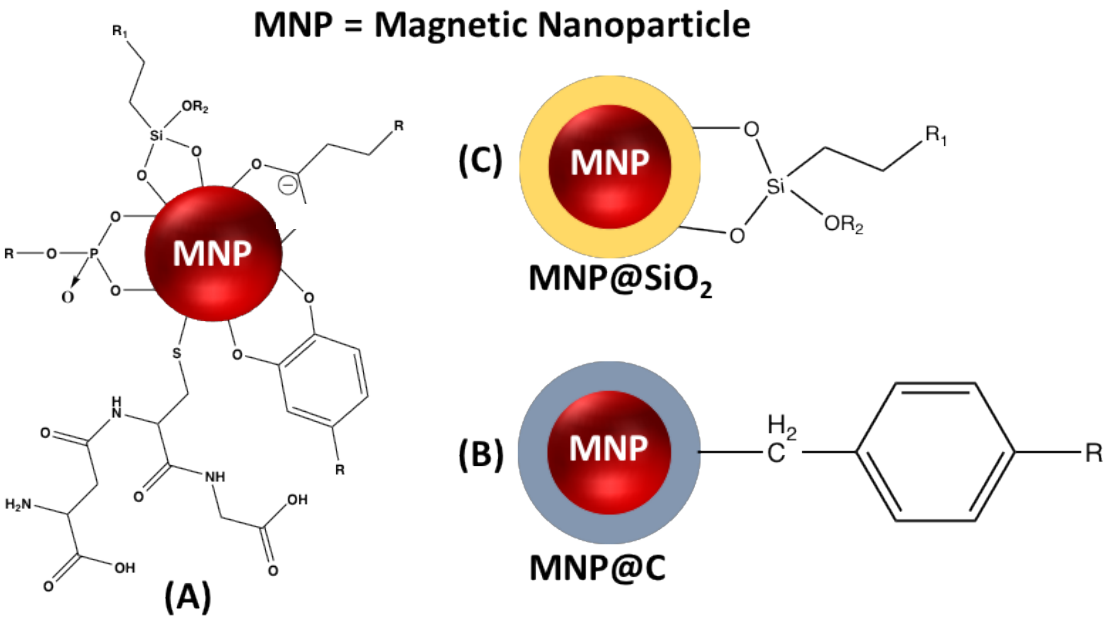

Figure 2.11: Different approaches to functionalize magnetic nanoparticles (MNPs): (A) iron oxide MNPs; (B) silica-coated MNPs and (C) carbon-coated MNPs [41]. [Adapted from reference [41]].

Heidari and co-worker [45] used isoniazide to functionalize the surface of the $Fe_3O_4@SiO_2$ magnetic nano-support (Figure 2.12). The isoniazide groups were used as linkers to immobilize palladium nanoparticles and prevent agglomeration on the surface of the $Fe_3O_4@SiO_2$ magnetic nano-support [45].

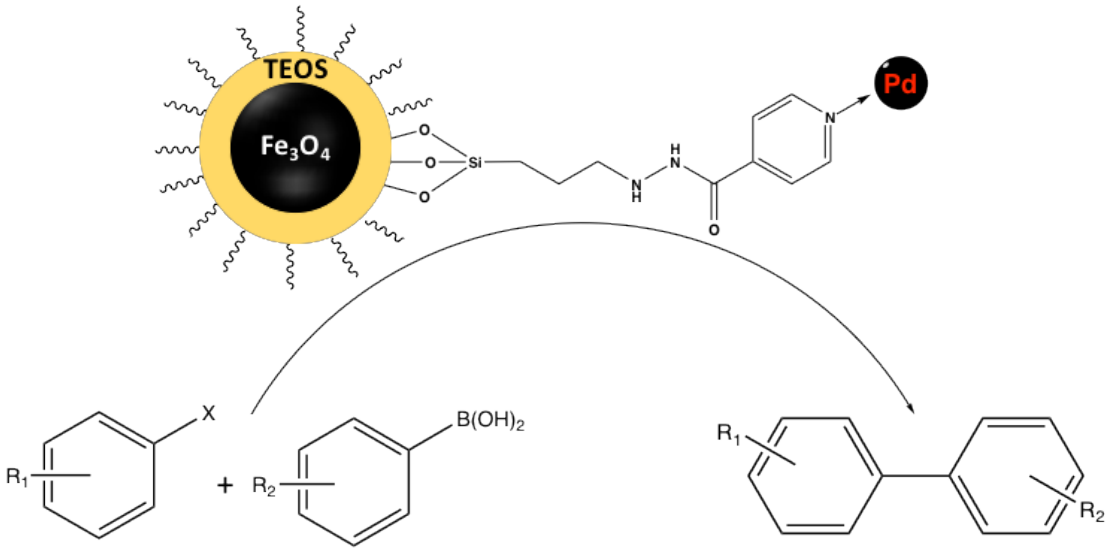

Figure 2.12: $Fe_3O_4@SiO_2$/isoniazide/Pd mediated Suzuki cross-coupling reaction [45]. [Adapted from reference [45]].

The resulting material, $Fe_3O_4@SiO_2$/isoniazide/Pd catalyst, was explored as a heterogeneous catalyst in Suzuki coupling reactions and good to excellent yields were obtained. The authors reported that the beneficial features of their system

include its generality, high efficiency and straightforward reusability of the heterogeneous catalyst through use of a magnet.

An interesting but slighly different approach was reportded by Khalili and co-workers [12], who supported palladium nanoparticles on an amino-vinyl silica functionalized magnetic carbon nanotube (CNT). Their core–shell contains CNT@Fe_3O_4@SiO_2-Pd in which the functionalized SiO_2 helps with stabilization of Pd nanoparticles and is also responsible for the reduction of Pd(II) to Pd(0) without the need for adding external reducing agents (Figure 2.13). This catalyst was sucesfully applied to Heck and Suzuki cross-coupling reactions and high yields were obtained. In addition, the catalyst exhibited good recyclability, and was used for six consecutive recycles without a significant loss in catalytic activity.

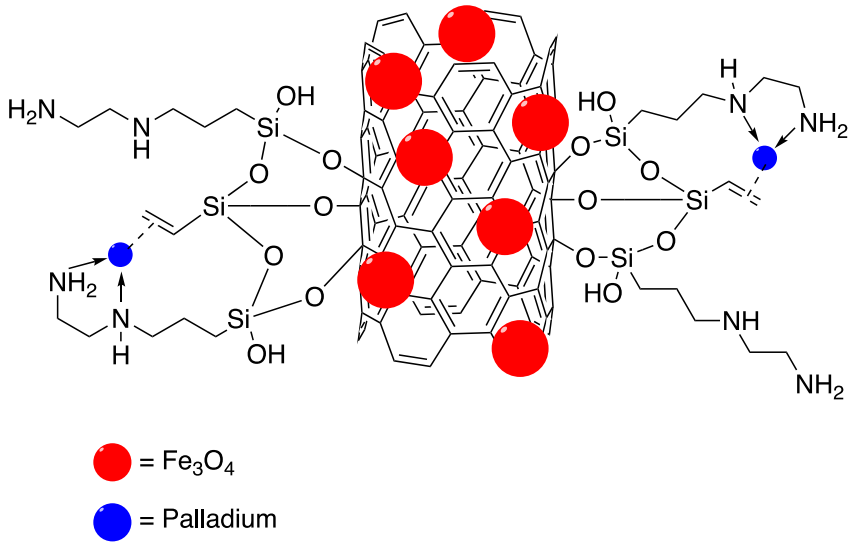

Figure 2.13: A graphical illustration of the CNT@Fe_3O_4@SiO_2-Pd catalyst [12]. [Adapted from reference [12]].

There are also numerous examples where organopalladium complexes, instead of palladium nanoparticles, have been immobilised on magnetic supports [46, 47]. Recently, Collinson and co-workers [46] prepared a [(NHC)Pd(allyl)Cl] complex, bearing an *N*-heterocyclic carbene (NHC) and immobilised it on silica-coated magnetic nanoparticles (Scheme 2.5). Their strategy tries to combine the high activity of palladium–NHC catalysts with the facile separation and recyclability of a heterogeneous catalyst. The catalyst was then explored on Suzuki coupling reactions and good to excellent yields were obtained with a variety of substrates. However, the immobilised palladium complex could not be reused because the catalyst was disassembled or decomposed under Suzuki coupling reaction conditions. The recycled catalyst only achieved 20% yield compared to the 90% yield that was obtained in its first use. The authors

suspected that the base was responsible for the detachment of the magnetic silica linker.

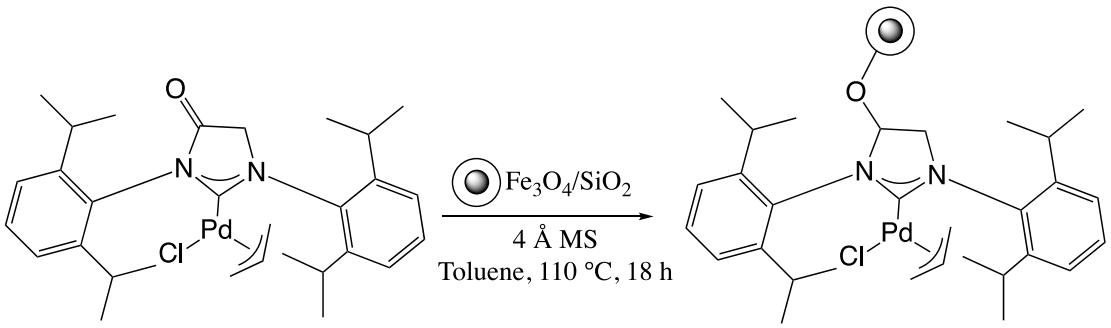

Scheme 2.5: Immobilisation of the [(NHC)Pd(allyl)Cl] complex on silica-coated magnetic nanoparticles [46]. [Adapted from reference [46]].

Better results were obtained by Fareghi-Alamdari et al. [47] who supported bis(*N*-heterocyclic carbene) palladium complex on silica coated magnetic nanoparticles (Figure 2.14).

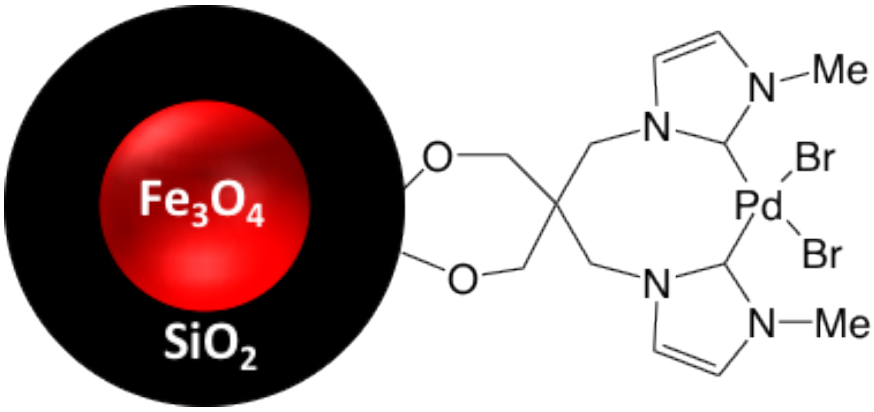

Figure 2.14: bis(*N*-heterocyclic carbene) palladium complex supported on silica coated magnetic nanoparticles [47]. [Adapted from reference [47]].

Their catalyst was efficiently used for Suzuki coupling reactions and at the end of the reaction, it was separated though application of an external magnet and recycled for six consecutive times. Hence, it not easy to identify the reaction parameters that caused the Collinson and co-workers [46] catalytic system to be unrecyclable because the reaction conditions are different (Table 2.4). However, the most obvious difference is the choice of the base; Collinson and co-workers used NaOH, which is very harsh, while Fareghi-Alamdari et al. used K_2CO_3. Hence, optimisation of reaction conditions is crucial in developing efficient and more robust catalytic systems.

Table 2.4: The reaction conditions for Suzuki cross-coupling reactions catalysed by supported palladium complexes in references [65] and [66].

	Reaction conditions		
	Solvent	Base	Temperature (°C)
Collinson et al. [46]	Isopropanol	NaOH	60
Fareghi-Alamdari et al. [47]	DMF/H_2O	K_2CO_3	80

In summary, the literature survey shows that remarkable progress has been made regarding the activity and recyclability of magnetic nanoparticle-based catalytic systems. However, thorough leaching and recyclability tests are still needed for most reported magnetic catalytic systems to unequivocally confirm that the magnetic palladium supported catalysts are responsible for the observed catalytic activity and not the leached material [35].

2.2.5 Polymer supported palladium nanoparticles

Literature reports have repeatedly shown that palladium nanoparticles can be efficiently supported on polymer frameworks [48-55]. Recently, Nemygina and co-workers immobilised various palladium precursors ($PdCl_2$, $PdCl_2(CH_3CN)_2$, and $PdCl_2(PhCN)_2$) on amino-functionalized hyper-crosslinked polystyrene [56]. They then evaluated the influence of palladium oxidation state (Pd(II) or Pd(0)) on the rate of Suzuki cross-coupling of 4-bromoanisole and phenylboronic acid. Their results revealed that the catalyst impregnated with a $PdCl_2(CH_3CN)_2$ precursor resulted in better catalytic activity (Scheme 2.6). The $PdCl_2(CH_3CN)_2$ precursor was believed to be more active because it experienced less hydrolysis and precipitation in comparison with $PdCl_2$ and $PdCl_2(PhCN)_2$ under Suzuki coupling reaction conditions. Lastly, they observed that unreduced, Pd(II) containing precatalyst were more active [56].

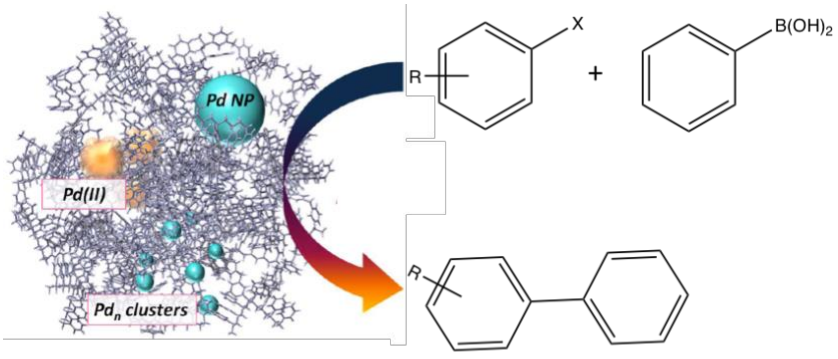

Scheme 2.6: Catalysts of Suzuki cross-coupling based on functionalized hyper-crosslinked polystyrene [56]. [Adapted from reference [56]].

Another interesting strategy for immobilising palladium on a polymer was reported by Li and co-workers [57], who synthesised a robust and flexible cellulose sponge using a dual-cross-linking cellulose nanofiber (CNF) with γ-glycidoxypropyltrimethoxysilane (GPTMS) and polydopamine (PDA) (Scheme 2.7). The characterisation results revealed that the palladium nanoparticles were homogeneously dispersed on the surface of the cellulose nanofiber with a narrow size distribution. The catalyst was successfully applied to heterogeneous Suzuki and Heck cross-coupling reactions. Leaching of palladium was negligible and the catalysts could be conveniently separated from the products and reused [57].

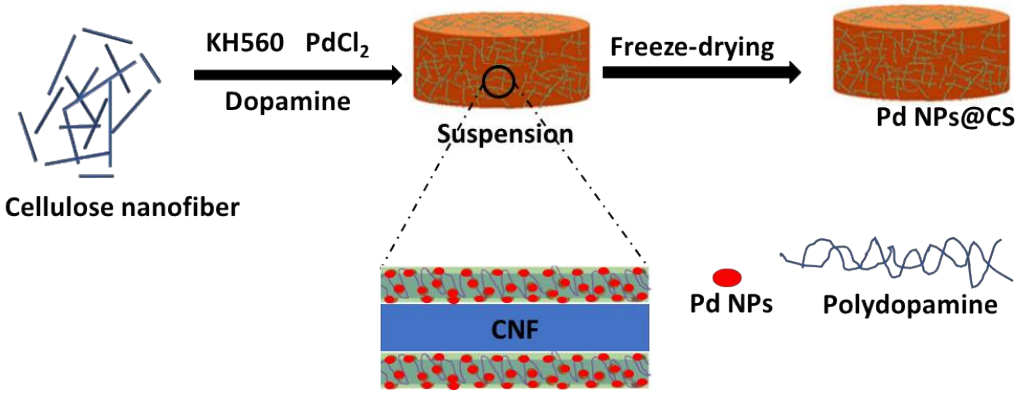

Scheme 2.7: Schematic of the stepwise formation of cellulose sponge supported palladium nanoparticles [57]. [Adapted from reference [57]].

2.2.6 Palladium nanoparticles immobilized on hybrid inorganic-organic material

The hybrid inorganic–organic materials are crystalline systems in which both inorganic and organic structural elements co-exist within a single phase [58]. These hybrid inorganic–organic materials are gaining popularity in cross-coupling reactions due to their tunable pore size, high surface areas, high crystallinity, and structural diversity [59-65]. Most hybrid inorganic–organic materials are synthesised through functionalization of the support surface with appropriate functional groups. This allows for a better control of the dimensions, dispersion and stability of the palladium nanoparticles. Metal-organic frameworks (MOFs) are one of the most popular classes of hybrid inorganic–organic materials and they are frequently explored as suitable palladium supports in heterogeneous cross-coupling reactions. For example, Shaikh and co-workers [66] used a zeolitic imidazolate framework (ZIF) to develop robust ZIF-supported palladium nanoparticles as a heterogeneous catalyst for Heck cross-coupling reactions (Figure 2.15). The Pd/ZIF catalyst was found to be highly efficient and could be re-used up to four times without any loss in catalytic efficiency [66].

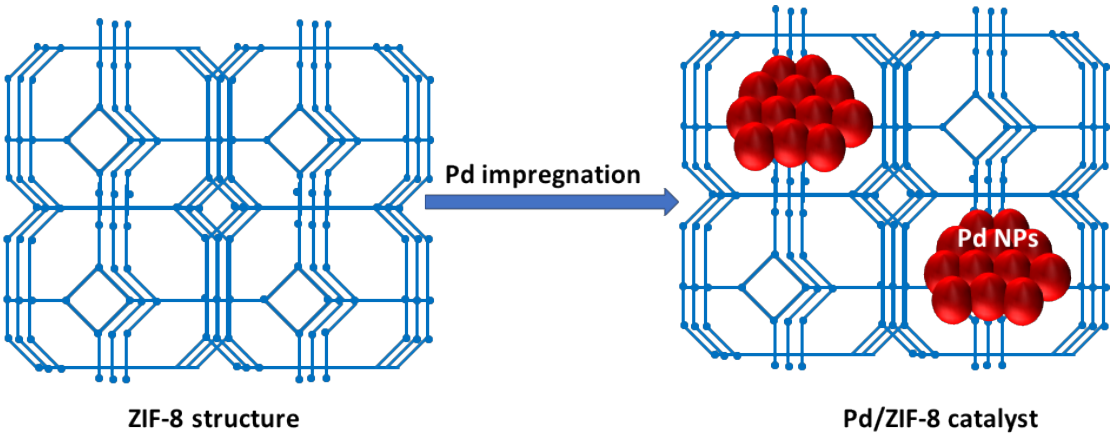

Figure 2.15: Graphical illustration of the Pd/ZIF-8 catalyst.

Another interesting example was reported by Kozell et al. [67] who immobilised palladium nanoparticles on zirconium phosphate glycine diphosphonate nanosheets (ZPGly). The immobilization of palladium nanoparticles on ZPGly nanosheets provided a stable catalyst with high palladium content (up to 22 wt %). This Pd@ZPGly-15 catalyst proved to be highly efficient in catalysing Suzuki and Heck cross-couplings reactions. Suprisingly, the authors reported that their catalytic system operates as an efficient "heterogeneous" system, even though 3-5 ppm of palladium leached (Table 2.5). In addition, a "release and catch" mechanism was proposed in which soluble active palladium species are released from the solid Pd@ZPGly-15 catalyst during the oxidative addition of the halide and then re-deposited on the ZPGly support as a consequence of the reductive elimination step at the end of the reaction [67].

Table 2.5: Suzuki cross-coupling reaction between 4-bromo benzene and phenylboric acid catalysed by Pd@ZPGly-15 catalyst [67].

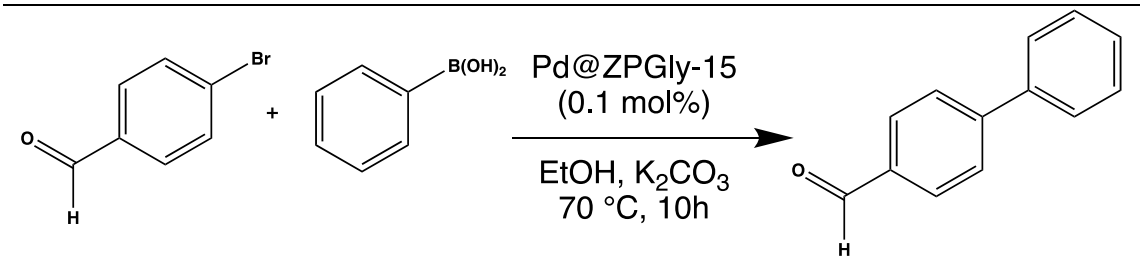

Entry	Yield (%)	Pd Leaching (ppm)
Run 1	98	5
Run 2	98	3
Run 3	98	3

A magnetically separable version of a hybrid organic-inorganic support was recently reported by Omar and co-workers [68]. They supported palladium on magnetically separable organic-silica hybrid nanoparticles that were functionalized with ionic liquid groups (Figure 2.16). The presence of ionic liquid

groups within the framework of the hybrid nanoparticles enhanced the stability of the palladium nanoparticles on the organic-silica nanoparticles. The resultant Pd/MNP@IL-SiO_2 catalyst was efficiently applied in Heck and Suzuki cross-coupling reactions and it demonstrated high catalytic activity (Figure 2.16). The Pd/MNP@IL-SiO_2 catalyst was also easily separated from the reaction mixture by application of an external magnetic field and the catalyst could be recycled over five times without a significant loss in its catalytic activity. In conclusion, the authors envisaged that this and similar catalytic systems could pave a way for the desired bridging of homogeneous and heterogeneous catalysis.

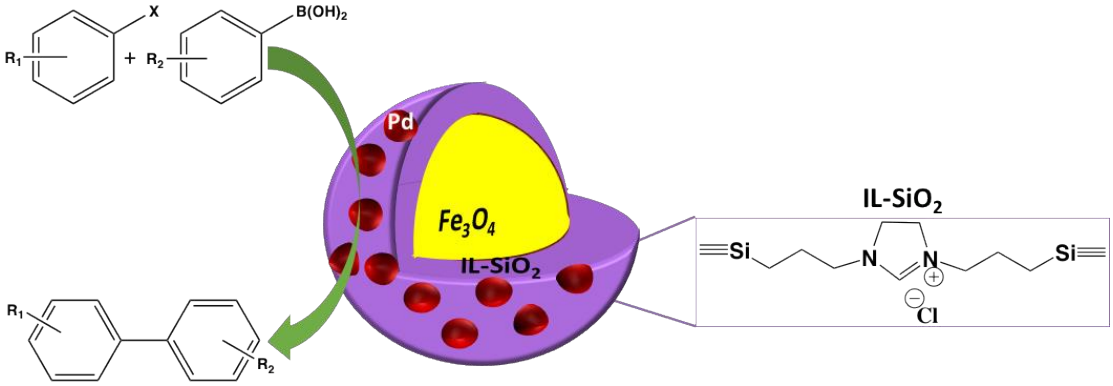

Figure 2.16: Suzuki cross-coupling reactions catalysed by the Pd/MNP@IL-SiO_2 catalyst [68]. [Adapted from reference [68]].

Another special type of hybrid organic-inorganic support was reported by Lin et al. who prepared a retrievable Pd/CMC@$Ce(OH)_4$ catalyst for Suzuki coupling-reactions [69]. In this system, $Ce(OH)_4$ was coated with carboxymethylcellulose (CMC) to form a hybrid organic-inorganic CMC@$Ce(OH)_4$ support (Scheme 2.8). Carboxymethylcellulose has a large number of inherent carboxylate (–COO–) and hydroxyl (–OH) groups on its molecular chain. Thus, CMC is an excellent cation exchange agent, which makes it an excellent support for stabilization of palladium nanoparticles. While ceria has a unique ability of forming oxygen vacancies that reduce Ce^{4+} to Ce^{3+} and create an excess of negative charge on its surface. The excess negative charge facilitates the coordination of palladium nanoparticles to the surface, as discussed earlier. These interactions have been shown to be crucial in preventing leaching and agglomeration of catalytic palladium nanoparticles.

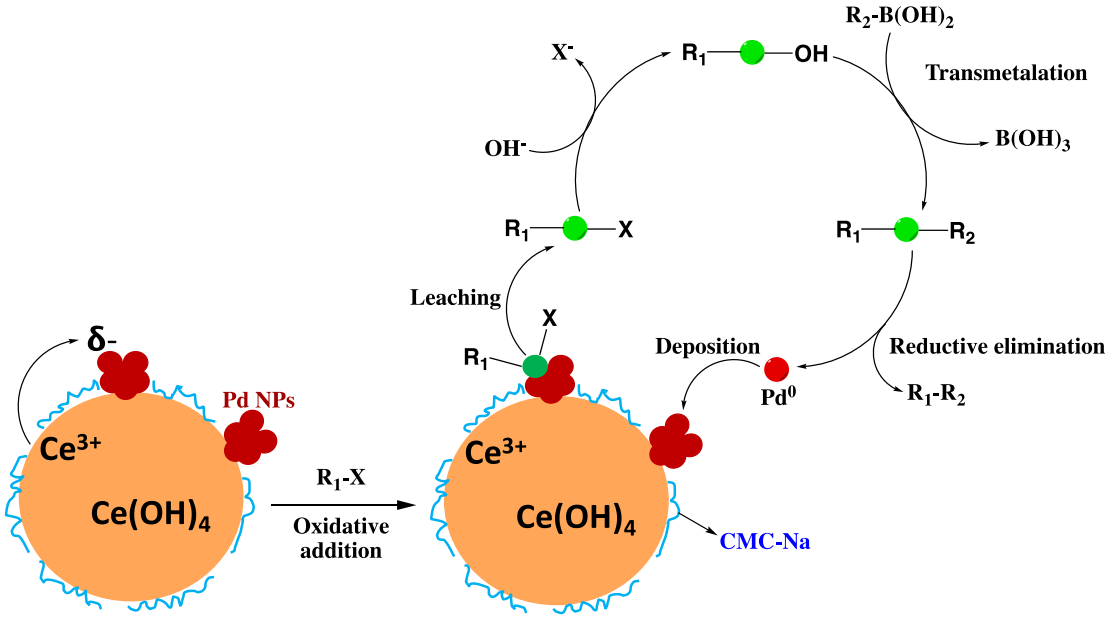

Scheme 2.8: Illustrative diagram of the conceptual mechanism of the Suzuki reaction catalyzed by Pd/CMC@Ce(OH)$_4$. [69]. [Adapted from reference [69]].

The Pd/CMC@Ce(OH)$_4$ catalyst was applied to the Suzuki cross-coupling reaction and good to excellent yields were obtained. It is believed that the activity of the catalyst was enhanced synergistically by the unique redox properties of Ce(OH)$_4$ (Ce^{3+}/Ce^{4+}) and the coordination with the functional (carboxyl and hydroxyl) groups of the hybrid CMC@Ce(OH)$_4$ support. Moreover, the catalyst could be easily separated by simple filtration and reused at least for five times without losing its activity. However, it was observed that Pd(0) species leached from the hybrid support during the reaction and were re–deposited onto the support at the end of the reaction. Therefore, the reaction mechanism is homogeneous in nature and the leached palladium species are the "true active species".

2.3 The nature of the "true" active Pd species

The true nature of the active catalyst when a palladium containing solid material is employed as a catalyst is still a highly debated issue in the field of cross-coupling reactions [70]. In most research papers, the "true nature" of the active form of palladium is ambiguous; claims exist in the literature supporting both soluble molecular and nanoparticle catalysts, as well as truly heterogeneous insoluble Pd catalysts (Scheme 2.9) [70-72]. More specifically, the question is whether the oxidative addition of the aryl halide (Ar–X) occurs on the surface of the solid catalyst (heterogeneous catalysis) or on leached metal atoms (homogeneous catalysis). On the basis of recent studies, there is a convergence of findings that recognise the solid pre-catalyst as a "reservoir" of soluble catalytically active palladium species [2, 19, 22, 73, 74]. Hence, these authors believe that oxidative addition of the aryl halide occurs on the leached palladium

atom in the solution, rendering the reaction homogeneous irrespective of the nature of the solid pre-catalyst. But, there is still a distinct minority of researchers who claim to have developed truly heterogeneous systems with catalysis taking place on the surface of the solid palladium based heterogeneous catalyst [26].

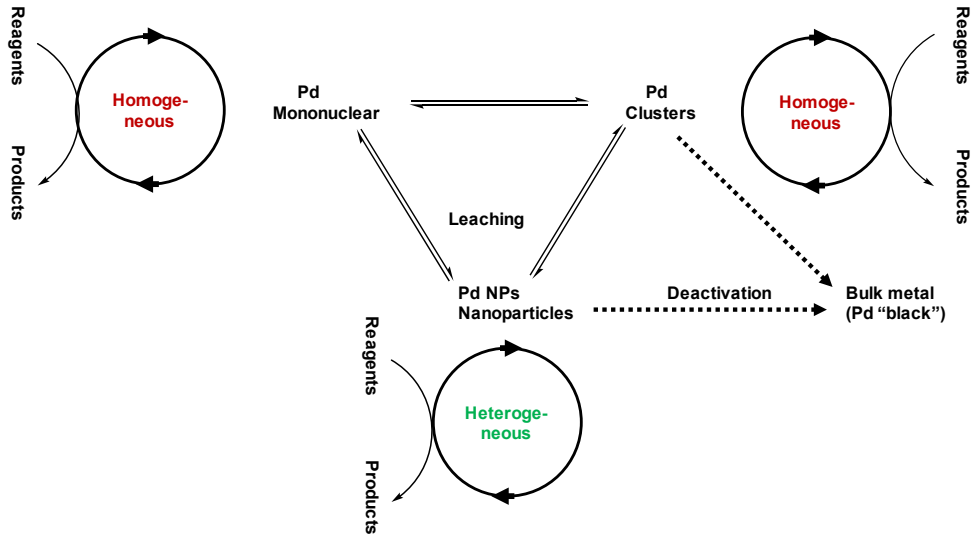

Scheme 2.9: A graphical illustration for the multiple species catalysis in palladium catalyzed cross coupling reactions [74]. [Adapted from reference [74]].

Hence, at the moment it is hard to say what the nature of the true catalyst is due to the dynamic nature of the reported catalytic systems for cross-coupling reactions. It is still difficult to predict which approach of catalyst design should be considered as superior. In any case, almost all of the reported Pd based heterogeneous catalytic systems try to relate the effectiveness of their systems on the nature of the palladium precatalyst and the optimised reaction conditions. Both the nature of the precatalyst and the reaction conditions determine the catalytic activity, recoverability and recyclability of the developed catalytic system. Although, most reported heterogeneous catalytic systems do not completely remove the palladium catalyst at the end of the reaction, in order to limit the metal contamination of the final product (''release-and-catch'' strategy). Therefore, identifying the true catalyst is critically important for future advances in the rational design of C-C cross-coupling catalysts.

2.4 Motivation and objectives of the current study

The importance of carbon-carbon bond forming reactions is well documented in literature. The numerous Nobel Prizes in Chemistry received by researchers in this area of research the industrial importance of C-C bond forming reactions has generated great interest. In addition, the unavailability of a universally trusted

catalytic system for these reactions means that there is room for new contributions towards designing an ideal catalytic system.

The literature survey has shown that almost all forms of palladium can be used as precatalysts for converting reactive substrates, while specifically designed catalysts are needed for difficult substrates.

1. Thus, the first objective is to design a highly active catalyst that can catalyze even the less reactive or deactivated substrates.
    a. An easy to synthesize catalyst that is moisture and thermally stable.
    b. A catalyst that can catalyze a wide range of substrates with high efficiency (high TONs and TOFs)
    c. The aim is to develop a catalyst system that retains the advantages of both the homogeneous and heterogeneous systems (quasi-heterogeneous or semi-heterogeneous).
2. The second objective is to develop a catalytic system that can minimize palladium metal contamination of the product.
    a. The aim is to develop a heterogeneous catalytic system that will allow the recovery and re-usability of the catalyst, leaving little to no palladium metal in the product solution.
3. Lastly, the aim is to investigate the nature of the active catalyst in cross-coupling reactions.
    a. The intention is to gain better understanding of cross-coupling reactions, to hopefully be in a better position to propose the nature of the reaction mechanism for heterogeneous cross-coupling reactions.

Conventionally, supported palladium based catalysts are used for developing heterogeneous variants of C-C cross-coupling reactions. The use of palladium based solid-solution oxides ($Pd_xCe_{1-x}O_{2-\delta}$) as catalysts have rarely been explored in C-C cross-coupling reactions. Hence, it was deemed worthwhile to explore palladium substituted ceria based catalysts, because ceria has received good reviews as a host or a support for metal nanoparticles (Figure 2.17). This catalyst design should easily meet the set catalytic activity objectives because substitution of palladium ions into the ceria lattice greatly improves the dispersion of palladium. Since palladium is the active component, increasing its dispersion will increase the number of exposed reactive sites, and as a result, increases the reactivity of the catalyst. Hence, the aim is to carefully prepare and characterize the single-phase, $Pd_xCe_{1-x}O_{2-\delta}$ based solid solution oxides and then explore them as suitable catalysts for Heck-Mizoroki, Sonogashira and Suzuki-Miyaura cross-coupling reactions.

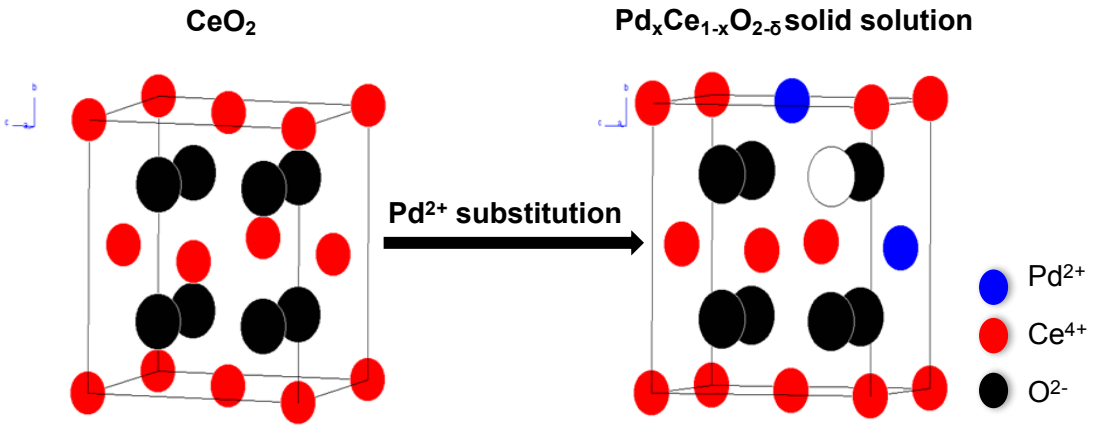

Figure 2.17: The graphical illustration of the fluorite structure of pure ceria and palladium-substituted ceria.

2.5 Reference:

1. A.V. Astakhov, O.V. Khazipov, A.Y. Chernenko, D.V. Pasyukov, A.S. Kashin, E.G. Gordeev, V.N. Khrustalev, V.M. Chernyshev, V.P. Ananikov, *Organometallics*, 36 (2017) 1981-1992.
2. M. Pagliaro, V. Pandarus, R. Ciriminna, F. Béland, P. Demma Carà, *ChemCatChem*, 4 (2012) 432-445.
3. A. Corma, H. Garcia, *Topics in Catalysis*, 48 (2008) 8-31.
4. F.X. Felpin, T. Ayad, S. Mitra, *European Journal of Organic Chemistry*, 2006 (2006) 2679-2690.
5. T. Asefa, A. V. Biradar, S. Das, K. K. Sharma, R. Silva, *Nanocatalysts for the Heck coupling reactions: Nanocatalysis: Synthesis and Applications, John Wiley & Sons, Inc, New Jersey*, 2013, pp. 11-50.
6. I.B. Chorkendorff, J.W. Niemantsverdriet, *Introduction to Catalysis: Concepts of Modern Catalysis and Kinetics, WILEY-VCH Verlag GmbH & Co. KGaA, Weinheim*, 2003, pp. 1-22.
7. M. Manuel, J.S. César, R. José Rafael, *Current Organic Chemistry*, 16 (2012) 1128-1150.
8. P. Veerakumar, P. Thanasekaran, K.L. Lu, S.B. Liu, S. Rajagopal, *ACS Sustainable Chemistry and Engineering*, 5 (2017) 6357-6376.
9. A. Leyva-Perez, *Dalton Transactions*, 46 (2017) 15987-15990.
10. B. Lakshminarayana, L. Mahendar, P. Ghosal, G. Satyanarayana, C. Subrahmanyam, *ChemistrySelect*, 2 (2017) 2700-2707.
11. S.N. Jadhav, A.S. Kumbhar, C.V. Rode, R.S. Salunkhe, *Green Chemistry*, 18 (2016) 1898-1911.
12. D. Khalili, A.R. Banazadeh, E. Etemadi-Davan, *Catalysis Letters*, 147 (2017) 2674-2687.
13. A.H. Labulo, B.S. Martincigh, B. Omondi, V.O. Nyamori, *Journal of Materials Science*, 52 (2017) 9225-9248.
14. L. Yang, G. Cheng, L. Xing, C. Cheng, L. Xia, *Method for activating carbon nanotube-supported palladium nanoparticle catalyst and application thereof: Liaoning University, People's Republic of China*. 2017, pp. 1-9. CN106902817A

15. M. Hosseini-Sarvari, Z. Razmi, M.M. Doroodmand, *Applied Catalysis A: General*, 475 (2014) 477-486.
16. A. Del Zotto, S. Colussi, A. Trovarelli, *Inorganica Chimica Acta*, 470 (2018) 275-283.
17. K. Köhler, R.G. Heidenreich, S.S. Soomro, S.S. Pröckl, *Advanced Synthesis & Catalysis*, 350 (2008) 2930-2936.
18. M. Gruttadauria, F. Giacalone, R. Noto, *Green Chemistry*, 15 (2013) 2608-2618.
19. F. Amoroso, S. Colussi, A. Del Zotto, J. Llorca, A. Trovarelli, *Catalysis Letters*, 143 (2013) 547-554.
20. J.H. Adair, E. Suvaci, J. Sindel, *Surface and Colloid Chemistry: Encyclopedia of Materials: Science and Technology (Second Edition), Elsevier, Oxford*, 2001, pp. 1-10.
21. M. Kosmulski, *Compilation of PZCs/IEPs: Surface charging and point of zero charge, Taylor & Francis Group, Boca Raton, Florida,* 2009, pp. 101-524.
22. A. Del Zotto, D. Zuccaccia, *Catalysis Science & Technology*, 7 (2017) 3934-3951.
23. P. Bera, M.S. Hegde, *RSC Advances*, 5 (2015) 94949-94979.
24. T. Cwele, N. Mahadevaiah, S. Singh, H.B. Friedrich, *Applied Catalysis B: Environmental*, 182 (2016) 1-14.
25. T. Cwele, N. Mahadevaiah, S. Singh, H.B. Friedrich, A.K. Yadav, S.N. Jha, D. Bhattacharyya, N.K. Sahoo, *Catalysis Science & Technology*, 6 (2016) 8104-8116.
26. S.R. Sanjaykumar, B.D. Mukri, S. Patil, G. Madras, M.S. Hegde, *Journal of Chemical Sciences*, 123 (2011) 47-54.
27. A. Gupta, U.V. Waghmare, M.S. Hegde, *Chemistry of Materials*, 22 (2010) 5184-5198.
28. P.A. Deshpande, M.S. Hegde, G. Madras, *AIChE Journal*, 56 (2010) 1315-1324.
29. M.S. Hegde, G. Madras, K.C. Patil, *Accounts of Chemical Research*, 42 (2009) 704-712.
30. A.S. Burange, R. Shukla, A.K. Tyagi, C.S. Gopinath, *ChemistrySelect*, 1 (2016) 2673-2681.
31. G.J. Lichtenegger, M. Maier, M. Hackl, J.G. Khinast, W. Gössler, T. Griesser, V.S.P. Kumar, H. Gruber-Woelfler, P.A. Deshpande, *Journal of Molecular Catalysis A: Chemical*, 426 (2017) 39-51.
32. B. Karimi, F. Mansouri, H.M. Mirzaei, *ChemCatChem*, 7 (2015) 1736-1789.
33. C. Feng, J. Liu, J. Gui, L. Liu, *Yingyong Huaxue*, 32 (2015) 19-26.
34. T. Cheng, D. Zhang, H. Li, G. Liu, *Green Chemistry*, 16 (2014) 3401-3427.
35. R.B.N. Baig, R.S. Varma, *Chemical Communications*, 49 (2013) 752-770.
36. L.M. Rossi, M.A.S. Garcia, L.L.R. Vono, *Journal of the Brazilian Chemical Society*, 23 (2012) 1959-1971.
37. C. Xiao, N. Yan, Y. Kou, *Cuihua Xuebao*, 30 (2009) 753-764.
38. E. Mulahmetovic, G.C. Hargaden, *Review Journal of Chemistry*, 7 (2017) 373-398.
39. A. Elhampour, F. Nemati, *Organic Preparations and Procedures International*, 49 (2017) 443-458.

40. R. Hudson, Y. Feng, R.S. Varma, A. Moores, *Green Chemistry*, 16 (2014) 4493-4505.
41. L.M. Rossi, N.J.S. Costa, F.P. Silva, R. Wojcieszak, *Green Chemistry*, 16 (2014) 2906-2933.
42. M. Nasrollahzadeh, S. Mohammad Sajadi, A. Rostami-Vartooni, M. Khalaj, *Journal of Molecular Catalysis A: Chemical*, 396 (2015) 31-39.
43. C. Xie, Y. Liu, S. Yu, *Qingdao Keji Daxue Xuebao, Ziran Kexueban*, 36 (2015) 237-244.
44. B.S. Kumar, R. Anbarasan, A.J. Amali, K. Pitchumani, *Tetrahedron Letters*, 58 (2017) 3276-3282.
45. F. Heidari, M. Hekmati, H. Veisi, *Journal of Colloid and Interface Science*, 501 (2017) 175-184.
46. H. Fan, Z. Qi, D. Sui, F. Mao, R. Chen, J. Huang, *Chinese Journal of Catalysis*, 38 (2017) 589-596.
47. A. Taher, M. Choudhary, D. Nandi, S. Siwal, K. Mallick, *Applied Organometallic Chemistry*, 32 (2017) e3898.
48. F. Ashouri, M. Zare, M. Bagherzadeh, *Comptes Rendus Chimie*, 20 (2017) 107-115.
49. C.A. Wang, Y.W. Li, X.M. Hou, Y.F. Han, K. Nie, J.P. Zhang, *ChemistrySelect*, 1 (2016) 1371-1376.
50. X. Liu, X. Zhao, M. Lu, *Journal of Organometallic Chemistry*, 768 (2014) 23-27.
51. B. Kodicherla, P. Perumgani C, S. Keesara, M.R. Mandapati, *Inorganica Chimica Acta*, 423 (2014) 95-100.
52. P. Aravinda Reddy, A. Babul Reddy, G. Ramachandra Reddy, N. Subbarami Reddy, *Journal of Heterocyclic Chemistry*, 50 (2013) 1451-1456.
53. B. Tamami, F.N. Dodeji, *Journal of the Iranian Chemical Society*, 9 (2012) 841-850.
54. N.A. Nemygina, L.Z. Nikoshvili, A.V. Bykov, A.I. Sidorov, V.P. Molchanov, M.G. Sulman, I.Y. Tiamina, B.D. Stein, V.G. Matveeva, E.M. Sulman, L. Kiwi-Minsker, *Organic Process Research & Development*, 20 (2016) 1453-1460.
55. Y. Li, L. Xu, B. Xu, Z. Mao, H. Xu, Y. Zhong, L. Zhang, B. Wang, X. Sui, *ACS Applied Materials & Interfaces*, 9 (2017) 17155-17162.
56. J.M. Collinson, J.D.E.T. Wilton-Ely, S. Diez-Gonzalez, *Catalysis Communications*, 87 (2016) 78-81.
57. R. Fareghi-Alamdari, M.S. Saeedi, F. Panahi, *Applied Organometallic Chemistry*, 31 (2017) e3870.
58. C.N.R. Rao, A.K. Cheetham, A. Thirumurugan, *Journal of Physics: Condensed Matter*, 20 (2008) 1-21.
59. Y. Wang, L. Dou, H. Zhang, *ACS Applied Materials & Interfaces*, 9 (2017) 38784-38795.
60. N. Arsalani, A. Akbari, M. Amini, E. Jabbari, S. Gautam, K.H. Chae, *Catalysis Letters*, 147 (2017) 1086-1094.
61. H. Woo, K. Lee, K.H. Park, *ChemCatChem*, 6 (2014) 1635-1640.
62. X. Jing, F. Sun, H. Ren, Y. Tian, M. Guo, L. Li, G. Zhu, *Microporous Mesoporous Materials*, 165 (2013) 92-98.
63. K. Qu, L. Wu, J. Ren, X. Qu, *ACS Applied Materials & Interfaces*, 4 (2012) 5001-5009.

64. H. Yang, Z. Ma, Y. Qing, G. Xie, J. Gao, L. Zhang, J. Gao, L. Du, *Applied Catalysis A: General*, 382 (2010) 312-321.
65. B. Wang, Y.l. Gu, L. Yang, J. Suo, *Fenzi Cuihua*, 17 (2003) 468-480.
66. M.N. Shaikh, M. Abdul Aziz, A. Helal, A.N. Kalanthoden, Z.H. Yamani, *ChemistrySelect*, 2 (2017) 9052-9057.
67. V. Kozell, T. Giannoni, M. Nocchetti, R. Vivani, O. Piermatti, L. Vaccaro, *Catalysts*, 7 (2017) 186-206.
68. S. Omar, R. Abu-Reziq, *Journal of Physical Chemistry C*, 118 (2014) 30045-30056.
69. B. Lin, X. Liu, Z. Zhang, Y. Chen, X. Liao, Y. Li, *Journal of Colloid and Interface Science*, 497 (2017) 134-143.
70. P. Veerakumar, P. Thanasekaran, K.L. Lu, K.C. Lin, S. Rajagopal, *ACS Applied Materials and Interfaces*, 5 (2017) 8475-8490.
71. Yin, J. Liebscher, *Chemical Reviews*, 107 (2007) 133-173.
72. R. Chinchilla, C. Nájera, *Chemical Reviews*, 107 (2007) 874-922.
73. N.T.S. Phan, M. Van Der Sluys, C.W. Jones, *Advanced Synthesis & Catalysis*, 348 (2006) 609-679.
74. V.P. Ananikov, I.P. Beletskaya, *Organometallics*, 31 (2012) 1595-1604.

Chapter 3

$Pd_{0.09}Ce_{0.91}O_{2-\delta}$: A sustainable ionic solid-solution precatalyst for heterogeneous, ligand free Heck coupling reactions.

Abstract

A quick and easy method for the preparation of Pd^{2+} metal ion substituted in ceria, $Pd_{0.09}Ce_{0.91}O_{2-\delta}$ solid solution oxide, is described. The $Pd_{0.09}Ce_{0.91}O_{2-\delta}$ solid solution oxide was fully characterized by XRD, ICP-OES, BET, XPS, SEM, EDX, TEM, TGA and Raman spectroscopy. All characterization techniques strongly suggested that Pd^{2+} was successfully incorporated into the lattice structure of ceria. The effect of the reaction conditions on the catalytic properties of the $Pd_{0.09}Ce_{0.91}O_{2-\delta}$ solid solution catalyst initially was studied in detail with the model Heck reaction of iodobenzene and methylacrylate to obtain optimum reaction conditions. The $Pd_{0.09}Ce_{0.91}O_{2-\delta}$ solid solution catalyst then afforded substituted alkenes in good to excellent yields under these optimum reaction conditions. Steric and electronic effects were also studied, and were found to influence the catalytic activity. Characterization of the used catalyst suggests that Pd^{2+} in $Pd_{0.09}Ce_{0.91}O_{2-\delta}$ is reduced *in situ* to Pd^0 when employed in the Heck cross-coupling reactions. The catalyst was easily recovered by centrifuge and reused for three times without significant loss of catalytic efficiency.

Keywords: Pd^{2+} substituted ceria; solution combustion; nanoparticles; Heck coupling reaction.

3.1 Introduction

Palladium catalyzed Heck coupling reactions are a well-known and a well-established technique in organic chemistry and the pharmaceutical industry [1]. The Heck coupling reaction is now considered to be one of the most useful and practical tools in modern organic synthesis [2]. It involves the construction of a carbon-carbon (C-C) bond through a chemical reaction between an unsaturated halide and an alkene in the presence of a base and a palladium catalyst to form substituted alkenes [3,4]. These C-C bonds are of great importance in organic chemistry and are essential for all life on earth [5-10]. Several reviews have been published [11-16].

The most common catalytic systems used for Heck coupling reactions involve homogenous palladium-phosphine complexes, such as $PdCl_2(PPh_3)_2$ or $Pd(PPh_3)_4$, in the presence of a base [11-18]. Many ligands and catalysts have also been reported, but they are largely not available commercially and do not find extensive use [19,20]. This is mostly because the phosphine ligands are oxygen sensitive (easily oxidized) [17]. Furthermore, the efficient separation and subsequent recycling of homogenous palladium catalysts and ligand remains a challenge and an aspect of economic relevance [19,20].

As a result, the use of ligand-free heterogeneous palladium catalyst is often desirable because it permits easy handling, simple recovery and recyclability of the palladium catalyst. The increasing number of reports indicates that there is a growing interest in finding heterogeneous variants of Heck coupling reactions [6,7,20-26]. Most classes of heterogeneous catalysts described in literature involve immobilization of homogeneous Pd containing catalysts onto insoluble polymeric supports or solid inorganic supports. Frequently used supports are activated carbon [7], molecular sieves [27], metal oxides [8-10,28,29] and polymers [30,31].

Heterogeneous catalysis with the noble metal ion substituted in solid-state materials, such as in simple and complex oxides, is not well understood [32-34]. However, some authors of the present work have published some papers addressing the synthesis and catalytic behavior of binary oxide-based compounds substituted with noble metal ions to make ionic catalysts [35-37]. Hedge and co-workers have also published numerous papers addressing solution combustion synthesis and application of noble metal ionic catalysts [38-50]. All reports have shown that substitution of Pd^{2+} ions within the CeO_2 lattice allows for complete palladium dispersion, which, as a result, increases the activity of the ceria-based catalysts [38,51].

However, the 2 mol% level of Pd substitution usually investigated for these materials is at the detection limit of phase identification by conventional powder X-ray diffraction [51]. Thus, in most cases it is unclear whether the Pd is incorporated into the lattice structure of CeO_2 or is deposited on the surface of CeO_2 as PdO [51]. In this regard, we thought it would be worthwhile to prepare, and evaluate the phase composition and physicochemical properties of, a higher Pd-substituted $Pd_xCe_{1-x}O_{2-\delta}$ (9 mol% Pd) solid solution oxide by solution combustion. This ionic $Pd_{0.09}Ce_{0.91}O_{2-\delta}$ solid solution oxide was then tested on Heck cross-coupling reactions. Using an air, moisture and thermally stable heterogeneous $Pd_{0.09}Ce_{0.91}O_{2-\delta}$ solid solution catalyst should offer simplicity of workup, recyclability and minimization of metallic waste. It should also offer higher turnover numbers since complete dispersion is achieved in similar Pd^{2+} ion substituted CeO_2 materials [38].

3.2 Experimental

3.2.1 Catalyst synthesis

Cerium ammonium nitrate [$(NH_3)Ce(NO_3)_6$, 99.9%], palladium chloride [$PdCl_2$, anhydrous, 60% Pd basis], urea [CH_4N_2O, 99.9%] were obtained from Sigma-Aldrich and were used without further purification.

3.2.2 Solution combustion synthesis of the $Pd_{0.09}Ce_{0.91}O_{2-\delta}$ oxide

The following materials were synthesized using an adaptation of a reported procedure [36]. For the synthesis of $Pd_{0.09}Ce_{0.91}O_{2-\delta}$ (6.7 wt% Pd), 2 mmol of $PdCl_2$ were dissolved in 10 mL of HCl (32%) in a borosilicate dish, and once all the $PdCl_2$ had dissolved, 40 mL of deionized water, 18 mmol of $(NH_3)Ce(NO_3)_6$, and 72 mmol CH_4N_2O (urea) were added. The solution was stirred at 100 °C to evaporate water and form a gel. The formed gel was introduced into a muffle furnace pre-heated to 120 °C, the furnace temperature was then increased gradually to 600 °C over 30 min, and maintained at that temperature for 5 h. A dark brown solid product was obtained. For the synthesis of blank CeO_2, the above procedure was followed without the addition of $PdCl_2$.

3.2.3 Catalyst characterization

A Bruker D8 Advance diffractometer, equipped with an XRK900 furnace, generator (40 kV and 40 mA) and a Cu $K\alpha_{1/2}$ source (λ = 1.5406 Å) was used to record the powder X-ray diffraction patterns of the samples. The structures were refined by the Rietveld method using the Full Prof Suite-2000 program. The average crystallite size (D) and lattice strain (ε) of CeO_2 and $Pd_{0.09}Ce_{0.91}O_{2-\delta}$ were estimated from the modified Rietveld method and Williamson-Hall (W-H) plots (1).

$$\beta_{hkl}\cos\theta = \frac{K\lambda}{D} + 4\varepsilon\sin\theta \qquad (1)$$

X-ray photoelectron spectra (XPS) were recorded with a Thermo Scientific Multilab 2000 spectrometer equipped with the Al Kα radiation source (1486.6 eV). All the binding energies were referenced to the C(1s) peak (284.5 eV).

ICP-OES was performed using a Perkin Elmer Optical Emission Spectrometer Optima 5300 DV. The standards (1000 ppm Ce and Pd) were purchased from Fluka.

Raman spectroscopy was carried out using an Advanced 532 series spectrometer (NIR Spectrometer) utilizing Nuspec software, equipped with a visible laser of 514 nm.

Brunauer–Emmett–Teller (BET) surface area measurements were determined using a MicroMetrics TriStar 3000 porosimeter with N_2 as probe gas. About 0.4 g of each powder sample was degased overnight at 200 °C using a Micromeritics FlowPep 060 instrument prior to analysis.

SEM images and EDX data were obtained with a Jeol JSM-6100 scanning microscope using a Bruker signal processing unit detector. The analysis was performed at random points along the surface of the catalyst. The samples were first mounted on aluminium stubs using double-sided carbon tape; they were then coated with gold using a Polaron E5100 coating unit.

For TEM analysis, the samples were viewed on Joel JEM-1010 Electron Microscope. For high resolution TEM (HR-TEM) and scanning electron microscopy (STEM) analysis, the samples were viewed on Joel JEM-2100 Electron Microscope and the images captured were analysed using iTEM software. The powder samples were ultrasonically dispersed in ethanol and supported on a perforated carbon film mounted on a copper grid prior to analysis.

TGA analysis was conducted with a TA SDT Q600 instrument under nitrogen flowing at 50 ml/min and at a temperature ramp rate of 10 °C/min from room temperature up to 1000° C with ca. 10 mg of sample.

3.2.4 General procedure for Heck cross-coupling reactions

A dry two-necked pear-shaped flask, equipped with a condenser containing a stirrer bar and 3 mL of DMF was charged with the aryl halide (2 mmol), olefin (1.5 eq.), triethylamine (1.5 eq.) and catalyst $Pd_{0.09}Ce_{0.91}O_{2-\delta}$ (0.3 mol% Pd). The reaction mixture was heated and stirred at 130 °C. A GC/MS (PerkinElmer Inc.–Clarus 560 S GC/MS; PONA column: 50 m × 0.15mm) was used for monitoring the progress of the reaction and for product identification. After the reaction had gone to completion, the reaction mixture was cooled to room temperature and filtered. The filtrate was extracted with ethyl acetate, hexane and brine (1:3:3). The organic layer was dried with sodium sulphate and the solvent was then evaporated under reduced pressure. The residue was finally purified by flash chromatography on silica gel using ethyl acetate as the eluent.

3.3 Results and discussion

3.3.1 Physicochemical properties investigation

The microstructural parameters of the $Pd_{0.09}Ce_{0.91}O_{2-\delta}$ sample were determined using Rietveld refinement; the experimental, calculated and difference curves

were plotted and are shown in Figure 3.1. The observed peaks in the X-ray patterns of $Pd_{0.09}Ce_{0.91}O_{2-\delta}$ correspond only to the ceria phase with the fluorite structure (JCPDS 34-0394). The STEM-EDX (Figure 3.1, insert) confirmed the presence of Pd and also shows that palladium is homogeneously dispersed in the ceria lattice. The absence of the Pd^0 and/or PdO phase in the X-ray pattern of the $Pd_{0.09}Ce_{0.91}O_{2-\delta}$ sample suggests that the Pd^{2+} ions were successfully incorporated into the ceria lattice. The incorporation of the Pd^{2+} into the ceria lattice came with the expected physicochemical changes to ceria. The peak for the [111] plane shifts to lower 2 theta values upon the introduction of Pd^{2+} into the ceria lattice. The 2 theta value of the [111] plane shifts from 28.86° in pure CeO_2 to 28.83° in the $Pd_{0.09}Ce_{0.91}O_{2-\delta}$ sample. This shift is associated with increases in lattice parameters that cause the ceria lattice to be strained [51]. Table 3.1 shows that the lattice parameter *a* increases from 5.411(9) Å in CeO_2 to 5.424(9) Å in $Pd_{0.09}Ce_{0.91}O_{2-\delta}$. The XRD, XPS, ICP-OES, BET, SEM-EDS, TEM, TGA and Raman analyses for the CeO_2 sample are enclosed in Appendix 1.

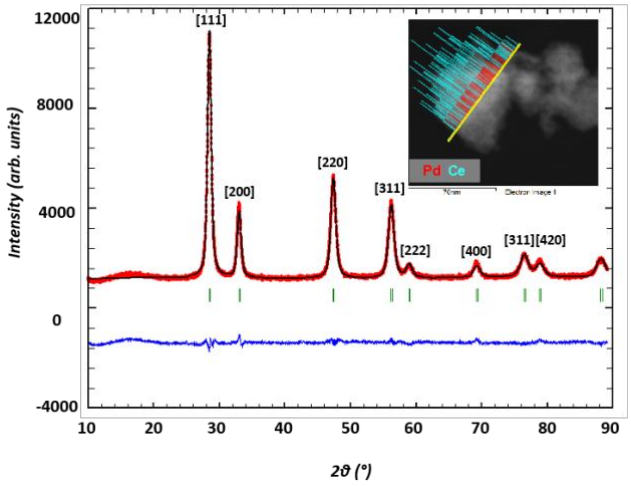

Figure 3.1: Rietveld refined XRD pattern of $Pd_{0.09}Ce_{0.91}O_{2-\delta}$ and its STEM-EDX image (insert)

The Williamson-Hall plot was used to estimate the average crystallite size and lattice strain of the samples (Table 3.1). The $Pd_{0.09}Ce_{0.91}O_{2-\delta}$ sample showed about three times more lattice strain than pure ceria prepared by the same route (Table 3.1). The increased lattice strain in the $Pd_{0.09}Ce_{0.91}O_{2-\delta}$ sample indicates that lattice distortion occurs upon introduction of Pd^{2+} ions in the CeO_2 lattice [37,51]. The average crystallite size decreases slightly with the incorporation of the Pd^{2+} ions into the CeO_2 lattice. The average crystallite size of the blank CeO_2 is 19 nm, while that of $Pd_{0.09}Ce_{0.91}O_{2-\delta}$ decreased to 17 nm.

Table 3.1: Structural parameters of the investigated materials obtained from the XRD profiles.

	Rietveld refinement	Williamson-Hall method		TEM
	Lattice parameter a (Å)	Lattice strain ($\times 10^{-3}$)	Crystallite size (nm)	Average particle size (nm)
CeO_2	5.411(9)	0.9	19	22
$Pd_{0.09}Ce_{0.91}O_{2-\delta}$	5.424(9)	3	17	19

An assessment of recent reports on $Pd_xCe_{1-x}O_{2-\delta}$ solid solutions suggests that there is no conventional opinion to explain why the lattice parameter increases with the increasing concentration of Pd^{2+} ions [51]. We are of a view that the lattice parameters increase due to the formation of larger Ce^{3+} (1.23 Å) ions and the creation of more oxygen vacancies upon introduction of Pd^{2+} ions into the ceria lattice. The increase in the lattice parameters then causes uniform lattice strain and a decrease in crystallite size. The formation of Ce^{3+} ions, that are larger than Ce^{4+} (0.97 Å) ions, was confirmed by XPS results (Figure 3.2).

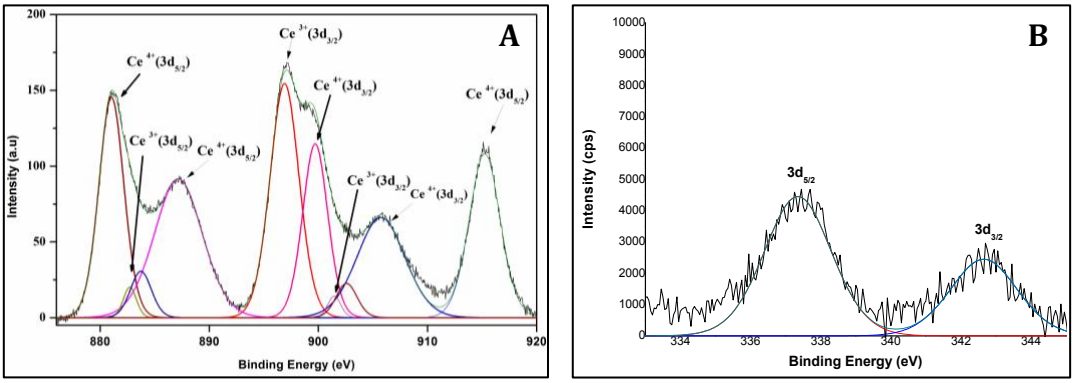

Figure 3.2: Core level XPS of (A) Ce (3d) and (B) Pd (3d) in $Pd_{0.09}Ce_{0.91}O_{2-\delta}$ catalyst.

The oxidation states of Pd and Ce in the $Pd_{0.09}Ce_{0.91}O_{2-\delta}$ catalyst were determined by XPS and core level XPS of Pd (3d) of $Pd_{0.09}Ce_{0.91}O_{2-\delta}$ as shown in Figure 3.2. The Pd (3d) doublet lines were analysed to obtain the electronic state of palladium and the binding energy for Pd ($3d_{5/2}$) was found to be equal to 337.5 eV, which is typical for Pd^{2+} in the catalyst [37,51,52]. This main state of palladium was attributed to individual palladium ions localized in the ceria lattice of the $Pd_{0.09}Ce_{0.91}O_{2-\delta}$ solid solution oxide [51,53]. The elevated binding energy of the satellite peak at 342.5 eV further suggests that the palladium ions are localized in the ceria lattice.

Hence, the analysis of the Pd (3d) doublet lines strongly suggests that the environment of Pd^{2+} ions in the $Pd_{0.09}Ce_{0.91}O_{2-\delta}$ solid solution oxide is different from the oxygen environment in PdO, since the Pd ($3d_{5/2}$) line for PdO oxide is in the range of 336.7–337.0 eV [51,54]. The Ce^{4+} ($3d_{5/2}$) peak obtained at 881.5 eV is a characteristic of Ce^{4+} in CeO_2. Thus, partial filling of the valley between 881 eV and its satellite at 886 eV shows that Ce is in a mixed valence state (+4 and +3) since the Ce^{3+} (3d) in Ce_2O_3, is characterized by Ce^{3+} ($3d_{5/2}$) at 885.1 eV [52]. The ratios of oxidation states present in the catalyst were calculated as Ce^{4+}:Ce^{3+} of 4:1. Core level XPS of Ce(3d) in CeO_2 is shown in Appendix 1 (Figure A1.4). The Ce^{4+}($3d_{3/2}$) peak obtained at 882.5 eV is characteristic of Ce^{4+} in CeO_2.

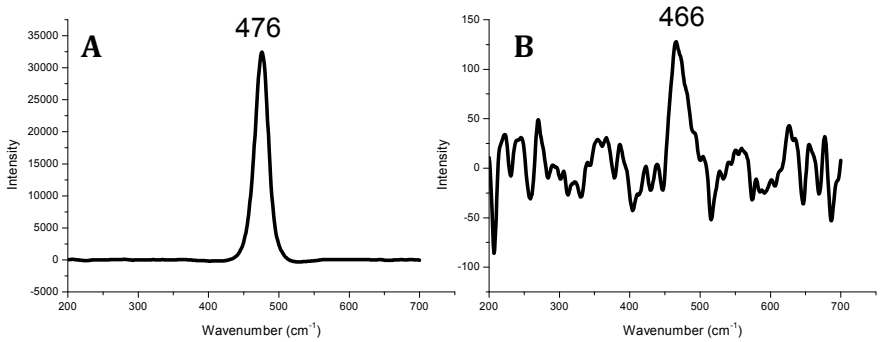

Figure 3.3: Raman spectra of (a) CeO_2 and (b) $Pd_{0.09}Ce_{0.91}O_{2-\delta}$

Raman spectroscopy was employed to comparatively analyze the CeO_2 and $Pd_{0.09}Ce_{0.91}O_{2-\delta}$ samples and the results are shown in Figure 3.3. The peak at 465–480 cm^{-1} corresponds to the F_{2g} vibrational mode of oxygen ions in the [CeO_8] cubic subunit of the CeO_2 structure [37,51]. In blank CeO_2 this peak appears at 476 cm^{-1}, while for $Pd_{0.09}Ce_{0.91}O_{2-\delta}$ it shifts to a lower wavenumber of 466 cm^{-1} (Figure 3.3). The bands at ca. 550 and 650 cm^{-1}, which are weak for blank CeO_2 and more intense for the $Pd_{0.09}Ce_{0.91}O_{2-\delta}$ sample, are assigned to the defect-induced vibrational mode (D-mode) [37,51]. The absence of a PdO peak (≈660 cm^{-1}) in the $Pd_{0.09}Ce_{0.91}O_{2-\delta}$ sample further suggests that the Pd^{2+} ions are fully dispersed in the lattice of CeO_2 and not deposited as PdO on its surface (Appendix 1, Figure A1.6).

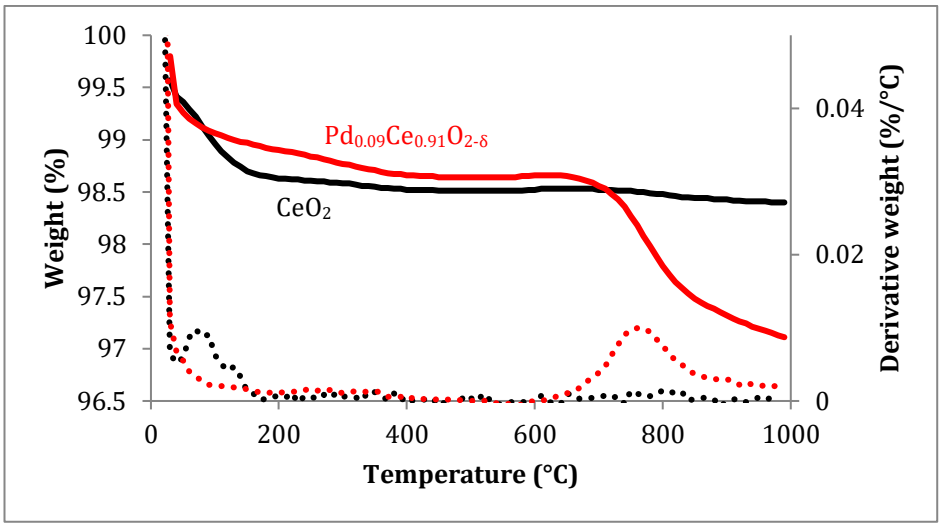

Figure 3.4: The TGA and DTA analysis of the investigated materials; (black) CeO_2 and (red) $Pd_{0.09}Ce_{0.91}O_{2-\delta}$

The Thermogravimetric analysis (TGA) (Figure 3.4, solid lines) and differential thermal analysis (DTA) curves (Figure 3.4, dotted lines) of the CeO_2 and $Pd_{0.09}Ce_{0.91}O_{2-\delta}$ samples are shown in Figure 3.4. The two samples show an initial weight loss is the temperature range of 30-150 °C. Powdered CeO_2 is known to be slightly hydroscopic and it also absorbs small amount of carbon dioxide from the atmosphere. Thus, for the ceria samples, the weight loss observed below 150 °C can be attributed to both water and carbon dioxide loss. Furthermore, no weight loss was observed from 150-1000 °C in the ceria sample. For the $Pd_{0.09}Ce_{0.91}O_{2-\delta}$ sample, a second weight loss was observed at 760 °C (DTA) due to the thermal dissociation of the Pd-O bond to form metallic palladium [34,55]. Furthermore, the smooth nature of the weight loss change suggests that there are no intermediates formed before complete reduction to metallic palladium, implying that the reduction to the metallic state occurs in one step.

The elemental composition of the samples was analyzed using EDS. The EDS spectrum of CeO_2 shows the presence of three elements; cerium, oxygen and chlorine (from HCl), while the EDS spectrum of the $Pd_{0.09}Ce_{0.91}O_{2-\delta}$ sample shows the presence of palladium in addition to the other three elements (Figure 3.5). The SEM images of CeO_2 and $Pd_{0.09}Ce_{0.91}O_{2-\delta}$ samples have very similar surface morphology (Figure 3.5). In both samples, the particles are present in the form of different sized lumps or flakes with round-shaped structures. These types of structures are generated due to the nature of the solution combustion synthesis method, where gases escape giving rise to porosity. The BET surface area of the $Pd_{0.09}Ce_{0.91}O_{2-\delta}$ sample was found to be 19 m^2/g.

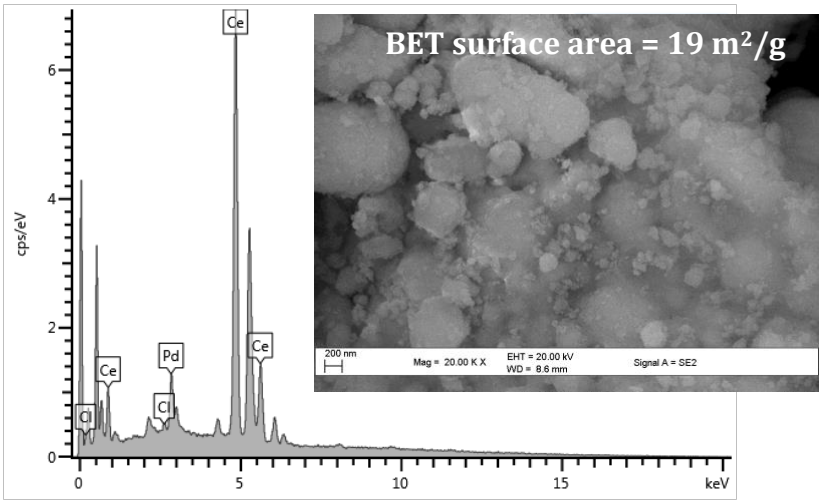

Figure 3.5: SEM/EDX $Pd_{0.09}Ce_{0.91}O_{2-\delta}$

Figure 3.6A shows the TEM image of the $Pd_{0.09}Ce_{0.91}O_{2-\delta}$ sample with average particle size 19 nm. These particles are spherical in shape. No particles associated with PdO or Pd nanoparticles were observed in the $Pd_{0.09}Ce_{0.91}O_{2-\delta}$ TEM images. Qiao et al. and other researchers have reported Pd particles as cubic and rectangular shaped particles [56-59]. Hence, the absence of these cubic and rectangular shaped particles in the $Pd_{0.09}Ce_{0.91}O_{2-\delta}$ sample further suggests that Pd^{2+} ions are substituted into the lattice structure of CeO_2, and are not supported on the surface of CeO_2 as PdO.

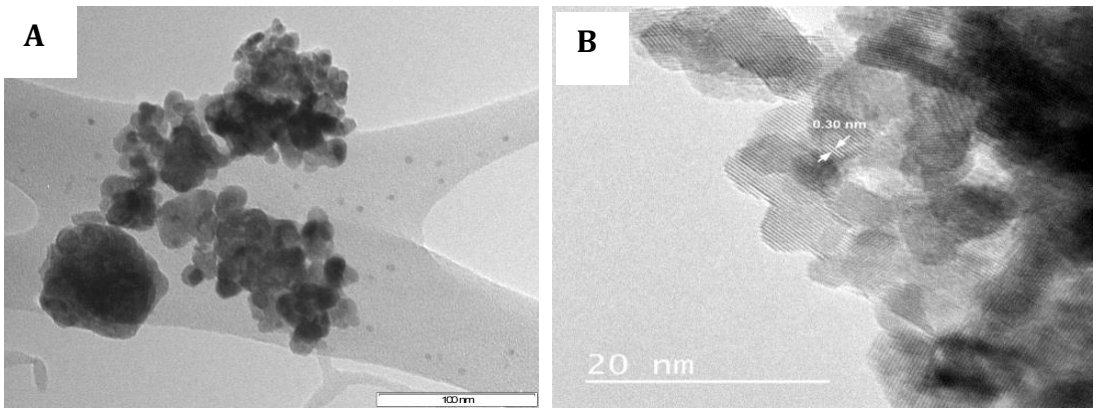

Figure 3.6: (A) TEM (B) HR-TEM images of $Pd_{0.09}Ce_{0.91}O_{2-\delta}$

The HR-TEM image of the solution combustion synthesized $Pd_{0.09}Ce_{0.91}O_{2-\delta}$ sample show lattice fringes of 0.30 nm (Figure 3.6B). There were no lattice fringes associated with PdO or Pd nanoparticles observed [60]. Again, the absence of PdO lattice fringes and the presence of peaks due to Pd in the EDS spectrum (Figure 3.5) of the $Pd_{0.09}Ce_{0.91}O_{2-\delta}$ sample further indicates that the Pd^{2+} ions are completely substituted into the CeO_2 lattice.

3.3.2 Catalyst activity investigation

To establish efficient Heck coupling conditions for the $Pd_{0.09}Ce_{0.91}O_{2-\delta}$ catalyst, methylacrylate and iodobenzene were used as model coupling partners. With this catalyst, neither copper salts nor activating ligands were necessary. In fact, addition of triphenylphosphine inhibited the reactions (Appendix 1, Table A1.5). The effect of each reaction parameter was then investigated and the optimum reaction conditions are highlighted in Table 3.2. Excellent yields were only obtained with polar aprotic solvents (DMF, benzonitrile and DMSO) and DMF was chosen as the solvent in further studies since it allowed easier product isolation. The reactions were more rapid at 130 °C and 1.5 olefin equivalence was found to be the optimum olefin loading. Potassium carbonate and triethylamine gave comparable yields, however, triethylamine was chosen as the base in further studies because it simplifies catalyst recovery. K_2CO_3 requires successive washes with water to remove it from the recovered catalyst. It was also found that for the model coupling partners, complete iodobenzene conversion was achieved in two hours with catalyst loading as low as 0.05 mol% (based on Pd). However, a 0.3 mol% loading was chosen for further studies to allow shorter reaction times for less reactive coupling partners. Further catalyst testing was carried out under the reaction conditions highlighted in bold in Table 3.2.

Table 3.2: Optimisation of reaction conditions for Heck coupling reactions

Reaction parameters	
Reaction temperature	25, 80 and **130** °C
Solvent	Anisole, benzonitrile, **DMF**, DMSO, toluene, water and xylene
Base	K_2CO_3 and **$(CH_3CH_3)_3N$**
Olefin equivalence	1, **1.5** and 2
Catalyst loading (based on Pd)	0.05, 0.1, **0.3**, 0.5 and 1 mol%

A wide range of olefins and aryl halides were then tested to investigate functional group tolerance, steric and electronic effects under optimum reaction conditions using $Pd_{0.09}Ce_{0.91}O_{2-\delta}$ as a catalyst. It is reported that both steric and electronic factors can favour arylation at the terminal position of the olefin or on the more exposed carbon [3,61,62]. Two sets of experiments were carried out to learn more about the catalyst activity. First, the olefins were varied and the aryl halide was kept constant as iodobenzene (Table 3.3 and 3.4). Secondly, the aryl halides were varied and the olefin was kept constant as methylacrylate (Table 3.5).

Aliphatic and aromatic olefins with electron withdrawing and donating group were arylated with iodobenzene and the results are tabulated in Table 3.3.

Entries 1-5 in Table 3.3 are of aliphatic olefins with varying functional groups. It was observed that olefins with electron withdrawing groups are easily arylated (Entries 1, 2, 4 and 5), with reaction times of less than an hour. However, Entry 3, which shows an olefin with an electron-donating group, has a longer reaction time. Entries 6-10 show the arylation of various styrene derivatives. The arylation of styrene (Entry 6) goes to completion in 2 hours, however, three products formed; predominantly *trans*-stilbene (78%), and *cis*-stilbene (19%) and 1,1-diphenylethene as minor products. These side products were not observed in the arylation of other styrene derivatives. The styrene derivative with a methyl or methoxy group as a substituent took longer to go to completion (Table 3.3, Entries 8, 9). This further confirms that electron donating substituents on olefins slow down the reaction. Hence, the electronic effect controls the catalyst activity for both cyclic and acyclic olefins.

Table 3.3: Investigation of electronic effects and functional group tolerances of functionalised olefins.

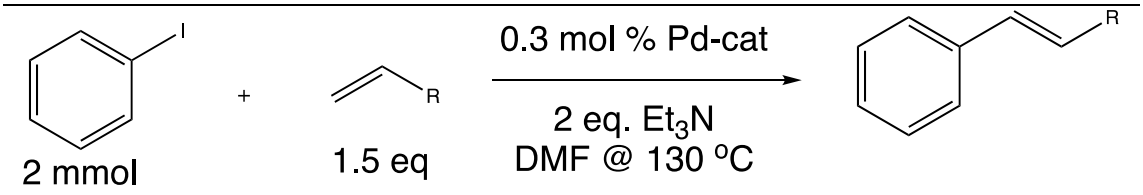

Entry	Alkene	Reaction time (h)	Isolated yield (trans) (%)	TON
1	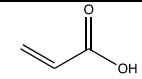	1	90	300
2	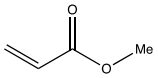	1	95	317
3	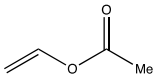	24	75	250
4	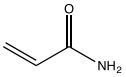	1	96	320
5	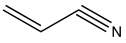	1	79	263
6	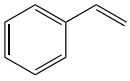	2	78	260
7	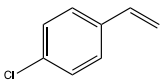	2	89	297
8	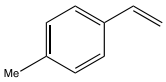	24	90	300
9	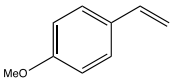	24	92	307
10	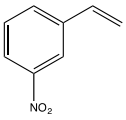	1	90	300

To investigate any possible steric effects, the reactivity of methylacrylate, ethyl crotonate and isobutylmethacrylate with iodobenzene was monitored (Table 3.4). It was found that steric effects play a major role in the catalysis. Thus, the reaction with methyacrylate went to completion in an hour, while it took 12 and 70 hours for isobutylmethacrylate and ethyl crotonate to react to completion, respectively. Isobutylmethacrylate (Table 3.4, Entry 2) has a 1,1 disubstitution and ethyl crotonate (Table 3.4, Entry 3) is 1,2-disubstituted. Thus, isobutylmethacrylate has a more exposed carbon-carbon double bond than ethyl crotonate, and hence it reacts faster. In conclusion, the Heck cross coupling reactions favour electron deficient and less hindered (less substituted) olefins.

Table 3.4: Investigation of steric effects on the Heck coupling reactions

Entry	Alkene	Reaction time (h)	Isolated yield (trans) (%)	TON
1	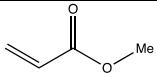	1	95	317
2	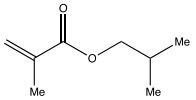	12	97	323
3	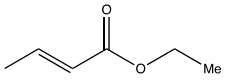	70	96	320

Table 3.5: Investigating the effect of varying the aryl iodide on the Heck coupling reactions.

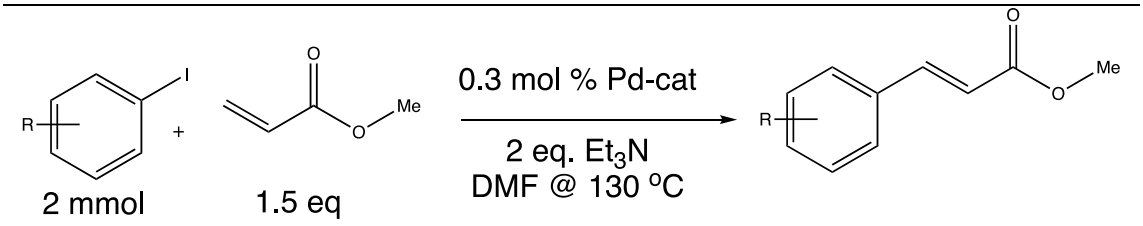

Entry	R	Reaction time (h)	Isolated yield (% trans)	TON
1	H	1	95	317
2	4-OH	2	75	250
3	4-CH_3	1	98	327
4	3-CH_3	3	96	320
5	4-NH_2	2	95	317
6	3-NH_2	4	92	307
7	4-$COCH_3$	2	90	300
8	3-$COCH_3$	2	94	313
9	4-NO_2	30	71	237
10	3-NO_2	7	75	250
11	3-CF_3	2	93	310

The scope of reactivity of various aryl halides was then investigated. It was found that aryl bromides and chlorides do not react under our optimum conditions. Various aryl iodides were then investigated to gain better understanding of the catalyst activity. With aryl iodides, both the electronic effect and substituent position effect were explored (Table 3.5). We found that most aryl iodides gave comparative reaction times; the electronic effect did not greatly influence the reactions (with an exception of iodonitrobenzenes). It was also observed that the position of the substituent on the aryl iodide has some influence in the reaction rate. Thus, Entries 3-4 show that the position of the methyl group influences the arylation rate of iodotoluene in that 4-iodotoluene is more reactive than 3-iodotoluene. The substituent position effect is more pronounced in Entries 9-10. In this case, 4-nitroiodobenzene is far less reactive than 3-nitroiodobenzene. It is unclear at this point how the substituents on aryl iodides affect the reactivity of the catalyst, however, the initial observation is that electron rich aryliodides are coupled more efficiently to methyl acrylate than to electron deficient aryliodides. This is discussed further in the reaction mechanism section.

Table 3.6: Performance comparison of the present catalyst in Heck cross coupling reactions of iodobenzene and styrene against other related heterogeneous catalysts.

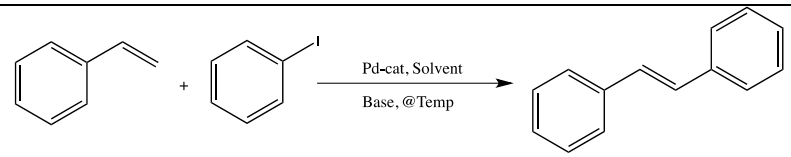

Entry	Catalyst	Reaction conditions	Time /h	Yield/%	[Ref.]
1	Pd/C 5% (0.05 mol% Pd)	Isooctane, H_2O, Aliquant 336, 100 °C	20	46	[63]
2	Pd-NPs/ZrO_2 (0.3 mol% Pd)	H_2O, TBAOH, 90 °C	4	81	[64]
3	Pd-complex/TiO_2 (0.12 mol% Pd)	MeOH, Na_2CO_3, 65 °C	7	30	[65]
4	$Ce_{0.98}Pd_{0.02}O_{2-\delta}$ (1.52 mol% Pd)	DMF, K_2CO_3, 130 °C	6	64	[66]
5	TiO_2@Pd (1 mol%)	DMF, $(CH_3CH_2)_3N$, 140 °C	10	93	[19]
6	$Pd_{0.09}Ce_{0.91}O_{2-\delta}$ (0.3 mol% Pd)	DMF, $(CH_3CH_2)_3N$, 130 °C	2	78	This paper

The product yield (stilbene) of the present catalytic system was compared to other heterogeneous, ligand-free palladium catalyzed Heck coupling reactions reported in literature (Table 3.6) [63-66]. The stilbene yield in this work was found to be comparable to those obtained by Nasrollahzadeh et al. and Monopoli

et al. [19,64]. However, the present catalyst system gives better results than those reported by Perosa et al., Karami et al. and Sanjaykmar et al. [63,65,66].

3.3.3 Used catalyst characterisation

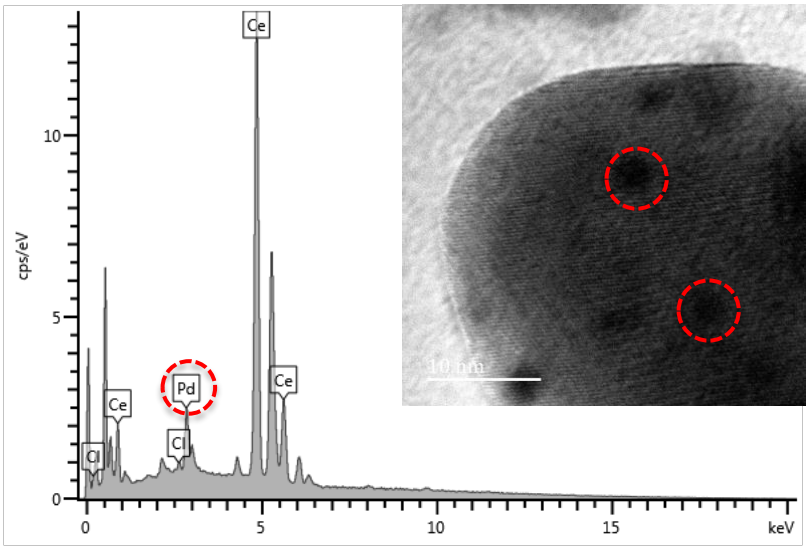

Figure 3.7: The EDS spectrum and TEM image (insert) of the recovered catalyst

The EDS spectrum of the used catalyst shows that it still contains palladium (Figure 3.7). It further indicated that the surface concentration of palladium in the used catalyst is not significantly different to that of the fresh catalyst. The TEM image of the used catalyst shows the presence of palladium nanoparticles on the surface of ceria, this indicates that palladium ions are extruded from the lattice of ceria during the reaction (Figure 3.7, insert).

The XRD pattern of the recovered catalyst also shows that the fluorite structure of the catalyst was intact; however, there is a small peak at 40° 2-θ, indicating the presence of Pd^0. This further suggests that Pd^{2+} ions are extruded from the lattice of ceria and sit on the surface as palladium nanoparticles (Figure 3.8). In addition, the STEM images of the used catalyst also show Pd^0 particles deposited on ceria (Figure 3.8, insert). This thus suggests that the single phase $Pd^{2+}_{0.09}Ce_{0.91}O_{2-\delta}$ solid solution is not the active species and that catalysis occurs instead over the reduced two phase Pd^0/CeO_2. Misch *et al.* reported similar observations for $Ce_{1-x}Pd_xO_{2-\delta}$ catalyzed C-H bond activation [33]. In their system, the $Ce_{1-x}Pd_xO_{2-\delta}$ material did not become active until it was significantly reduced by ethylene and hydrogen flowing over the catalyst.

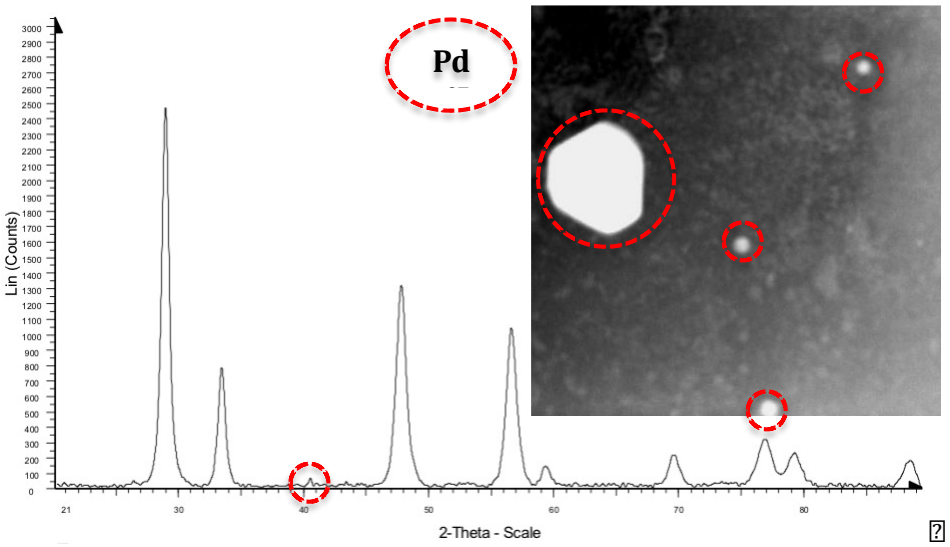

Figure 3.8: The XRD pattern and STEM image (insert) of the recovered catalyst

3.3.4 Catalyst leaching and recyclability tests

A mixture of $Pd_{0.09}Ce_{0.91}O_{2-\delta}$, iodobenzene, methylacrylate and triethylamine in DMF was stirred for an hour at 130 °C. After completion of the reaction, the catalyst was separated by centrifuge. (a) The mother liquor was analysed by ICP-OES for palladium content. (b) To the recovered catalyst, fresh substrates were added, namely iodobenzene, methylacrylate, triethylamine, and stirred in DMF at 130 °C for an hour. After completion of the reaction, the catalyst was separated by centrifuge, and parts (a) and (b) were repeated. This process was repeated three times and the results are tabulated in Table 3.7.

Table 3.7: Leaching and recyclability test[a]

	Reaction time/h	% Conversion	Amount Pd leached (ICP) / ppm
Cycle 1	1	100	0.35
Cycle 2	1	98	0.35
Cycle 3	1	98	0.25

[a]Pd content in fresh catalyst = 390 ppm

The catalyst was recycled successfully three times without any significant loss in activity. However, the ICP results show that there was a minimal metal contamination of the products; a total of about 0.25% of palladium leached out of the $Pd_{0.09}Ce_{0.91}O_{2-\delta}$ solid solution over the three cycles. When the filtrate from cycle one was stirred with methylacrylate and 3-iodoacetophenone only 15% conversion was achieved in two hours, as compared to 100% conversion with the fresh catalyst. This implies that the reaction mechanism of the filtrate is

different to that of the fresh catalyst. Although these results suggest that the $Pd_{0.09}Ce_{0.91}O_{2-\delta}$ catalysed Heck coupling reactions are largely heterogeneous, reports in literature have shown that supported palladium catalyst are mostly reservoirs of active soluble zerovalent palladium species [2,67-70]. Thus there is a possibility of a dissolution-recapture mechanism, with ceria acting like a Pd^0 scavenger. In any case, the $Pd_{0.09}Ce_{0.91}O_{2-\delta}$ precatalyst has proven effective in minimisation of metallic waste and allows for simplification of work-up.

3.3.5 Proposed mechanism

There are two main proposed mechanisms for the palladium catalysed Heck coupling reaction using homogeneous catalysts, namely the Pd^0/Pd^{2+} and Pd^{2+}/Pd^{4+} catalytic cycles. For the heterogeneous Heck reaction discussed here, the mechanism is not clear. However, the catalytic activity data and the physicochemical properties of the fresh and used catalyst suggest that the reaction follows a Pd^0/Pd^{2+} catalytic cycle (Scheme 3.1). The XRD diffractogram and HR-TEM images of the used catalyst suggest that palladium extrudes from the ceria lattice and is deposited as palladium nanoparticles on the surface of ceria. Hence, we proposed that the first step in the reaction mechanism is 'pre-activation' which allows $Pd^{2+}{}_{0.09}Ce_{0.91}O_{2-\delta}$ to enter the catalytic cycle as Pd^0/CeO_2 (**1**). The Pd^{2+} ions in the fresh catalyst are reduced *in situ* by DMF and/or triethylamine to Pd^0 [14,71,72]. Since Pd^0 is more electron rich than Pd^{2+}, it allows for oxidative addition of the aryl iodide, which marks the beginning of the catalytic cycle (**2**).

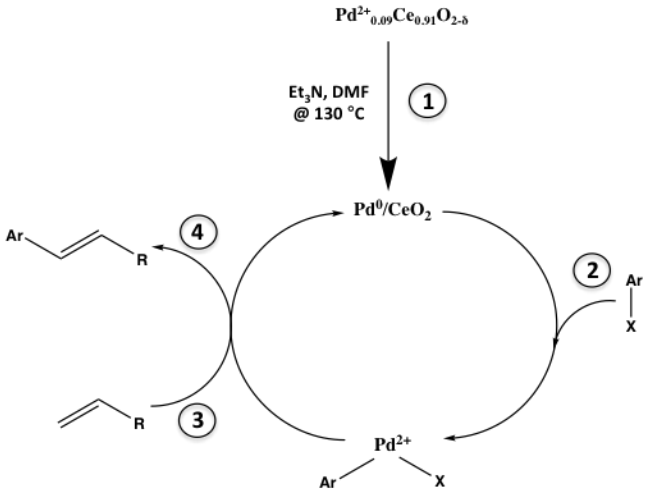

Scheme 3.1: Proposed Heck coupling reaction mechanism catalysed by the $Pd_{0.09}Ce_{0.91}O_{2-\delta}$ precatalyst.

The olefin coordinates and forms a pi complex with palladium (**3**). The catalytic results suggest that this olefin insertion is likely the rate-determining step. The oxidative addition step cannot be the rate-limiting step, since varying aryl

iodides gave comparable activity. Similar observations were reported by de Vries et al., who suggested that oxidative addition only becomes a rate-determining step under ligand-free Heck coupling of aryl bromide [73]. Olefin insertion is then followed by β-hydride elimination, and the dissociation of the product moiety liberates the reaction product (**4**). The active catalyst is then regenerated through reductive elimination of hydrogen by the base triethylamine.

3.4 Conclusions

In conclusion, a more highly Pd substituted ceria catalyst (9 mol%), $Pd_{0.09}Ce_{0.91}O_{2-\delta}$ was prepared, characterized by various techniques and shown to be catalytically active towards the Heck coupling reaction between aryl iodides and alkenes. The physicochemical properties of this material indicate that the Pd^{2+} ions are substituted in the lattice structure of ceria and not deposited on its surface as PdO. However, used catalyst characterisation revealed that the catalysis occurs over the reduced two phase Pd^0/CeO_2 and not on the as prepared monophasic $Pd_{0.09}Ce_{0.91}O_{2-\delta}$. Good to excellent yields of substituted olefins were obtained with the $Pd_{0.09}Ce_{0.91}O_{2-\delta}$ precatalyst when tested on ligand-free Heck coupling reactions. The Heck reactions were also shown to be affected by electronic and steric effects. Electron deficient olefins react more rapidly compared to electron rich olefins. In addition, an olefin with a more exposed carbon-carbon double bond also reacts more rapidly. Finally, the active catalyst (Pd^0/CeO_2) can be easily recovered and reused for at least three times without any significant loss in efficiency and only a negligible amount of palladium was detected in the product solution (0.35 ppm).

3.5 Acknowledgements

We would like to express our gratitude to Mintek and the Department of Science and Technology, South Africa (Advanced Metals Initiative program) for financial support. The authors would also like to thank Dr M Shozi, Dr S Mohamed, Dr S Singh and the rest of the UKZN catalysis research group for helpful discussions.

3.6 References

1. J.C. Hierso, *Angewandte Chemie International Edition*, 53 (2014) 920-922.
2. A. Biffis, M. Zecca, M. Basato, *Journal of Molecular Catalysis A: Chemical*, 173 (2001) 249-274.
3. R.F. Heck, J.P. Nolley, *Journal of Organic Chemistry*, 37 (1972) 2320-2322.
4. T. Mizoroki, K. Mori, A. Ozaki, *Bulletin of the Chemical Society of Japan*, 44 (1971) 581-581.
5. S. Sisodiya, L.R. Wallenberg, E. Lewin, O.F. Wendt, *Applied Catalysis A: General*, 503 (2015) 69-76.

6. J. Xiao, Z. Lu, Y. Li, *Industrial & Engineering Chemistry Research*, 54 (2015) 790-797.
7. X.U. Qijie, S.H.I. Wenzhong, Z.U.O. Chunshan, L.I.U. Dayong, Y.A.N.G. Chun, Z.H.A.O. Xiang, L.I.U. Pengcheng, *Chinese Journal of Applied Chemistry*, 32 (2015) 428-437.
8. C. Battilocchio, B.N. Bhawal, R. Chorghade, B.J. Deadman, J.M. Hawkins, S.V. Ley, *Israel Journal of Chemistry*, 54 (2014) 371-380.
9. M. Hosseini-Sarvari, Z. Razmi, M.M. Doroodmand, *Applied Catalysis A: General*, 475 (2014) 477-486.
10. C. Pavia, F. Giacalone, L.A. Bivona, A.M.P. Salvo, C. Petrucci, G. Strappaveccia, L. Vaccaro, C. Aprile, M. Gruttadauria, *Journal of Molecular Catalysis A: Chemical*, 387 (2014) 57-62.
11. A. de Meijere, F.E. Meyer, *Angewandte Chemie International Edition*, 33 (1995) 2379-2411.
12. I.P. Beletskaya, A.V. Cheprakov, *Chemical Reviews*, 100 (2000) 3009-3066.
13. D. Mc Cartney, P.J. Guiry, *Chemical Society Reviews*, 40 (2011) 5122-5150.
14. L. Yin, J. Liebscher, *Chemical Reviews*, 107 (2007) 133-173.
15. K. Köhler, R.G. Heidenreich, J.G. Krauter, J. Pietsch, *Chemistry: A European Journal*, 8 (2002) 622-631.
16. A. Kumbhar, *Topics in Current Chemistry*, 375 (2016) 2-29.
17. M. Islam, P. Mondal, K. Tuhina, A.S. Roy, *Journal of the Brazilian Chemical Society*, 22 (2011) 319-326.
18. H. Doucet, *Angewandte Chemie International Edition*, 53 (2014) 629-629.
19. M. Nasrollahzadeh, A. Azarian, A. Ehsani, M. Khalaj, *Journal of Molecular Catalysis A: Chemical*, 394 (2014) 205-210.
20. A. Banazadeh, A. Pirisedigh, F. Aryanasab, H. Salimi, S. Shafiei-Haghighi, *Inorganica Chimica Acta*, 429 (2015) 132-137.
21. J.W. Brown, N.N. Jarenwattananon, T. Otto, J.L. Wang, S. Gloggler, L. Bouchard, *Catalysis Communications*, 65 (2015) 105-107.
22. B. Movassagh, F.S. Parvis, M. Navidi, *Applied Organometallic Chemistry*, 29 (2015) 40-44.
23. A. Naghipour, A. Fakhri, *Catalysis Communications*, 73 (2016) 39-45.
24. S. Sobhani, Z.M. Falatooni, S. Asadi, M. Honarmand, *Catalysis Letters*, 146 (2015) 255-268.
25. S. Sobhani, Z. Zeraatkar, F. Zarifi, *New Journal of Chemistry*, 39 (2015) 7076-7085.
26. L. You, W. Zong, G. Xiong, F.; Ding, S. Wang, B. Ren, I. Dragutan, V. Dragutan, Y. Sun, *Applied Catalysis A: General*, 511 (2016) 1-10.
27. J. Demel, M. Lamac, J. Cejka, P. Stepnicka, *ChemSusChem*, 2 (2009) 442-451.
28. Z. Li, J. Chen, W. Su, M. Hong, *Journal of Molecular Catalysis A: Chemical*, 328 (2010) 93-98.

29. A.R. Hajipour, N.S. Tadayoni, Z. Khorsandi, *Applied Organometallic Chemistry*, 30 (2016) 590-595.
30. N. Kann, *Molecules*, 15 (2010) 6306-6331.
31. S.J. Tabatabaei Rezaei, A. Shamseddin, A. Ramazani, A. Mashhadi Malekzadeh, P. Azimzadeh Asiabi, *Applied Organometallic Chemistry*, 31 (2017) e3707.
32. J.A. Kurzman, J. Li, T.D. Schladt, C.R. Parra, X. Ouyang, R. Davis, J.T. Miller, S.L. Scott, R. Seshadri, *Inorganic Chemistry*, 50 (2011) 8073-8084.
33. L.M. Misch, J.A. Kurzman, A.R. Derk, Y.I. Kim, R. Seshadri, H. Metiu, E.W. McFarland, G.D. Stucky, *Chemistry of Materials*, 23 (2011) 5432-5439.
34. J.A. Kurzman, L.M. Misch, R. Seshadri, *Dalton Transactions*, 42 (2013) 14653-14667.
35. M. Narayanappa, V.D.B.C. Dasireddy, H.B. Friedrich, *Applied Catalysis A: General*, 135 (2012) 135-143.
36. T. Cwele, N. Mahadevaiah, S. Singh, H.B. Friedrich, *Applied Catalysis B: Environmental*, 182 (2016) 1-14.
37. T. Cwele, N. Mahadevaiah, S. Singh, H.B. Friedrich, A.K. Yadav, S.N. Jha, D. Bhattacharyya, N.K. Sahoo, *Catalysis Science & Technology*, 6 (2016) 8104-8116.
38. M.S. Hegde, G. Madras, K.C. Patil, *Accounts of Chemical Research*, 42 (2009) 704-712.
39. T. Baidya, G. Dutta, M.S. Hegde, U.V. Waghmare, *Dalton Transactions*, (2009) 455-464.
40. T. Baidya, A. Gupta, P.A. Deshpandey, G. Madras, M.S. Hegde, *Journal of Physical Chemistry C*, 113 (2009) 4059-4068.
41. P. Bera, K.C. Patil, V. Jayaram, G.N. Subbanna, M.S. Hegde, *Journal of Catalysis*, 196 (2000) 293-301.
42. P. Bera, K.R. Priolkar, P.R. Sarode, M.S. Hegde, S. Emura, R. Kumashiro, N.P. Lalla, *Chemistry of Materials*, 14 (2002) 3591-3601.
43. A. Gayen, K.R. Priolkar, P.R. Sarode, V. Jayaram, M.S. Hegde, G.N. Subbanna, S. Emura, *Chemistry of Materials*, 16 (2004) 2317-2328.
44. A. Gupta, A. Kumar, U.V. Waghmare, M.S. Hegde, *Chemistry of Materials*, 21 (2009) 4880-4891.
45. S. Roy, M.S. Hegde, *Catalysis Communications*, 9 (2008) 811-815.
46. S. Roy, A. Marimuthu, M.S. Hegde, G. Madras, *Catalysis Communications*, 9 (2008) 101-105.
47. P. Singh, M.S. Hegde, *Dalton Transactions*, 39 (2010) 10768-10780.
48. P. Singh, M.S. Hegde, *Chemistry of Materials*, 21 (2009) 3337-3345.
49. P. Singh, M.S. Hegde, J. Gopalakrishnan, *Chemistry of Materials*, 20 (2008) 7268-7273.
50. K.C. Patil, M.S. Hegde, T. Rattan, S.T. Aruna*, Chemistry of Nanocrystalline Oxide Materials: Combustion Synthesis, Properties and Applications; World Scientific: 5 toh tuck link, Singapore*, 2008, pp. 9-41.

51. R.V. Gulyaev, T.Y. Kardash, S.E. Malykhin, O.A. Stonkus, A.S. Ivanova, A.I. Boronin, *Physical Chemistry Chemical Physics*, 16 (2014) 13523-13539.
52. R.V. Gulyaev, A.I. Stadnichenko, E.M. Slavinskaya, A.S. Ivanova, S.V. Koscheev, A.I. Boronin, *Applied Catalysis A: General*, 439 (2012) 41-50.
53. K.R. Priolkar, P. Bera, P.R. Sarode, M.S. Hegde, S. Emura, R. Kumashiro, N.P. Lalla, *Chemistry of Materials*, 14 (2002) 2120-2128.
54. S. Colussi, A. Gayen, M. Farnesi Camellone, M. Boaro, J. Llorca, S. Fabris, A. Trovarelli, *Angewandte Chemie International Edition*, 48 (2009) 8481-8484.
55. S. Hinokuma, H. Fujii, M. Okamoto, K. Ikeue, M. Machida, *Chemistry of Materials*, 22 (2010) 6183-6190.
56. Z.A. Qiao, Z. Wu, S. Dai, *ChemSusChem*, 6 (2013) 1821-1833.
57. H. Zhang, M. Jin, Y. Xia, *Angewandte Chemie International Edition*, 51 (2012) 7656-7673.
58. W. Niu, L. Zhang, G. Xu, *Nanoscale*, 5 (2013) 3172-3181.
59. Y. Xia, Y. Xiong, B. Lim, S.E. Skrabalak, *Angewandte Chemie International Edition*, 48 (2009) 60-103.
60. C. Rossy, J. Majimel, M.T. Delapierre, E. Fouquet, F.X. Felpin, *Applied Catalysis A: General*, 482 (2014) 157-162.
61. A. King, N. Yasuda, *In Organometallics in Process Chemistry, Springer Berlin Heidelberg,* 2004, pp. 205-245.
62. E. Mieczyńska, A. Gniewek, I. Pryjomska-Ray, A. M. Trzeciak, H. Grabowska, M. A. Zawadzki, *Applied Catalysis A: General*, 393 (2011) 195-205.
63. A. Perosa, P. Tundo, M. Selva, S. Zinovyev, A. Testa, *Organic & Biomolecular Chemistry*, 2 (2004) 2249-2252.
64. A. Monopoli, A. Nacci, V. Calò, F. Ciminale, P. Cotugno, A. Mangone, L.C. Giannossa, P. Azzone, N. Cioffi, *Molecules*, 15 (2010) 4511-4525.
65. K. Karami, M.B. Shehni, N. Rahimi, *Applied Organometallic Chemistry*, 27 (2013) 437-443.
66. S.R. Sanjaykumar, B. Mukri, S. Patil, G. Madras, M.S. J. Hegde, *Chemical Science*, 123 (2011) 47-54.
67. F. Zhao, B.M. Bhanage, M. Shirai, M. Arai, *Chemistry: A European Journal*, 6 (2000) 843-848.
68. P. Albers, J. Pietsch, S.F. Parker, *Journal of Molecular Catalysis A: Chemical*, 173 (2001) 275-286.
69. J.A. Gladysz, *Recoverable and Recyclable Catalysts, John Wiley & Sons, Ltd: Chichester, United Kingdom*, 2009, pp. 1-45.
70. R.L. Augustine, S.T. O'Leary, *Journal of Molecular Catalysis A: Chemical*, 95 (1995) 277-285.
71. A. Jutand, *The Mizoroki-Heck Reaction, John Wiley & Sons, Ltd., Chichester, United Kingdom,* 2009, pp. 6-50.

72. J.P. Collman, R.G. Finke, J.R. Norton, *Principles and Applications of Organotransition Metal Chemistry, 2nd ed., University Science Books, Mill Valley, California,* 1987, pp. 1145-1146.
73. A.H.M. de Vries, J.M.C.A. Mulders, J.H.M. Mommers, H.J.W. Henderickx, J.G. de Vries, *Organic Letters*, 5 (2003) 3285-3288.

Chapter 4

$Pd_{0.02}Ce_{0.98}O_{2-\delta}$: A copper- and ligand-free quasi-heterogeneous catalyst for aquacatalytic Sonogashira cross-coupling reactions.

Abstract

A $Pd_{0.02}Ce_{0.98}O_{2-\delta}$ solid solution oxide was synthesized in one-step using a urea-assisted solution combustion method. XRD, ICP-OES, BET, XPS, SEM, EDX, TEM, TGA and Raman spectroscopy were used to study the structural and electronic properties of the as-prepared $Pd_{0.02}Ce_{0.98}O_{2-\delta}$ catalyst. The catalyst testing results revealed that the $Pd_{0.02}Ce_{0.98}O_{2-\delta}$ system performs as an efficient precatalyst for the Sonogashira cross-coupling reactions under copper- and ligand-free conditions. A wide range of iodoarenes were efficiently coupled to phenylacetylene with good to excellent isolated yields. A thorough investigation through a series of suitable experiments explicitly showed that the Sonogashira cross-coupling reaction is accomplished via a quasi-heterogeneous mechanism by the leached Pd(0) species. As a result, the $Pd_{0.02}Ce_{0.98}O_{2-\delta}$ lost some activity upon recycling.

Keywords: Pd^{2+} substituted ceria, solution combustion, nanoparticles and Sonogashira coupling reactions.

4.1 Introduction

The Sonogashira cross-coupling reaction is a great procedure for C-C bond formation between vinyl- or aryl halides and terminal alkynes [1-3]. Sonogashira *et al.* discovered it in 1975 by recognizing that the addition of copper(I) iodide significantly accelerates the alkenylation reaction that was conventionally catalysed by palladium–phosphane complexes [1,3]. Their discovery gained great interest since the products of this reaction are important intermediates in the synthesis of organic materials, pharmaceuticals and natural products [1-8]. For example, the Sonogashira coupling procedure is used in the synthesis of the drug Terbinafine, which is used as an antifungal agent [9,10].

In most cases, the conventional Sonogashira coupling reactions are carried out under homogeneous conditions, which involve using palladium complexes such as $[PdCl_2(PPh_3)_2]$ or $[Pd(PPh_3)_4]$ (3–5 mol%), a catalytic amount of a Cu salt (3-

10 mol%) and an amine in large excess [1,3,11,12]. The use of copper salts as co-catalysts accelerates the Sonogashira reaction greatly, however, its presence in the reaction gives alkyne dimers [13]. This leads to the generation of an undesired homocoupling product of the alkyne upon oxidation. Thus, the reaction must be conducted under inert atmosphere if a Cu salt is to be used as a co-catalyst [13]. Furthermore, the above-mentioned standard conditions require a high loading of palladium and involve use of phosphine ligands that are usually oxygen sensitive [5]. In addition, the efficient separation and subsequent recycling of homogenous palladium catalysts and ligand remains a challenge and an aspect of environmental and economic relevance [14].

Intensive studies on heterogenization of Sonogashira coupling reactions with the objective to combine the benefits of both heterogeneous and homogeneous catalysis have been carried out during the last three decades [15]. In this direction, researchers have immobilised Pd on solid supports such as activated carbon (charcoal) [16], zeolites [17], metal oxides [5,6,14,18] (MgO, ZnO, TiO_2, ZrO_2, Fe_2O_3, CeO_2, etc.), clays [19], alkaline earth salts ($CaCO_3$, $BaSO_4$, $BaCO_3$, $SrCO_3$) [20] and organic polymers [21,22]. However, the leaching of palladium from the catalyst is still the main problem, even though most researchers have reported that their catalysts can be recycled by the redeposition of Pd onto the support [23]. This is due to the quasi-heterogeneous mechanism of the Sonogashira cross-coupling reaction via the solvated palladium clusters [24].

Hence, quasi-heterogeneous catalysis has developed into a new stream in catalysis and it is a promising approach for bridging heterogeneous and homogeneous catalysis [15]. Quasi-heterogeneous catalysis relies on the fact that nano-supports have a large surface areas, thus they can retain the activity and selectivity of the supported catalysts [15,25].

In this regard, we thought it would be worthwhile to develop a general catalytic system for a copper- and ligand-free quasi-heterogeneous Sonogashira coupling reaction catalyzed by a nano $Pd_{0\cdot02}Ce_{0\cdot98}O_{2-\delta}$ solid solution oxide. To the best of our knowledge, $Pd_xCe_{1-x}O_{2-\delta}$ based solid-solution oxides have never been investigated on the Sonogashira coupling reactions. Using an air, moisture and thermally stable quasi-heterogeneous $Pd_{0.02}Ce_{0.98}O_{2-\delta}$ solid solution oxide should offer higher activity, simplicity of workup, recyclability and minimization of metallic waste.

4.2 Experimental section

Cerium ammonium nitrate [$(NH_3)Ce(NO_3)_6$, 99.9%], palladium chloride [$PdCl_2$, 60%], urea [CH_4N_2O, 99.9%] were obtained from Sigma-Aldrich and were used without further purification.

4.2.1 Procedure for synthesis of $Pd_{0.02}Ce_{0.98}O_{2-\delta}$

The monophasic $Pd_{0.02}Ce_{0.98}O_{2-\delta}$ solid-solution oxide was prepared using a one-step urea-assisted solution combustion synthesis method described earlier.[26] The catalyst synthesis method involved preparation of a redox combustion mixture composed of stoichiometric amounts of metal precursors [$(NH_4)_2Ce(NO_3)_6$ and $PdCl_2$] and urea [NH_2CONH_2] in the ratio of 1.0:3.77 respectively, dissolved in water. The solution was then stirred at 100 °C for 10 minutes to evaporate water and reduce its volume to ~20 mL. The boiling solution was then introduced into a muffle furnace pre-heated at 400 °C and was kept in the furnace overnight. A light brown solid was obtained.

4.2.2 Catalyst characterisation

A Bruker D8 Advance diffractometer, equipped with a XRK900 furnace, generator (40 kV and 40 mA) and a Cu $K\alpha_{1/2}$ source (λ = 1.5406 Å) was used to record the powder X-ray diffraction patterns of the samples. The structures were refined by the Rietveld method using the Full Prof Suite-2000 program. The average crystallite size (*D*) and lattice strain (ε) of CeO_2 and $Pd_{0.02}Ce_{0.98}O_{2-\delta}$ were estimated from the modified Rietveld method and Williamson-Hall (W-H) plots.

ICP-OES was performed using a Perkin Elmer Optical Emission Spectrometer Optima 5300 DV. Standards (1000 ppm Ce and Pd) were purchased from Fluka.

Brunauer–Emmett–Teller (BET) surface area measurements were determined using a MicroMetrics TriStar 3000 porosimeter with N_2 as probe gas. About 0.4 g of each powder sample was degased overnight at 200 °C using a Micromeritics FlowPep 060 instrument prior to analysis.

SEM images were obtained with a Jeol JSM-6100 scanning microscope using a Bruker signal processing unit detector. The analysis was performed at random points along the surface of the catalyst. The samples were first mounted on aluminium stubs using a double-sided carbon tape; they were then coated with gold using a Polaron E5100 coating unit.

For TEM analysis, the samples were viewed on Joel JEM-1010 Electron Microscope. For high resolution TEM (HR-TEM) and scanning electron microscopy (STEM) analysis, the samples were viewed on Joel JEM-2100 Electron Microscope and the images captured were analysed using iTEM software. The powder samples were ultrasonically dispersed in ethanol and supported on a perforated carbon film mounted on a copper grid prior to analysis.

4.2.3 Catalyst testing: general procedure for Sonogashira coupling reactions

A dry two necked pear-shaped flask containing a stirrer bar, a condenser, 2 mL of H_2O and 6 mL of acetonitrile was charged with an aryl halide (2.3 mmol), phenylacetylene (2 eq.), triethylamine (5 eq.) and catalyst $Pd_{0.02}Ce_{0.98}O_{2-\delta}$ (0.05 mol% Pd). The reaction mixture was stirred and (usually) heated to 82 °C and its progress was monitored by GC and GC-MS. The iodoarene conversion was used to estimate the catalytic activity, using biphenyl as an internal standard. After the reaction had gone to completion, the reaction mixture was filtered and the filtrate was extracted with ethyl acetate and brine. The organic layer was then evaporated under reduced pressure and the residue was purified by flash chromatography on silica gel using EtOAc/hexane (8/2) as an eluent. The structure of the coupling product was confirmed by ^{1}H and ^{13}C NMR spectroscopy and the results were consistent with those reported in literature for substituted biphenylacetylenes [17].

4.2.4 General procedure for catalyst recovery and recyclability

The catalyst used in the first run was separated by centrifugation, washed with 5 mL acetonitrile, dried at 60 °C and reused as described for the fresh catalyst.

4.3 Results and discussion

The structural and electronic properties of the $Pd_{0\cdot02}Ce_{0\cdot98}O_{2-\delta}$ catalyst have been shown earlier by X-ray diffraction (XRD), XPS, XANES, Raman spectroscopy, EXAFS and high-resolution transmission electron microscopy (HR-TEM) [26]. The characterisation results indicated that the prepared material was a solid solution oxide with a fluorite structure. The Rietveld refined XRD profile of the prepared catalyst and the XPS of the Pd(3d) are shown in Figure 4.1.

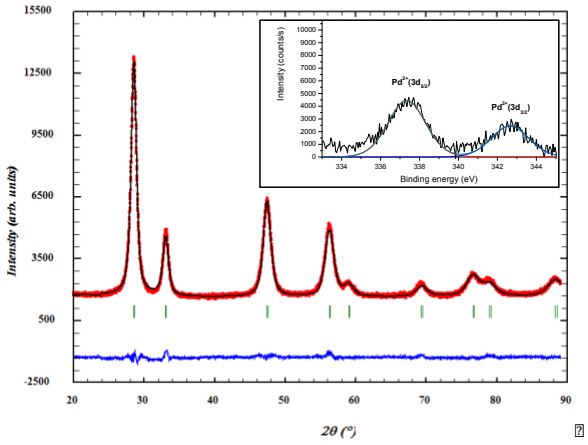

Figure 4.1: The Rietveld refined XRD patterns of $Pd_{0.02}Ce_{0.98}O_{2-\delta}$ and its XPS of Pd(3d) core level region (insert)

The X-ray pattern corresponds to a monophasic $Pd_{0.02}Ce_{0.98}O_{2-\delta}$ solid-solution oxide with a fluorite structure as reported earlier [26]. The insert in Figure 4.1 shows the XPS of the Pd(3d). The binding energy of Pd($3d_{5/2}$) and Pd($3d_{3/2}$) at 337.5 and 342.5 eV respectively, confirm that Pd is in the +2 oxidation state. The crystallite size and the lattice strain were estimated employing Williamson-Hall (W-H) plots and equation (1). The lattice strain in the $Pd_{0.02}Ce_{0.98}O_{2-\delta}$ sample was four times greater than in the CeO_2 sample (Table 4.1). This indicates that lattice distortion occurs upon introduction of Pd^{2+} ions in the CeO_2 lattice. The average crystallite size increased slightly with the incorporation of the Pd^{2+} ions into the CeO_2 lattice. The average crystallite size of the blank CeO_2 is 8 nm, while that of $Pd_{0.02}Ce_{0.98}O_{2-\delta}$ increased to 13 nm.

$$\beta_{hkl}\cos\theta = \frac{K\lambda}{D} + 4\varepsilon\sin\theta \qquad (1)$$

Table 4.1: Physicochemical properties of the synthesised materials.

Catalyst	Lattice parameter a (Å)	Lattice strain (10^{-3})	Crystallite size (nm)	Surface area (m^2/g)
CeO_2	5.4221	1.10	8	69
$Pd_{0.02}Ce_{0.98}O_{2-\delta}$	5.4200	4.20	13	58

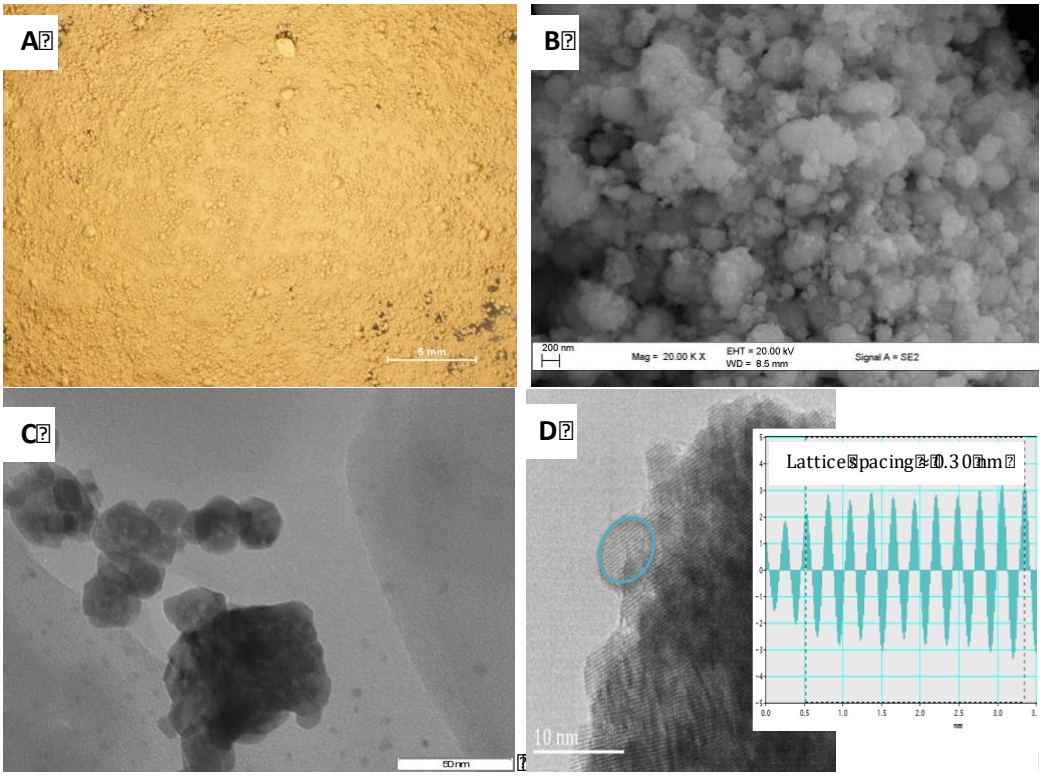

Figure 4.2: Light microscopy (A) SEM (B) TEM (C) and HR-TEM (D) analysis of the $Pd_{0.02}Ce_{0.98}O_{2-\delta}$ catalyst.

The SEM and TEM images of CeO_2 and $Pd_{0.02}Ce_{0.98}O_{2-\delta}$ samples have very similar morphology (Figure 4.2). In both samples, the particles are present in the form of different sized lumps or flakes with rounded shaped structures. These types of structures are generated due to the nature of the solution combustion synthesis method, where gases escape giving rise to porosity. The BET surface area of the $Pd_{0.02}Ce_{0.98}O_{2-\delta}$ sample was found to be 58 m^2/g (Table 4.1).

The catalytic performance of the as prepared $Pd_{0.02}Ce_{0.98}O_{2-\delta}$ solid-solution precatalyst was evaluated in the Sonogashira coupling of phenylacetylene and various haloarenes and the results are listed in Table 4.2. Optimisation of reaction conditions was conducted in order to develop a general catalytic system for the copper- and ligand-free $Pd_{0.02}Ce_{0.98}O_{2-\delta}$ catalysed Sonogashira coupling reaction. Solvent, temperature, alkyne loading, base and catalyst loading investigations were conducted using phenylacetylene (**1**) and iodobenzene (**2**) as model coupling partners (Scheme 4.1).

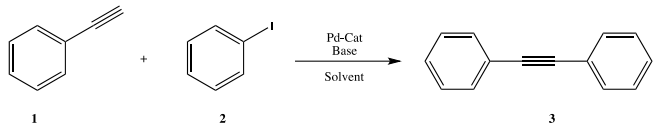

Scheme 4.1: The model Sonogashira cross-coupling reaction between phenylacetylene (1) and iodobenzene (2) leading to biphenylacetylene (3)

We first conducted investigations to find a solvent system that is conducive for the Sonogashira coupling reaction (Figure 4.3). The solvent systems investigated were: acetonitrile (CH_3CN), DMF, toluene (PhMe), "solvent-less" and H_2O/CH_3CN (1:3 v/v). Toluene gave the lowest conversion of 32 % after 8 hours, while "solvent-free" and acetonitrile conditions gave relatively high conversion of 68% and 80% respectively. DMF gave 100 % conversion in 3 hours, while H_2O/acetonitrile (1:3 v/v) went to completion in an hour. Hence, further investigations were conducted in H_2O/acetonitrile (1:3 v/v). Böhm et al. reported that the polarity and hydrogen bonding ability of the solvent are important in accelerating the reaction by stabilizing the ionic intermediates of the catalytic cycle [4]. The solvent investigation results agree well with the above statement, since the reaction conducted in toluene has the longest reaction time and the lowest % conversion, while those conducted in aqueous acetonitrile had the shortest reaction time and gave 100 % conversion of phenylacetylene. The Böhm et al. findings also indirectly address the nature of catalysis for most Sonogashira coupling procedures (discussed later).

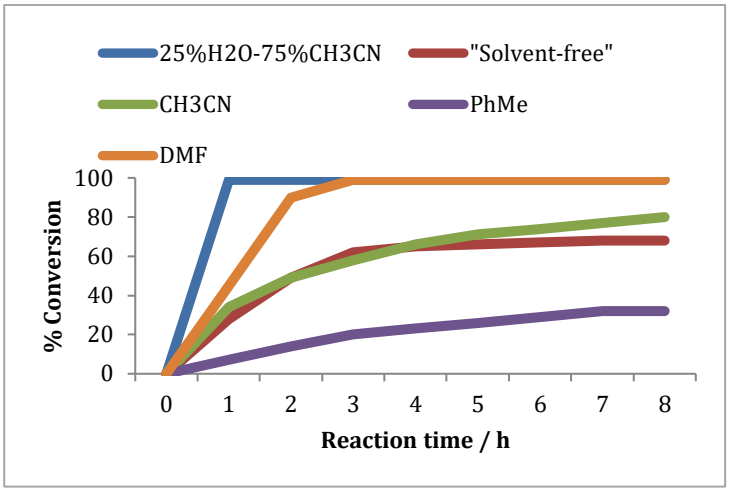

Figure 4.3: Solvent investigation results under the model Sonogashira coupling conditions. Reaction conditions: 2.3 mmol of iodobenzene, 1 mol% (based on Pd) of $Pd_{0.02}Ce_{0.98}O_{2-\delta}$, 2 equiv. phenylacetylene and 5 equiv. of Et_3N in a corresponding solvent system at 82 °C.

The choice of base is considered crucial in Sonogashira coupling reactions. The base is used to neutralise the acid (HX) formed as a by-product in this reaction [4]. In addition, the base plays a role in inhibiting the generation of a homo-coupling product (Glaser-type reaction) and its strength plays a key role in the deprotonation of terminal alkynes [4,27]. Amongst the investigated bases, triethylamine was found to be the best base under our reaction conditions (Table 4.2). The reaction went to completion in just an hour when triethylamine was used as base, while the reactions didn't go to completion with the other bases investigated (K_2CO_3, NaOH, CH_3COONa and Cs_2CO_3). It has been suggested that amines don't act as bases only, but also as weak coordinating ligands [28]. Hence, beside the observed solubility problem, when the inorganic bases were used, the fact that triethylamine can act as a coordinating base is thought to be a major reason for its superior performance.

Table 4.2: Investigating the effect of a base on the model Sonogashira cross-coupling reaction

Entry[a]	Base	Reaction time/h	Conversion/%
1	Cs_2CO_3	24	62
2	Et_3N	1	100
3	K_2CO_3	24	66
4	NaOAc	24	21
5	NaOH	24	48

[a]Reaction conditions: 2.3 mmol of iodobenzene, 1 mol% (based on Pd) of $Pd_{0.02}Ce_{0.98}O_{2-\delta}$, 2 equiv. phenylacetylene and 5 equiv. of the base in H_2O/acetonitrile (1:3 v/v) at 82 °C.

Three different temperatures were also investigated; 25, 50 and 82 °C (Figure 4.4). It was found that the reactions were most rapid under refluxing conditions (82 °C).

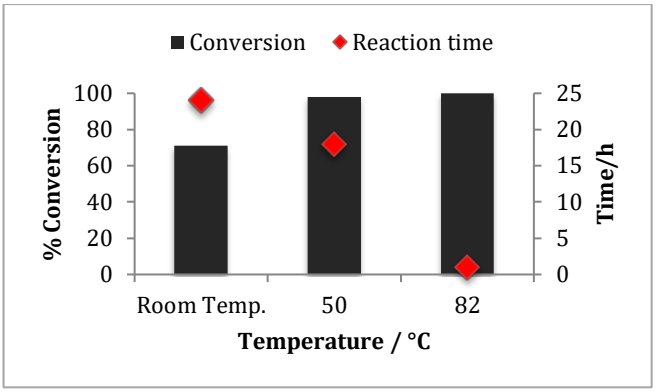

Figure 4.4: Investigating the effect of temperature on the model Sonogashira coupling reaction. Reaction conditions: 2.3 mmol of iodobenzene, 1 mol% (based on Pd) of $Pd_{0.02}Ce_{0.98}O_{2-\delta}$, 2 equiv. phenylacetylene and 5 equiv. of Et_3N in H_2O/acetonitrile (1:3 v/v) at investigated temperature.

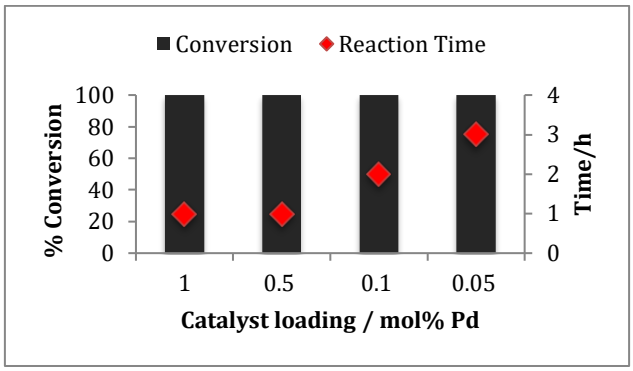

Figure 4.5: Catalyst loading investigation on the model Sonogashira coupling reaction. [a]Reaction conditions: 2.3 mmol of iodobenzene, 'X' mol% (based on Pd) of $Pd_{0.02}Ce_{0.98}O_{2-\delta}$, 2 equiv. phenylacetylene and 5 equiv. of Et_3N in H_2O/acetonitrile (1:3 v/v) at 82 °C.

Several experiments were conducted to find the lowest amount of the catalyst loading (based on Pd) that could efficiently catalyse the Sonogashira coupling reactions in reasonable reaction times (Figure 4.5). The investigations were initiated with catalyst loading between 0.05-1 mol%. For loadings of 0.1-1 mol%, the reaction was found to be to very fast, and the reaction went to completion in an hour. This fast reaction makes it difficult to monitor the substitution and electronic effect caused by the aryl halides. Hence, a catalyst loading of 0.05 mol% was investigated; this then gave a slower reaction that went to completion in 3 hours.

Table 4.3: Sonogashira cross-coupling of phenylacetylene with various iodoarenes to give substituted biphenylacetylenes under our optimum reaction conditions

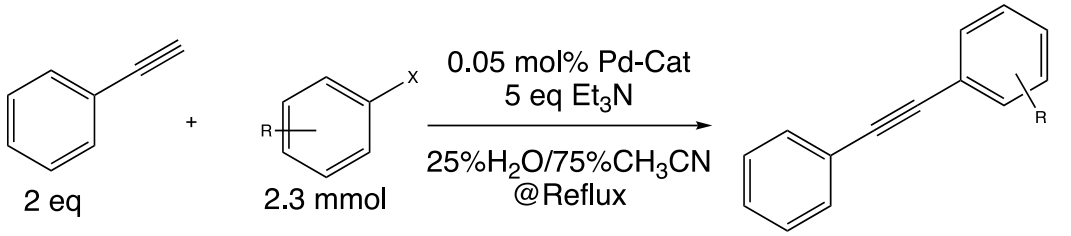

Entry	Iodoarene	Reaction time /h	Isolated yield / %
1	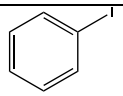	3	98
2	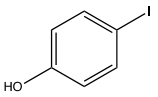	4	94
3	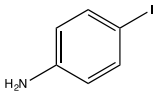	44	70
4	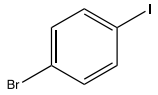	2	91
5	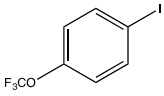	1	90
6	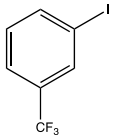	1	93
7	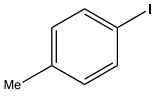	9	92
8	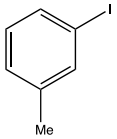	3	92
9	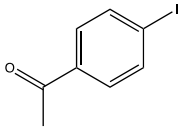	1	98
10	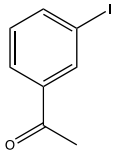	2	95
11	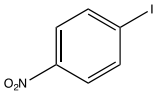	1	95
12	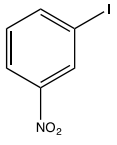	1	93

Hence, the obtained optimum conditions are limited to iodoarenes and aromatic alkynes as coupling partners only. Performance comparisons of the present catalyst in Sonogashira cross coupling reactions of iodobenzene and phenylacetylene against other related Cu- and ligand-free catalytic systems are shown in Table 4.4.

Table 4.4: Performance comparisons of catalysts in the reaction of iodobenzene and phenylacetylene under copper- and ligand free conditions.

Entry[ref]	Catalyst	Reaction conditions	Time /h	Yield /%
1[14]	Pd-$CoFe_2O_4$ (5 mol% Pd)	Ethanol, K_2CO_3, 70 °C	6	90
2[27]	Pd-2QC-MCM-41 (0.18 mol% Pd)	NMP, piperidine, 80 °C	3	99
3[5]	Pd-MgLa (1.5 mol% Pd)	DMF, Et_3N, 90 °C	10	90
4[19]	Pd^0/montmorill-onite (0.07 mol% Pd)	CH_3CN, Et_3N, 82 °C	3	90
5 (This paper)	$Pd_{0.02}Ce_{0.98}O_{2-\delta}$ (0.05 mol% Pd)	H_2O/CH_3CN (1:3), Et_3N, 82 °C	3	98

4.4 Leaching and recyclability test

A strong test for evaluating heterogeneity of a catalyst is the hot filtration test. To determine whether the reactions reported here were homogeneous or heterogeneous, a hot filtration test was performed for the Sonogashira coupling of phenylacetylene and iodobenzene. The catalyst was filtered-off from the reaction mixture after 5 min, and the hot filtrate was then allowed to react further under similar conditions. The reaction was then monitored every 15 min for 2 hours. Assessment of the rate of iodobenzene conversion from the fresh reaction and the hot filtration test suggests that the activity in the fresh reaction can be attributed to the Pd species in the solution (Figure 4.6). The fresh catalyst and the hot filtrate have almost identical reaction profiles (Figure 4.6). An ICP analysis of the filtered solution confirmed the presence of about 0.5 ppm of Pd in the hot filtrate.

Since the active catalytic phase was evidently the leached Pd, we attempted to determine the active Pd species using the mercury-poising test. Hg(0) is known to form amalgams with a variety of metals in their zero oxidation state [24].

Hence, if Pd dissociates from the solid $Pd_{0.02}Ce_{0.98}O_{2-\delta}$, it would bind with Hg(0) thereby quenching its catalytic activity. However, Pd in a raised oxidation state is not expected to be quenched by Hg(0) [24]. Thus, the mercury-poising test was used to establish whether bare Pd(0) did participate in catalysing the Sonogashira coupling reactions.

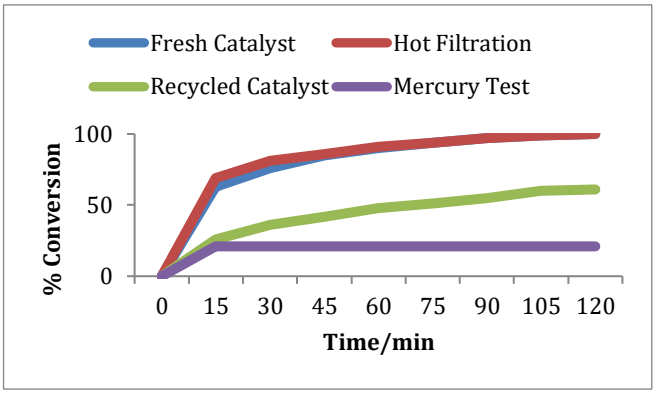

Figure 4.6: Reaction profiles of fresh catalyst, hot-filtration, recycled catalyst and mercury-poison tests.

To do the mercury poison test for the system described here, the $Pd_{0.02}Ce_{0.98}O_{2-\delta}$ catalyst was filtered-off from the reaction mixture after a reaction time of 5 min and 2.5 mmol Hg(0) was added to the hot reaction mixture. The reaction mixture was then allowed to react further under similar conditions, while monitoring the activity every 15 min. It was found that no further reaction occurred after 15 min. Thus, the analysis confirms the presence of Pd(0) in the solution, which in turn gives insight into the reaction mechanism. Hence, the $Pd_{0.02}Ce_{0.98}O_{2-\delta}$ catalyzed Sonogashira coupling reaction is essentially a quasi-heterogeneous catalytic process occurring over solvated Pd(0) clusters.

The recycled catalyst showed about 60 % conversion of iodobenzene in 2 hours. Hence, the recyclability test suggests that some of the leached Pd can redeposit on the CeO_2 support at the end of the Sonogashira reaction, and/or the $Pd_{0.02}Ce_{0.98}O_{2-\delta}$ serves as an active catalyst reservoir.

4.5 Proposed mechanism

The exact mechanism by which the quasi-heterogeneous $Pd_{0.02}Ce_{0.98}O_{2-\delta}$ catalyzed copper- and ligand-free Sonogashira coupling reaction occurs is still under examination. However, the catalytic activity results, leaching and recyclability tests seem to indicate that the reaction follows a Pd(0)/Pd(2+) mechanism (Scheme 4.2). We proposed that the first step in the reaction mechanism is 'pre-activation' which allows $Pd^{2+}{}_{0.02}Ce_{0.98}O_{2-\delta}$ to enter the catalytic cycle as Pd^0/CeO_2. The Pd(2+) ions in the fresh catalyst are reduced *in situ* by triethylamine and/or the solvent system (H_2O/acetonitrile) to Pd(0) [28,29].

Since Pd(0) is more electron rich than Pd(2+), it allows for oxidative addition of the iodoarene, which marks the beginning of the catalytic cycle. The alkyne coordinates and forms a pi complex with Pd and then the desired Sonogashira coupling product is generated through the reductive elimination step.

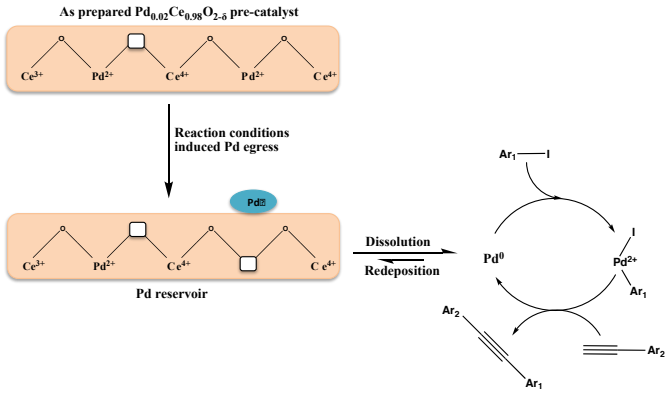

Scheme 4.2: A proposed reaction mechanism for $Pd^{2+}_{0.02}Ce_{0.98}O_{2-\delta}$ catalysed quasi-homogeneous Sonogashira cross-coupling reactions.

4.6 Conclusions

In conclusion, we have developed a general and simple process for Sonogashira coupling reactions using $Pd_{0.02}Ce_{0.98}O_{2-\delta}$ as a precatalyst. The catalyst was found to be very effective in a water/acetonitrile solvent system at 82 °C under ligand- and Cu-free reaction conditions. A wide range of iodorenes were coupled to phenylacetylene using this catalytic route. It was also found that the $Pd_{0.02}Ce_{0.98}O_{2-\delta}$ catalysed Sonogashira cross-coupling reactions are essentially a quasi-heterogeneous catalytic process occurring over solvated Pd(0) clusters. As a result, the recovered catalyst looses some activity upon recycle.

4.7 Acknowledgements

We would like to express our gratitude to Mintek and the Department of Science and Technology (Advanced Metals Initiative program) for financial support. The authors would also like to thank Dr AS Mohamed, Dr M Shozi and Dr S Singh for helpful discussions.

4.8 References

1. K. Sonogashira, Y. Tohda, N. Hagihara, *Tetrahedron Letters*, 16 (1975) 4467-4470.
2. S. Takahashi, Y. Kuroyama, K. Sonogashira, N. Hagihara, *Synthesis*, 1980 (1980) 627-630.
3. K. Sonogashira, *Journal of Organometallic Chemistry*, 653 (2002) 46-49.

4. V.P.W. Böhm, W.A. Herrmann, *European Journal of Organic Chemistry*, 2000 (2000) 3679-3681.
5. A. Cwik, Z. Hell, F. Figueras, *Tetrahedron Letters*, 47 (2006) 3023-3026.
6. M. Hosseini-Sarvari, Z. Razmi, M.M. Doroodmand, *Applied Catalysis A: General*, 475 (2014) 477-486.
7. D. Mujahidin, S. Doye, *European Journal of Organic Chemistry*, 2005 (2005) 2693-2693.
8. A.O. King, N. Yasuda, *Palladium-Catalyzed Cross-Coupling Reactions in the Synthesis of Pharmaceuticals: Organometallics in Process Chemistry, Springer Berlin Heidelberg, Berlin, Heidelberg*, 2004, pp. 205-245.
9. C. Torborg, M. Beller, *Advanced Synthesis & Catalysis*, 351 (2009) 3027-3043.
10. U. Beutler, J. Mazacek, G. Penn, B. Schenkel, D. Wasmuth, *Chimia*, 50 (1996) 154-156.
11. D.S. Rosa, F. Antelo, T.J. Lopes, N.F. de Moura, G.R. Rosa, *Quimica Nova*, 38 (2015) 605-608.
12. R. Ciriminna, V. Pandarus, G. Gingras, F. Béland, P. Demma Carà, M. Pagliaro, *ACS Sustainable Chemistry & Engineering*, 1 (2013) 57-61.
13. S. Sisodiya, L.R. Wallenberg, E. Lewin, O.F. Wendt, *Applied Catalysis A: General*, 503 (2015) 69-76.
14. S. Roy, K.K. Senapati, P. Phukan, *Research on Chemical Intermediates*, 41 (2015) 5753-5767.
15. R. Abu-Reziq, H. Alper, *Applied Sciences*, 2 (2012) 260.
16. C. Rossy, J. Majimel, M.T. Delapierre, E. Fouquet, F.X. Felpin, *Applied Catalysis A: General*, 482 (2014) 157-162.
17. L. Djakovitch, P. Rollet, *Advanced Synthesis & Catalysis*, 346 (2004) 1782-1792.
18. D.A. Kotadia, U.H. Patel, S. Gandhi, S.S. Soni, *RSC Advances*, 4 (2014) 32826-32833.
19. B.J. Borah, D.K. Dutta, *Journal of Molecular Catalysis A: Chemical*, 366 (2013) 202-209.
20. J.C. Barros, A.L.F. de Souza, P.G. de Lima, J.F.M. da Silva, O.A.C. Antunes, *Applied Organometallic Chemistry*, 22 (2008) 249-252.
21. Z.W. Ye, W.B. Yi, *Journal of Fluorine Chemistry*, 129 (2008) 1124-1128.
22. J.H. Kim, D.H. Lee, B.H. Jun, Y.S. Lee, *Tetrahedron Letters*, 48 (2007) 7079-7084.
23. R. Redon, N.G. Peña, F.R. Crescencio, *Recent Patents on Nanotechnology*, 8 (2014), 31-51.
24. A.J. Reay, I.J.S. Fairlamb, *Chemical Communucations,* 51 (2015), 16289-16307.
25. Y. Wu, D. Wang, P. Zhao, Z. Niu, Q. Peng, Y. Li, *Inorganic Chemistry*, 50 (2011) 2046-2048.

26. T. Cwele, N. Mahadevaiah, S. Singh, H.B. Friedrich, A.K. Yadav, S.N. Jha, D. Bhattacharyya, N.K. Sahoo, *Catalysis Science & Technology*, 6 (2016), 8104-8116.
27. K. Komura, H. Nakamura, Y. Sugi, *Journal of Molecular Catalysis A: Chemical*, 293 (2008) 72-78.
28. A. Tougerti, S. Negri, A. Jutand, *Chemistry: A European Journal*, 13 (2007) 666-676.
29. A. Jutand, S. Négri, A. Principaud, *European Journal of Inorganic Chemistry*, 2005 (2005), 631-635.

Chapter 5

PdCuCeO-TPAB: A new catalytic system for quasi-heterogeneous Suzuki-Miyaura cross-coupling reaction under ligand-free conditions in water.

Abstract

In this contribution, we report a simple and clean method for preparation of a single-phase $Pd_{0.04}Cu_{0.04}Ce_{0.92}O_{2-\delta}$ (PdCuCeO) solid-solution oxide and its application in quasi-heterogeneous Suzuki-Miyaura cross-coupling reactions. The catalyst was characterised fully and all the characterisation techniques strongly suggest that the Pd^{2+} and Cu^{2+} ions were succesfully incorporated into the lattice of ceria. The as-prepared PdCuCeO solid-solution oxide was tested on Suzuki-Miyaura cross-coupling reactions under ligand free conditions using water as a sole solvent and tetrapropylammonium bromide (TPAB) as a phase tranfer catalyst. It was discovered that TPAB acts as scavenger of Pd and the resulting material (Pd/TPAB) is able to catalyse the Suzuki-Miyaura coupling reaction. The Suzuki-Miyaura coupling of aryl iodides, bromides as well as activated aryl chlorides was efficiently performed by this PdCuCeO-TPAB catalytic system. The PdCuCeO-TPAB catalytic system also displayed good functional group tolerance and good to excellent isolated yields were obtained. Catalyst leaching and recyclability studies revealed that PdCuCeO acts as a Pd reservoir and that the reactions are essentially quasi-heterogeneous occuring over the recoverable Pd/TPAB aggregates. Only a negligible amount of palladium (<0.1 ppm) was detected by ICP-OES in the product solution.

Keywords: Suzuki cross coupling, solid-solution and Pd-subsituted ceria.

5.1 Introduction

The Suzuki–Miyaura (SM) cross-coupling reactions are characterized by the cross coupling of an organohalide or organotriflate and an aryl boronic acid to give a biaryl compound [1-3]. The SM cross-coupling reaction has become a useful strategy for the preparation of substituted biaryl compounds, which are essential building blocks for agricultural, pharmaceutical and engineering material industries [4-10]. The 2010 Nobel Prize in Chemistry, awarded to Akira Suzuki, Richard Heck and Ei-ichi Negishi, further demonstrated the significance of Pd-catalyzed cross coupling reactions [11]. Given the applicability of the SM

reactions, the design of a more sustainable procedure that uses inexpensive and easily prepared catalysts, environmentally friendly solvents and avoids the use of expensive ligands remains a goal of high practical value [12].

There is also a growing interest to finding a suitable replacement for palladium with cheaper metals such as iron, copper and nickel [13]. Moreover, Cu(I) salts and Cu_2O have been reported as co-reagents and co-catalysts in SM coupling reactions [14-19]. However, we think it is of equal importance to determine whether palladium catalysts can be better utilised to broaden their impressive reactivity [20]. Notably, Pd catalysts often display a higher reactivity than their alternatives, which enable them to easily catalyze less reactive substrates and achieve high catalyst turnover numbers (TONs) [21]. Furthermore, bimetallic nanoparticles supported on carbon (Pd-Cu/C, Pd-Ni/C and Pd-Ag/C) have also shown activity in SM coupling reactions [22]. The catalytic efficiency based on the yield of the desired product decreased in the following order: Pd-Cu/C > Pd/C > Pd-Ag/C > Pd-Ni/C [22,23]. Thathagar et al. also observed that the combined Pd/Cu nanoclusters displayed the highest activity among all the other combinations (Pd/Pt and Pd/Ru nanoclusters) [14].

Herein, we further investigated the Pd and Cu combination using the $Pd_{0.04}Cu_{0.04}Ce_{0.92}O_{2-\delta}$ (PdCuCeO) solid-solution oxide, instead of Pd-Cu/C or Pd/Cu nanoclusters, as a bimetallic catalyst for SM reactions. We have previously shown that substitution of Pd^{2+} and Cu^{2+} ions within the CeO_2 lattice allows for complete palladium and copper dispersion, which, as a result, increased the catalyst activity in CO oxidation [24,25] In addition, we also showed that the synergetic effect between palladium, copper and cerium ions improves the catalyst reducibility and as a result, it enhanced its performance in CO oxidation [24]. For this contribution, we wanted to further exploit the synergetic effect between Pd-Cu-Ce to hopefully enhance the reactivity of PdCuCeO in SM cross-coupling reactions.

Recently, a wealth of literature has been reported on supported Pd catalysts that catalyze SM cross-coupling reactions with high reactivity, good recyclability and minimal metal leaching [6-11,26-41]. However, the nature of the true catalyst is still unclear and the dominant view at present is that the mechanism of most C-C cross-coupling reactions is largely homogeneous irrespective of the type of catalyst precursor used [42-49]. Hence, the challenge of distinguishing heterogeneous from homogeneous catalysis when heterogeneous systems are developed is still a critical topic [7,9,42,50].

In this regard, we now report a “greener” and highly efficient procedure that can quasi-heterogeneously catalyse SM coupling using an easily prepared PdCuCeO solid-solution oxide that can be recovered and reused at end of the reaction. In

addition, we have eliminated the need for a ligand and utilise water as the sole solvent, since it is cheap, safe and environmentally friendly [27,31]. We also investigated the true nature of catalysis for this SM reaction by doing selective poisoning and hot-filtration tests.

5.2 Experimental

Cerium ammonium nitrate [$(NH_3)Ce(NO_3)_6$, 99.9%], palladium nitrate [$Pd(NO_3)_2$], copper nitrate [$Cu(NO_3)_2$], and urea [CH_4N_2O, 99.9%] were obtained from Sigma-Aldrich and were used without further purification.

5.2.1 Procedure for synthesis of $Pd_{0.04}Cu_{0.04}Ce_{0.92}O_{2-\delta}$

The monophasic $Pd_{0.04}Cu_{0.04}Ce_{0.92}O_{2-\delta}$ solid-solution oxide was prepared using a one-step urea-assisted solution combustion synthesis method described earlier [26]. The catalyst synthesis method involved preparation of a redox combustion mixture composed of stoichiometric amounts of metal precursors [$(NH_4)_2Ce(NO_3)_6$, $Pd(NO_3)_2$ and $Cu(NO_3)_2$] and urea [NH_2CONH_2] in the ratio of 1.0:3.68 respectively. The solution was then stirred at 150 °C for 10 minutes to evaporate water and reduce its volume to ≈20 mL. The boiling solution was then introduced into a muffle furnace pre-heated at 400 °C and was kept in the furnace for 5 hours. A light grey solid was obtained.

5.2.2 Catalyst testing: general procedure for coupling reactions

A dry two necked pear-shaped flask containing a stirrer bar, a condenser and 5 mL of H_2O was charged with an aryl halide (4.6 mmol), boric acid (2 eq.), Na_2CO_3 (3 eq.) and catalyst $Pd_{0.04}Cu_{0.04}Ce_{0.92}O_{2-\delta}$ (0.05 mol% Pd). The reaction mixture was stirred and (usually) heated to 100 °C and its progress was monitored by GC and GC-MS (the reaction mixture was homogenized with 5 mL of toluene). The aryl halide conversion was used to estimate the catalytic activity, using benzophenone as an internal standard. After the reaction had gone to completion, the reaction mixture was filtered and the filtrate was extracted with ethyl acetate and brine. Pure products were obtained by simple filtration through silica gel using ethyl acetate as solvent. The structure of the coupling product was confirmed by ^1H and ^{13}C NMR spectroscopy and the results were consistent with those reported in literature for substituted biphenyls.[8]

5.2.3 General procedure for catalyst recovery and recyclability

The catalyst used in the first run was separated by centrifugation, washed with 5 mL toluene and water, respectively, dried at 60 °C and reused as described for the fresh catalyst.

5.3 Results and discussion

The solution combustion synthesis method was used to prepare the bimetallic $Pd_{0.04}Cu_{0.04}Ce_{0.92}O_{2-\delta}$ (PdCuCeO) solid-solution oxide. This synthesis method was preferred because it is a relatively simple, quick and inexpensive method for synthesizing highly crystalline and pure noble metal substituted oxides [51-54]. We have recently shown the structural and electronic properties of this material using X-ray diffraction (XRD), XPS, XANES, Raman spectroscopy, EXAFS and high-resolution transmission electron microscopy (HR-TEM) [24]. The Rietveld refinement fits of XRD data for PdCuCeO correspond only to the ceria phase with the fluorite structure (JCPDS 34-0394). The absence of the PdO and CuO phases in the X-ray pattern of PdCuCeO supports its phase purity and also strongly suggests that Pd^{2+} and Cu^{2+} ions were successfully incorporated into the ceria lattice (Figure 5.1). The STEM-EDX (Figure 5.1, insert) confirmed the presence of Pd and Cu in the as-prepared PdCuCeO and also shows that both metals are homogeneously dispersed in the ceria lattice.

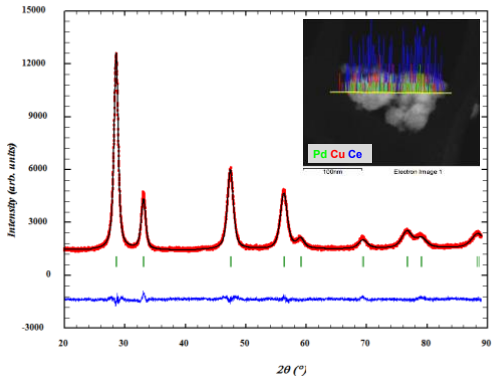

Figure 5.1: The Rietveld refined XRD patterns of PdCuCeO and its STEM-EDX image (insert)

Table 5.1: Physicochemical properties of prepared materials.

Catalyst	Metal loading (wt%)		Crystallite size (nm)	Surface area (m^2/g)
	Pd	Cu		
CuCeO	-	1.8	14	31
PdCeO	2.9	-	14	33
PdCuCeO	3.1	1.7	11	34

We also synthesised two monometallic ionic solid-solution oxides ($Pd_{0.04}Ce_{0.96}O_{2-\delta}$ [PdCeO] and $Cu_{0.04}Ce_{0.96}O_{2-\delta}$ [CuCeO]) as control materials. The chemical composition and some physicochemical properties of the studied materials are summarised in Table 5.1 and the rest of the characterisation data (XRD, TEM, SEM, EDS and TGA) is enclosed in Appendix 1 (Figure A1.4-A1.11). The Williamson-Hall method was used to estimate the average crystallite sizes of the prepared solid-solution oxides [24]. The three materials have similar physical

properties, their surface areas ranges between 31-34 m^2/g, while their crystallite sizes range from 11-14 nm (Table 5.1).

5.3.1 Assessment of catalyst activity

The catalyst testing studies began by assessing the effect of several variables on catalyst activity using iodobenzene and phenylboric acid as model coupling partners. First, water was chosen as the reaction medium, since one of our aims was to eliminate organic impurities and use water as sole solvent. We then investigated commonly used inorganic bases (K_2CO_3, Na_2CO_3, Cs_2CO_3, NaOH and *t*-BuOK) in the Suzuki-Miyaura coupling reactions. All the tested bases, except NaOH, gave identical results and Na_2CO_3 was chosen since it is the most commonly used base [55].

Table 5.2: Optimisation of reaction conditions

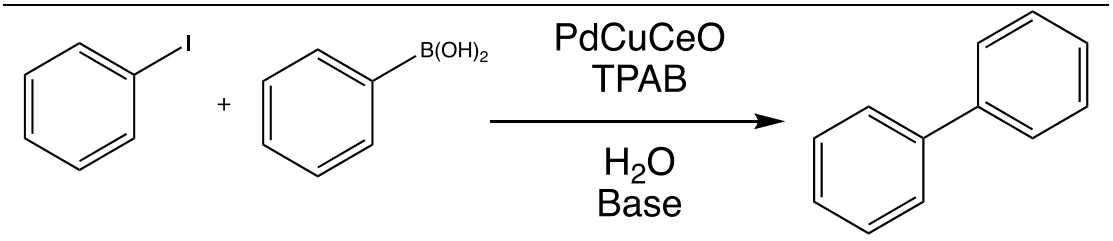

Entry[a]	Base	Catalyst loading (mol% Pd)	Temp. (°C)	Reaction time (h)	Yield (%)[c]
1	*t*-BuOK	0.5	100	1	100
2	K_2CO_3	0.5	100	1	100
3	Cs_2CO_3	0.5	100	1	100
4	Na_2CO_3	0.5	100	1	100
5	NaOH	0.5	100	3	100
6	TPAB	0.5	100	8	10
7	Na_2CO_3	0.5	60	1	100
8	Na_2CO_3	0.5	25	12	0
9[b]	Na_2CO_3	0.1	100	2	100
10[b]	Na_2CO_3	0.05	100	2	100

[a]Volume of water = 2 mL

[b]Volume of water = 5 mL

[c]GC yield

It was later realized that for bromoarenes and chloroarenes, the reactions don't proceed efficiently in the absence of a phase transfer catalyst, tetrapropyl ammonium bromide (TPAB) [56-59]. Hence, all the reactions were carried out in the presence of TPAB to allow for a good comparative study (Table 5.2).

Temperature and catalyst loading were also optimized and the optimum reaction conditions found are summarized in Table 5.3. There was no reaction at room temperature, while the reaction went to completion in an hour at 60 and 100 °C (Table 5.2). Further testing was carried out at 100 °C to allow for better miscibility of less water-soluble substrates and better reactivity for difficult substrate such as chloroarenes.

Table 5.3: Optimisation of reaction conditions

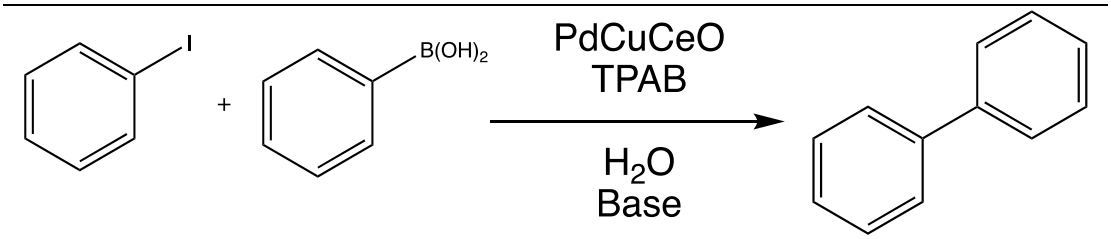

Reaction conditions	
Solvent	H_2O (5 mL)
Base	Na_2CO_3 (3 eq.)
Temperature	100 °C
Catalyst loading (Pd based)	0.05 mol%
Additive	TPAB (1 eq.)

Under the obtained optimum reaction conditions (Table 5.3), several control reactions were carried out using 2-bromoanisole and phenylboric acid as model coupling partners. 2-Bromoanisole is a highly deactivated coupling partner, thus it allows for a more reliable determination of the most robust catalytic system. The results showed that no reaction occurs in the absence of a palladium containing catalyst (Table 5.4). In addition, the palladium and copper containing catalyst (PdCuCeO) was the superior catalyst. Firstly, the data suggests that palladium is the active metal; secondly, it suggests that there is a synergetic effect between palladium and copper ions, since PdCuCeO was more active than PdCeO, while CuCeO was inactive. Hence, the synergetic effect between palladium and copper in PdCuCeO improves its catalyst performance. Further catalytic testing was thus carried out using the PdCuCeO solid-solution oxide.

Table 5.4: Investigating the most robust catalyst for SM cross-coupling reactions under optimum reaction condition.

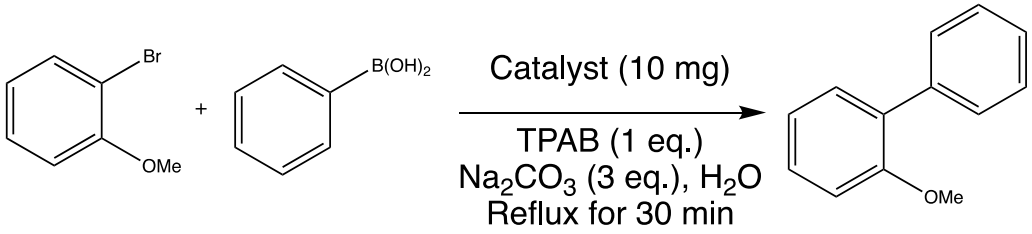

Entry	Catalyst	% Yield
1	No catalyst	No reaction
2	CuCeO	No reaction
3	PdCeO	20
4	PdCuCeO	48

To establish the versatility of the developed PdCuCeO catalyzed SM coupling reactions, the reactions of phenylboronic acids with iodoarenes, bromoarenes, and chloroarenes were further studied; the results are summarized in Tables 5.5 and 5.6. To allow for a good comparative study, the reaction time was fixed at 30 minutes, since using water as a sole solvent meant that we couldn't reliably and quantitatively monitor the progress of the reaction due to limited solubility of some substrates and products in the reaction medium.

The results show that the PdCuCeO catalysed SM cross-coupling reactions are efficient over a wide range of ortho-, meta- and para-substituted haloarenes and that various functional groups of the substituents are well tolerated. The PdCuCeO catalyst was highly active, achieving TOFs of up-to 3300 h^{-1} (Table 5.5). It was observed that electron-withdrawing substituents speed-up the reaction (Table 5.5, Entries 4-7 and 12-15), while electron-donating substituents slow down the catalytic activity (Table 5.5, Entries 2-3 and 9-10). The highly activated substrates reacted have identical TOFs since their reaction times are less than 30 minutes (which is fixed) and each reaction only yields the desired product.

Table 5.5: SM cross-coupling of iodo- and bromoarenes with phenylboric acid to give substituted biphenyls under our optimum reaction conditions

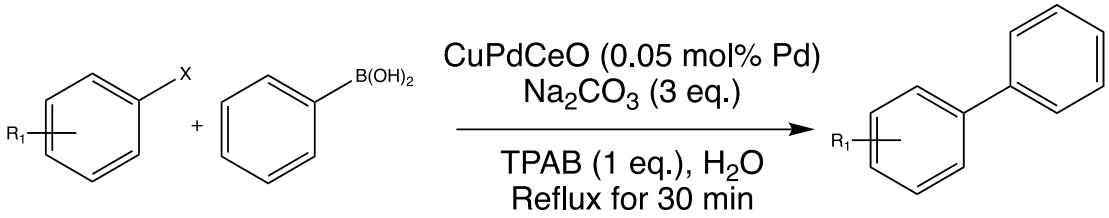

Entry	R_1—	X	% Yield	TOF /h^{-1}
1	H	I	85	2797
2	4-NH_2	I	62	2010
3	4-Me	I	72	2338
4	4-COH	I	100	3308
5	4-COMe	I	100	3308
6	3-CF_3	I	100	3308
7	4-NO_2	I	100	3308
8	H	Br	80	2630
9	4-Me	Br	73	2402
10	2-OMe	Br	48	1670
11	4-F	Br	88	2890
12	4-COH	Br	100	3308
13	4-COMe	Br	100	3308
14	4-CF_3	Br	100	3308
15	4-NO_2	Br	100	3308

Due to the success gained from the activation of aryl iodides and bromides, the study was extended to develop a procedure that facilitates efficient SM coupling of chloroarenes (Table 5.6). The synthesis of fine chemicals and phamaceuticals should benefit highly from the activation of chloroarenes, since these can serve as cheap and readily available starting materials. Unfortunately, chloroarenes are notoriously more difficult to activate than iodo- and bromoarenes. In our initial study, we focused on the coupling of unactivated chloroarenes (Table 5.6, Entry 1), however, sluggish results were obtained even when using 4.6 mol% Pd. Moderate to excellent yields were only obtained from coupling of activated chloroarenes with various phenylboric acids (Table 5.6, Entry 2-5). The activated chloroarenes also allowed for lower catalyst loading.

Table 5.6: SM cross-coupling of chloroarenes with various phenylboric acids to give substituted biphenyls

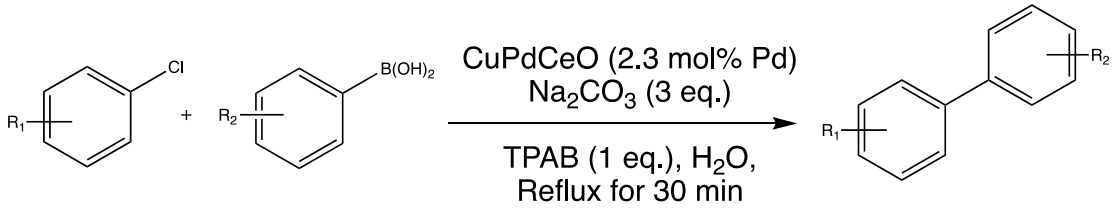

Entry	Chloroarene	R_2	%Yield	TOF /h^{-1}
1[a]		4-H	<5	<4
2[a]		4-Me	42	15
3[b]	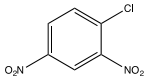	4-H	100	34
4[b]	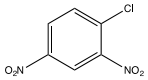	4-Me	100	34
5[b]	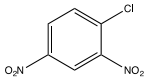	4-OMe	100	34

[a]Catalyst loading = 4.6 mol%
[b]Catalyst loading = 2.3 mol%

To evaluate the performance of the developed catalytic system, the product yield (4-acetylbiphenyl) of the present catalytic system was compared to other reported "heterogeneous" and ligand-less palladium catalyzed SM cross-coupling reactions that use water as sole solvent (Table 5.7). The yield of 4-acetylbiphenyl in this work was found to be comparable or better to most reported yields in literature. Furthermore, the present catalyst system gives superior TONs and TOFs than most reported catalytic systems that use water as a sole solvent (Tables 5.5 and 5.7) [12,59-63].

Table 5.7: Performance comparison of catalytic systems in SM coupling of 4-bromoacetophenone to phenylboric acid under 'heterogeneous', ligand-free conditions that use water as a sole solvent.

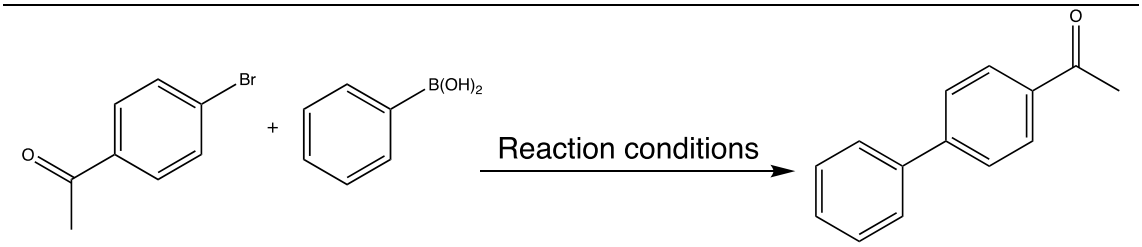

Entry	Catalyst [mol% Pd]	Reaction conditions	Time /h	Yield[a] /%	Ref.
1	Pd/C [0.05]	H_2O, CTAB, K_2CO_3, @60 °C	4	89 (445)	[60]
2	Pd/polymer [2]	H_2O, K_3PO_4, @100 °C	5	93 (9)	[61]
3	Pd/porous glass [0.45]	H_2O, K_2CO_3, TBAB, MW(300W), @150 °C	0.17	99 (12941)	[62]
4	Pd@SBA-15(C) [0.08]	H_2O, TBAB, K_2CO_3, @80 °C	1	97 (1212)	[63]
5	Pd/HAP [0.33]	H_2O, K_2CO_3, TBAB, @80 °C	4	94 (71)	[12]
6	PdNPs/ZrO_2 [0.1]	H_2O, TBAOH, @90 °C	14	90 (71)	[59]
7	PdCuCeO [0.05]	H_2O, Na_2CO_3, TPAB, @100 °C	0.5	100 (3308)	This paper

[a]Parentheses = TOF/h^{-1}

5.4 Catalyst leaching and recyclability studies

The SM cross-coupling reaction is often used by pharmaceutical industries in the synthesis of medicinal compounds. Thus it is important to quantify the residual metal in the product when developing heterogeneous systems. The requirement is that the residual metal must be kept below 5 ppm [57,64]. To distinguish homogeneous from heterogeneous catalysis and possibly determine the true nature of catalysis for these reactions in the present study we conducted a series

of investigations: catalyst recovery and recyclability, hot-filtration, selective poisoning tests and elemental analysis of the fresh and used catalyst. Phenylboric acid and 4-bromoacetophenone were used as model coupling partners for all the leaching and recyclability studies.

The catalyst was recovered quantitatively at the end of the reaction and reused three times. It was observed that the catalyst activity dropped with each subsequent recycle (Figure 5.2). Catalyst deactivation is usually caused by chemical, mechanical and/or thermal degradation of the heterogeneous catalyst. Herein, we only investigated chemical degradation (leaching) of the catalyst, since it is the most common catalyst deactivator for these types of reactions and its study could lead to a better understanding of the true nature of the catalysis [44,57]. To investigate the cause of deactivation we conducted elemental analysis of the reaction solution, fresh and used catalyst (Table 5.8). The metal content of the fresh and used catalyst were compared and it was observed that the fresh catalyst lost about 50% of Pd and Cu in its first use. However, only about 6% of the leached Pd was found in the reaction solution (Table 5.8).

Table 5.8: ICP-OES elemental analysis of the fresh and used PdCuCeO catalyst

	Pd loading (wt%)	Cu loading (wt%)	STEM-EDX image of used PdCuCeO
Fresh PdCuCeO	3.1	1.7	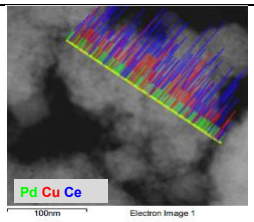
Used PdCuCeO	1.4	0.72	
Reaction solution	<0.1 ppm	3 ppm	

Catalyst poisoning tests were thus performed to further investigate the possible presence of leached, soluble palladium from the PdCuCeO pre-catalyst. This test was performed using ethylpyridine as poison, since pyridines are reported to bind strongly to Pd(II) [44,65]. Ethylpyridine was added along with the other reagents at the start of the reaction and then the reaction was stirred under similar conditions. The results in Figure 5.2 revealed that ethylpyridine addition did partially deactivate the catalyst, since the 4-bromoacetophenone conversion dropped to 40%. Hence, this test confirmed the presence of leached palladium in the TPAB-water mixture.

The hot filtration test was then performed to assess the activity of any leached palladium in the TPAB-water mixture. In the hot filtration test, a mixture of PdCuCeO, 4-bromoacetophenone, phenylboric acid, TPAB and Na_2CO_3 in water was stirred at 100 °C for 5 minutes. The catalyst was filtered off from the

reaction mixture after 5 min and the hot filtrate was then allowed to react further for 25 minutes under similar conditions. It was, however, noticed that during the hot filtration a significant quantity of TPAB precipitated out of the solution, hence the filtrate contained little to no TPAB. The results in Figure 5.2 show negligible activity in the filtrate, suggesting that there is very little soluble Pd present in the solution. The ICP elemental analysis of the filtrate also revealed that there was a very low amount of Pd (<0.1 ppm) left in the filtrate (Table 5.8). Hence, lack of activity is due to an insufficient amount of Pd in the filtrate to catalyse the Suzuki reaction.

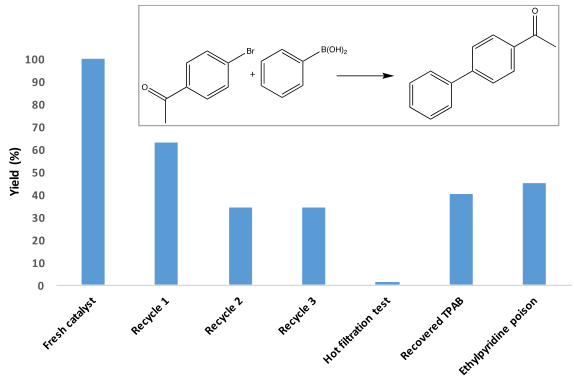

Figure 5.2: Catalyst leaching and recyclability studies

It was suspected that the Pd might have precipitated out with TPAB, since the ethylpyridine poison test confirmed the presence of Pd in the TPAB-water mixture. This then led us to recover TPAB and test its activity. The recovered TPAB gave about 40% conversion to the desired product. This suggest that TPAB acts as a scavenger of Pd and its aggregates are able to generate, in situ, highly dispersed palladium nanoparticles (Pd/TPAB) from simple PdCuCeO. Hence, the catalyst recyclability and leaching tests performed in the current work agree very well with the findings of other studies using Pd-doped metal oxides as precatalysts, and substantiate the hypothesis that the precatalysts act as a palladium reservoir, that slowly releases extremely reactive Pd species [37,60]. In our case, the released Pd is captured by TPAB and generates, in situ, a highly active quasi-heterogeneous Pd/TPAB catalyst (Scheme 5.1). We have termed the active catalyst system as PdCuCeO-TPAB. The catalytic cycle is then initiated by the oxidative addition of the aryl halide to palladium to form the organopalladium complex. In the presence of a base, this organopalladium complex reacts with boric acid via a transmetallation step and the desired product is then obtained via the reductive elimination step (Scheme 5.1). This special type of the Pd release/capture mechanism proved very advantageous, since it has potential to resolve the difficulties of catalyst separation and recovery and it greatly minimizes metal contamination of the products.

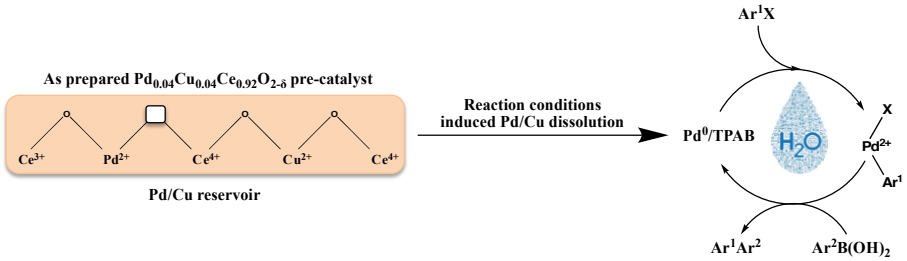

Scheme 5.1: Shows an illustration of the proposed reaction mechanism for the PdCuCeO-TPAB catalysed quasi-heterogeneous SM cross-coupling reactions.

5.5 Conclusions

In summary, we have demonstrated that the PdCuCeO-TPAB catalytic system can catalyse the Suzuki-Miyaura cross-coupling under milder and more environmentally friendly reaction conditions. The reactions were conducted in water as sole solvent and the addition of a ligand was unnecessary. The PdCuCeO-TPAB catalytic system also displayed good functional group tolerance and good to excellent isolated yields were obtained. Catalyst leaching and recyclability studies revealed that PdCuCeO acts as a Pd reservoir and that the reactions are essentially quasi-heterogeneous, occuring over recoverable Pd/TPAB aggregates. The TPAB aggregates generate, in situ, highly dispersed palladium nanoparticles from simple PdCuCeO. As as result, the PdCuCeO catalytic activity declined with each subsequent recycle. However, only a negligible amount of palladium (<0.1 ppm) was detected by ICP-OES in the product solution because most of the palladium is removed from the reaction solution by TPAB. Hence, this PdCuCeO-TPAB catalytic system has potential to resolve the difficulties of catalyst separation and recovery, since it greatly minimises metal contamination of the products.

5.6 Acknowledgements

We would like to express our gratitude to Mintek and the Department of Science and Technology South Africa (Advanced Metals Initiative program) for financial support. The authors would also like to thank Dr M Shozi, Dr S Mohamed, Dr S Singh and the rest of the UKZN catalysis research group for helpful discussions.

5.7 References

1. N. Miyaura, A. Suzuki, *Chemical Reviews*, 95 (1995) 2457-2483.
2. N. Miyaura, A. Suzuki, *Journal of the Chemical Society, Chemical Communications*, 20 (1979) 866-867.
3. N. Miyaura, K. Yamada, A. Suzuki, *Tetrahedron Letters*, 20 (1979) 3437-3440.
4. I. Maluenda, O. Navarro, *Molecules*, 20 (2015) 7528-7557.
5. X. Wu, Y. Wu, Z. Xin, Y. Ma, *Huaxue Tongbao*, 76 (2013) 778-785.

6. Y. Monguchi, H. Sajiki, *Yuki Gosei Kagaku Kyokaishi*, 70 (2012) 711-721.
7. M. Mora, C. Jimenez-Sanchidrian, J.R. Ruiz, *Current Organic Chemistry*, 16 (2012) 1128-1150.
8. F. Amoroso, S. Colussi, A. Del Zotto, J. Llorca, A. Trovarelli, *Journal of Molecular Catalysis A: Chemical*, 315 (2010) 197-204.
9. L. Wang, X. Bai, H. Fan, *Huaxue Yu Nianhe*, 32 (2010) 37-41.
10. Y. Monguchi, Y. Kitamura, T. Maegawa, H. Sajiki, *Kemikaru Enjiniyaringu*, 53 (2008) 256-261.
11. G.J. Lichtenegger, M. Maier, M. Hackl, J.G. Khinast, W. Gössler, T. Griesser, V.S.P. Kumar, H. Gruber-Woelfler, P.A. Deshpande, *Journal of Molecular Catalysis A: Chemical*, 426 (2017) 39-51.
12. N. Jamwal, M. Gupta, S. Paul, *Green Chemistry*, 10 (2008) 999-1003.
13. F.S. Han, *Chemical Society Reviews*, 42 (2013) 5270-5298.
14. M.B. Thathagar, J. Beckers, G. Rothenberg, *Journal of the American Chemical Society*, 124 (2002) 11858-11859.
15. M. Aufiero, F. Proutiere, F. Schoenebeck, *Angewandte Chemie International Edition*, 51 (2012) 7226-7230.
16. J.Z. Deng, D.V. Paone, A.T. Ginnetti, H. Kurihara, S.D. Dreher, S.A. Weissman, S.R. Stauffer, C.S. Burgey, *Organic Letters*, 11 (2009) 345-347.
17. S.K. Gurung, S. Thapa, A. Kafle, D.A. Dickie, R. Giri, *Organic Letters*, 16 (2014) 1264-1267.
18. J. Mao, J. Guo, F. Fang, S.J. Ji, *Tetrahedron*, 64 (2008) 3905-3911.
19. C.T. Yang, Z.Q. Zhang, Y.C. Liu, L. Liu, *Angewandte Chemie International Edition*, 50 (2011) 3904-3907.
20. A.J. Reay, I.J.S. Fairlamb, *Chemical Communications*, 51 (2015) 16289-16307.
21. C. Torborg, M. Beller, *Advanced Synthesis & Catalysis*, 351 (2009) 3027-3043.
22. S.J. Kim, S.D. Oh, S. Lee, S.H. Choi, *Journal of Industrial and Engineering Chemistry*, 14 (2008) 449-456.
23. R. Narayanan, *Molecules*, 15 (2010) 2124-2138.
24. T. Cwele, N. Mahadevaiah, S. Singh, H.B. Friedrich, A.K. Yadav, S.N. Jha, D. Bhattacharyya, N.K. Sahoo, *Catalysis Science & Technology*, 6 (2016) 8104-8116.
25. T. Cwele, N. Mahadevaiah, S. Singh, H.B. Friedrich, *Applied Catalysis B: Environmental*, 182 (2016) 1-14.
26. P. Das, W. Linert, *Coordination Chemistry Reviews*, 311 (2016) 1-23.
27. S. Paul, M.M. Islam, S.M. Islam, *RSC Advances*, 5 (2015) 42193-42221.
28. R. Cano, A.F. Schmidt, G.P. McGlacken, *Chemical Science*, 6 (2015) 5338-5346.
29. S. Horikoshi, N. Serpone, *Catalysis Science and Technology*, 4 (2014) 1197-1210.
30. S.K. Beaumont, *Journal of Chemical Technology and Biotechnology*, 87 (2012) 595-600.
31. M. Lamblin, L. Nassar-Hardy, J.C. Hierso, E. Fouquet, F.X. Felpin, *Advanced Synthesis and Catalysis*, 352 (2010) 33-79.
32. C.G. Frost, L. Mutton, Green Chemistry, 12 (2010) 1687-1703.
33. P. Lu, J. Lu, H. You, P. Shi, J. Dong, *Huaxue Jinzhan*, 21 (2009) 1434-1441.
34. K. Kaneda, *Yuki Gosei Kagaku Kyokaishi*, 61 (2003) 436-444.

35. M.R. Buchmeiser, *Bioorganic and Medicinal Chemistry Letters*, 12 (2002) 1837-1840.
36. M. Nishida, T. Tagata, *Yuki Gosei Kagaku Kyokaishi*, 62 (2004) 737-742.
37. S. Paul, M.M. Islam, S.M. Islam, *RSC Advances*, 5 (2015) 42193-42221.
38. K.V.S. Ranganath, S. Onitsuka, A.K. Kumar, J. Inanaga, *Catalysis Science and Technology*, 3 (2013) 2161-2181.
39. W.Y. Wu, F.Y. Tsai, *Huaxue*, 66 (2008) 117-125.
40. L. Yin, J. Liebscher, *Chemical Reviews*, 107 (2007) 133-173.
41. P. Ncube, T. Hlabathe, R. Meijboom, *Journal of Cluster Science*, 26 (2015) 1873-1888.
42. A.F. Schmidt, A.A. Kurokhtina, *Kinetics and Catalysis*, 53 (2012) 714-730.
43. K. Köhler, R.G. Heidenreich, J.G. Krauter, J. Pietsch, *Chemistry – A European Journal*, 8 (2002) 622-631.
44. Y. Ji, S. Jain, R.J. Davis, *The Journal of Physical Chemistry B*, 109 (2005) 17232-17238.
45. J.S. Chen, A.N. Vasiliev, A.P. Panarello, J.G. Khinast, *Applied Catalysis A: General*, 325 (2007) 76-86.
46. A. Biffis, M. Zecca, M. Basato, *European Journal of Inorganic Chemistry*, 2001 (2001) 1131-1133.
47. C. Pavia, F. Giacalone, L.A. Bivona, A.M.P. Salvo, C. Petrucci, G. Strappaveccia, L. Vaccaro, C. Aprile, M. Gruttadauria, *Journal of Molecular Catalysis A: Chemical*, 387 (2014) 57-62.
48. S. Reimann, J. Stötzel, R. Frahm, W. Kleist, J.D. Grunwaldt, A. Baiker, *Journal of the American Chemical Society*, 133 (2011) 3921-3930.
49. F. Zhao, M. Shirai, Y. Ikushima, M. Arai, *Journal of Molecular Catalysis A: Chemical*, 180 (2002) 211-219.
50. N.T.S. Phan, M. Van Der Sluys, C.W. Jones, *Advanced Synthesis Catalysis*, 348 (2006) 609-679.
51. T. Baidya, G. Dutta, M.S. Hegde, U.V. Waghmare, *Dalton Transactions*, 0 (2009) 455-464.
52. A.S. Mukasyan, P. Epstein, P. Dinka, *Proceedings of the Combustion Institute*, 31 (2007) 1789-1795.
53. M. Narayanappa, V.D.B.C. Dasireddy, H.B. Friedrich, *Applied Catalysis A: General*, 447–448 (2012) 135-143.
54. W. Wen, J.M. Wu, *RSC Advances*, 4 (2014) 58090-58100.
55. S. Kotha, K. Lahiri, D. Kashinath, *Tetrahedron*, 58 (2002) 9633-9695.
56. M. Lysen, K. Köhler, *Synlett*, 2005 (2005) 1671-1674.
57. K. Köhler, R.G. Heidenreich, S.S. Soomro, S.S. Pröckl, *Advanced Synthesis & Catalysis*, 350 (2008) 2930-2936.
58. M. Mora, C. Jiménez-Sanchidrián, J.R. Ruiz, *Journal of Molecular Catalysis A: Chemical*, 285 (2008) 79-83.
59. A. Monopoli, A. Nacci, V. Calò, F. Ciminale, P. Cotugno, A. Mangone, L.C. Giannossa, P. Azzone, N. Cioffi, *Molecules*, 15 (2010) 4511-4525.
60. A. Arcadi, G. Cerichelli, M. Chiarini, M. Correa, D. Zorzan, *European Journal of Organic Chemistry*, 2003 (2003) 4080-4086.
61. S.E. Lyubimov, A.A. Vasil'ev, A.A. Korlyukov, M.M. Ilyin, S.A. Pisarev, V.V. Matveev, A.E. Chalykh, S.G. Zlotin, V.A. Davankov, *Reactive and Functional Polymers*, 69 (2009) 755-758.

62. C. Schmöger, T. Szuppa, A. Tied, F. Schneider, A. Stolle, B. Ondruschka, ChemSusChem, 1 (2008) 339-347.
63. J. Zhi, D. Song, Z. Li, X. Lei, A. Hu, *Chemical Communications*, 47 (2011) 10707-10709.
64. P. Albers, J. Pietsch, S.F. Parker, *Journal of Molecular Catalysis A: Chemical*, 173 (2001) 275-286.
65. D.M. Argyle, H.C. Bartholomew, *Catalysts*, 5 (2015) 145-269.

Chapter 6

Summary and conclusion

The construction of carbon-carbon bonds remains highly topical and has a huge industrial potential. The carbon-carbon forming reactions are frequently employed in the building of complex and bioactive molecules that are developed as medicines and agrochemicals. In addition, the awarding of the 2010 Nobel Prize in chemistry to Richard F. Heck, Ei-ichi Negishi and Akira Suzuki for their work on palladium catalyzed cross-coupling reactions further emphasized the importance of this field. Hence, the objectives were to further explore this area of research with the aim of developing heterogeneous variants of carbon-carbon cross-coupling reactions. In addition, the aim was to develop catalysts with improved reactivity by incorporating Pd^{2+} ions in the lattice structure of ceria; as opposed to a more conventional approach that involves deposition of palladium nanoparticles on the surface of ceria. The three catalytic systems that were developed for Heck-Mizoroki, Sonogashira and Suzuki-Miyaura cross coupling reactions, all used palladium and ceria ($Pd_xCe_{1-x}O_{2-\delta}$) based solid-solution oxides as catalysts. All the solid-solution oxide catalysts were synthesised using a single-step urea-assisted solution combustion synthesis method. These solid solution oxides were fully characterized by XRD, ICP-OES, BET, XPS, SEM, EDX, TEM, TGA and Raman spectroscopy. The physicochemical properties of these materials strongly suggested that Pd^{2+} was successfully incorporated into the lattice structure of ceria and the formed solid-solid solution oxides were monophasic.

With regards to the catalytic system developed for ligand-free Heck-Mizoroki cross coupling reactions, a more highly Pd substituted ceria solid-solution oxide catalyst, $Pd_{0.09}Ce_{0.91}O_{2-\delta}$, was used. Good to excellent yields of substituted olefins were obtained with this solid-solution oxide catalyst. The Heck-Mizoroki cross coupling reactions were shown to be affected by electronic and steric effects. Electron deficient olefins reacted more rapidly compared to electron rich olefins, while an olefin with a more exposed carbon-carbon double bond also reacted more rapidly. The physicochemical properties indicated that the fresh $Pd_{0.09}Ce_{0.91}O_{2-\delta}$ catalyst is monophasic, with Pd^{2+} ions fully substituted in the lattice of ceria and not deposited on its surface as PdO. However, used catalyst characterisation revealed that the catalysis occurs over the reduced two phase Pd^0/CeO_2 and not on the as prepared monophasic $Pd_{0.09}Ce_{0.91}O_{2-\delta}$. Catalyst recovery and recyclability tests revealed that the active Pd^0/CeO_2 (formed *in situ*) catalyst could be easily recovered and reused for several times without any

significant loss in efficiency. Only a negligible amount of palladium was detected in the product solution (0.35 ppm) when the catalyst leaching studies were conducted. Hence, it was concluded that under the developed catalytic system, the Heck-Mizoroki cross coupling reactions are largely heterogeneous, and operate under a release-captured mechanism.

The development of a catalytic system that could catalyse Sonogashira cross coupling reactions was performed using $Pd_{0.02}Ce_{0.98}O_{2-\delta}$ solid-solution oxide as a catalyst. Optimized reaction conditions revealed that the $Pd_{0.02}Ce_{0.98}O_{2-\delta}$ catalyst was more active when triethylamine was used as a base in a water/acetonitrile solvent system at 82 °C. These reactions were performed under ligand- and Cu-free reaction conditions. The developed catalytic system efficiently generated substituted biphenylacetylene in good to excellent yields through the cross coupling reaction of phenylacetylene and a wide range of iodoarenes using only 0.05 mol% catalyst loading. The Sonogashira cross-coupling reactions are strongly affected by the electronic nature of the substituents and their position on the iodoarene. Electron withdrawing functional groups (e.g. $-NO_2$) tend to speed-up the reaction, while electron donating functional groups (e.g. $-CH_3$) decrease the reactivity of the catalyst. Unfortunately, these reactions are limited to iodoarenes, since bromo- and chloroarenes proved difficult to catalyse. A thorough analysis of the reaction profiles from the catalyst leaching and recyclability experiments explicitly displayed that the Sonogashira cross-coupling reactions are accomplished via a quasi-heterogeneous mechanism by the leached Pd(0) species. As a result, the recovered $Pd_{0.02}Ce_{0.98}O_{2-\delta}$ lost some activity upon recycling. Although a negligible amount of palladium (0.5 ppm) was found in the product solution, additional developments are still required to further enhance the recoverability and recyclability of the $Pd_{0.02}Ce_{0.98}O_{2-\delta}$ catalyst.

Lastly, this work demonstrated that the synergetic effect between palladium, copper and cerium greatly enhanced the reactivity of $Pd_{0.04}Cu_{0.04}Ce_{0.92}O_{2-\delta}$ (PdCuCeO) solid-solution oxide in Suzuki-Miyaura cross coupling reactions. The Pd^{2+} and Cu^{2+} co-substituted ceria (PdCuCeO) solid-solution oxide displayed the highest activity compared to the mono-substituted $Pd_{0.04}Ce_{0.96}O_{2-\delta}$ and $Cu_{0.04}Ce_{0.96}O_{2-\delta}$ solid-solution oxides. The reactions were conducted under more environmentally friendly reaction conditions than conventional systems, since water was used as a sole solvent and no ligand was added. The addition of tetrapropylammonium bromide (TPAB) as phase transfer catalyst generated a robust PdCuCeO-TPAB catalytic system (*in situ*) that was able to catalyse even deactivated bromo- and chloroarenes. In addition, the PdCuCeO-TPAB catalytic system displayed good functional group tolerance and good to excellent yields of substituted biaryls were obtained.

A thorough investigation through a series of suitable experiments clearly displayed that PdCuCeO acts as a Pd reservoir. The TPAB aggregates generate, in situ, highly dispersed palladium nanoparticles from PdCuCeO to form recoverable Pd/TPAB aggregates. Hence, it was concluded that the Suzuki-Miyaura cross-coupling reactions occur over the recoverable Pd/TPAB aggregates under quasi-heterogeneous conditions. As a result, the PdCuCeO catalytic activity declined with each subsequent recycle. The leached palladium doesn't stay in the product solution, it precipitates out as Pd/TPAB aggregates. Hence, only a negligible amount of palladium (<0.1 ppm) was detected by ICP-OES in the product solution. Hence, this PdCuCeO-TPAB catalytic system is not only greener and highly efficient, it also has a potential to resolve the difficulties of catalyst separation and recovery of the expensive palladium catalyst, and as a result, it minimises metal contamination of the products.

In summary, the current studies have proven to be highly relevant and contribute greatly to understanding and development of heterogeneous variants of palladium catalysed C-C cross coupling reactions. In our research group (UKZN Catalysis Research Group) alone, these studies have inspired the design of three addition research projects. The first two research projects are being carried out by two Masters students, Miss Zanele Vundla and Mrs Nolwazi Chonco. Miss Vundla is trying to develop more robust catalytic systems that use palladium-substituted ceria-zirconia ($Pd_xZr_yCe_{1-x-y}O_{2-\delta}$) to limit palladium leaching and enhance its recoverability and recyclability under Heck cross-coupling reactions. Mrs Chonco is trying to develop a more robust catalytic system for Suzuki cross-coupling reactions by exploiting the synergetic effect between various metal combinations, $Pd_xM_yZr_zCe_{1-x-y-z}O_{2-\delta}$ (M = Fe, Cu and Ni). The third project looks at developing chemoselective and heterogeneous catalytic systems for one-pot double cross-coupling reactions of aryl dihalides into synthetically useful unsymmetrically substituted arenes (Scheme 6.1). In this study, $Pd_xZr_yCe_{1-x-y}O_{2-\delta}$ is used as a catalyst to perform sequential double cross-coupling reactions (Heck-Suzuki, Heck-Sonogashira, Suzuki-Sonogashira or Heck-Heck).

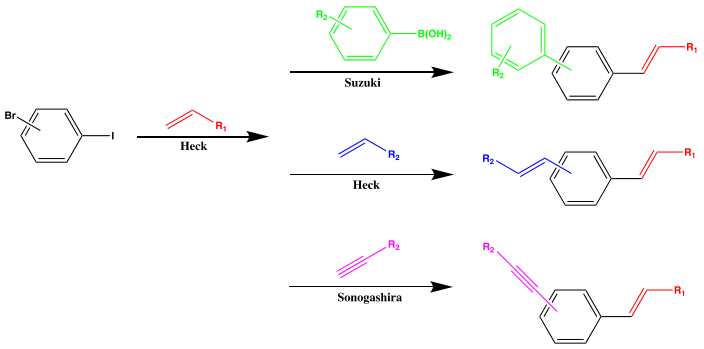

Scheme 6.1: Selected examples of CePdO catalysed double C-C cross-coupling reactions

Appendix 1

Supplementary information for Chapter 3

A1.1 Experimental procedure for the synthesis of PdO/CeO_2

For the synthesis of PdO/CeO_2, 2 mmol of $PdCl_2$ were dissolved in 10 mL of HCl (32%) in a borosilicate dish and, after all the $PdCl_2$ had dissolved, 40 mL of deionized water, 3 g of CeO_2 and 72 mmol CH_4N_2O (urea) were added. The suspension was stirred at 100 °C to evaporate water and form a slurry. The redox slurry was introduced into a furnace pre-heated at 120 °C, then the furnace temperature was increased gradually to 600 °C over 30 minutes and maintained there for 5 hours. The solid product obtained was characterized using various techniques and the results were compared to those of the solution combustion synthesized $Pd_{0.09}Ce_{0.91}O_{2-\delta}$ solid-solution oxide.

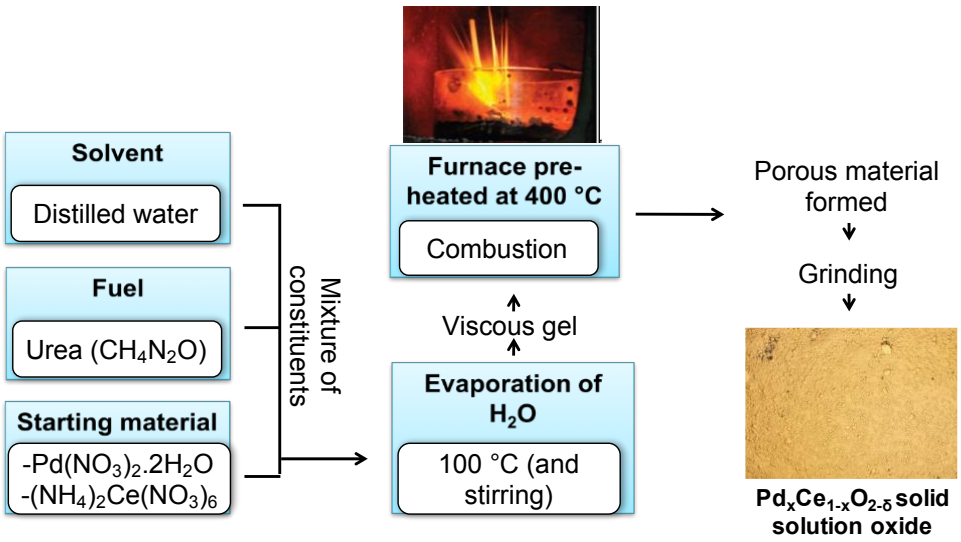

Scheme A1.1: A general illustration of the solution combustion synthesis method for preparation of $Pd_xCe_{1-x}O_{2-\delta}$ based solid-solution oxides.

A1.2 Catalyst characterization

A1.2.1 XRD analysis

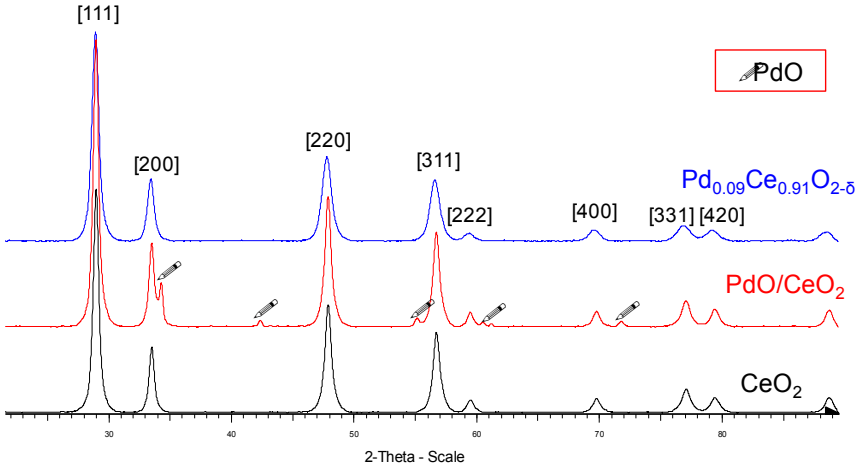

Figure A1.1: XRD patterns of the as-prepared samples

Table A1.1: Structural parameters of the investigated samples obtained from their XRD profiles.

Sample	a (Å)	V (Å^3)	R_F	R_B	χ^2
CeO_2	5.411(9)	158.43	1.94	3.61	1.74
$Pd_{0.09}Ce_{0.91}O_{2-\delta}$	5.424(9)	159.57	1.58	3.12	1.92
PdO/CeO_2	5.415(3)	158.78	2.35	4.53	1.89

A1.2.2 ICP-OES analysis

Table A1.2: ICP-OES elemental analysis of the $Pd_{0.09}Ce_{0.91}O_{2-\delta}$ sample

	Metal concentration (mg/L)[a]	**Amount (mmol)**
Ce	92.2	0.3291
Pd	6.8	0.03217

[a]Mass of catalyst digested = 0.0510g

A1.2.3 BET, SEM-EDS and TEM analysis

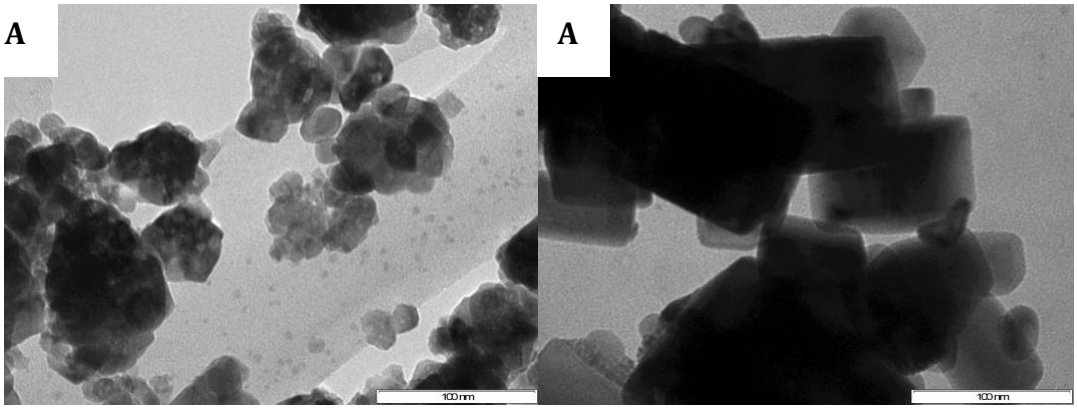

Figure A1.2: TEM images of (A) CeO_2 and (B) PdO/CeO_2

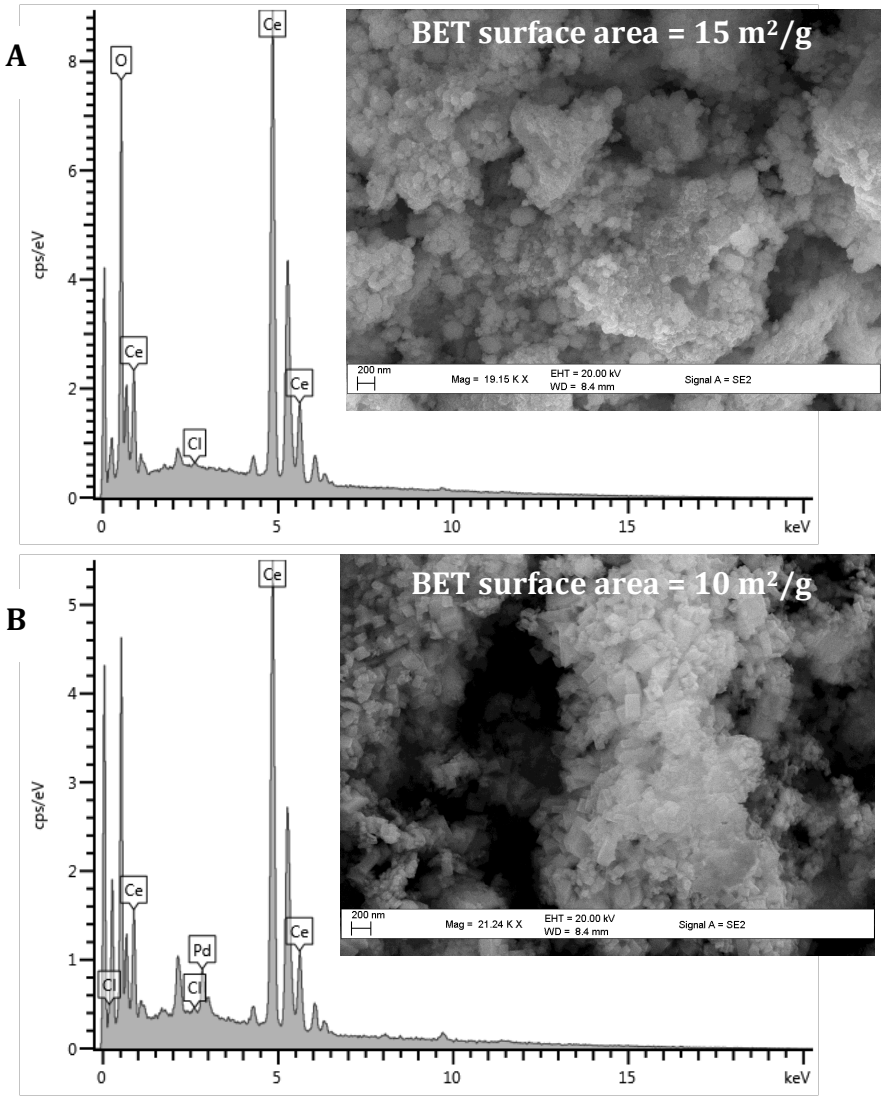

Figure A1.3: SEM/EDX image of (A) CeO_2 and (B) PdO/CeO_2

A1.2.4 XPS analysis

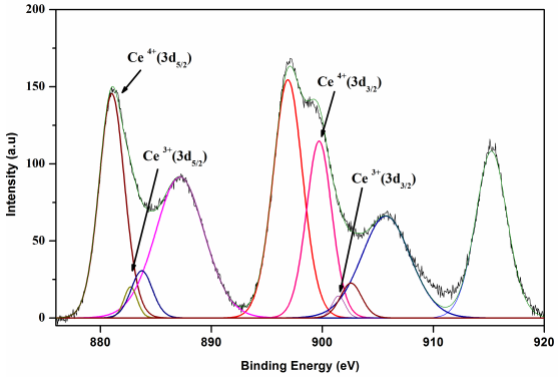

Figure A1.4: Core level XPS of Ce (3d) in the $CeO_{2-\delta}$ sample.

A1.2.5 Thermogravimetric analyses (TGA) and differential thermal analysis (DTA)

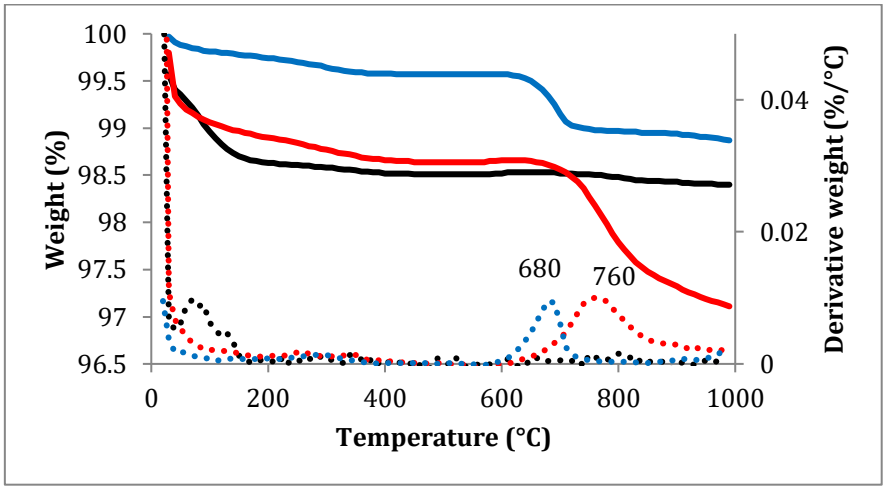

Figure A1.5: TGA and DTA analysis of the investigated materials; (black) CeO_2, (red) $Pd_{0.09}Ce_{0.91}O_{2-\delta}$ and (blue) PdO/CeO_2

A1.2.6 Raman spectroscopy analysis

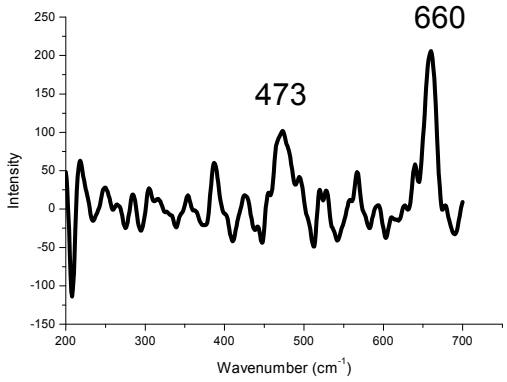

Figure A1.6: Raman spectrum of PdO/CeO_2

A1.3 Catalyst testing: Optimisation of reaction conditions

Table A1.3: Solvent and base investigations[a]

Solvent	Base	Time/h	%Yield
Anisole	K_2CO_3	6	<5
	Et_3N	6	73
Benzonitrile	K_2CO_3	6	<5
	Et_3N	6	96
DMF	K_2CO_3	6	93
	Et_3N	6	95
DMSO	K_2CO_3	6	87
	Et_3N	6	84
Toluene	K_2CO_3	6	<5
	Et_3N	6	45
Xylene	K_2CO_3	6	<5
	Et_3N	6	36

[a]Reaction conditions: 2 mmol of iodobenzene, 0.5 mol% (based on Pd) of $Pd_{0.09}Ce_{0.91}O_{2-\delta}$, 1.5 equiv. methyl acrylate and 2 equiv. of 'base' in 'solvent' at 130 °C.

Table A1.4: Temperature investigation

Temperature/°C	Reaction time/h	% Yield[a]
Room temperature	6	No reaction
80	6	20
130	1	95

[a]Reaction conditions: 2 mmol of iodobenzene, 0.5 mol% (based on Pd) of $Pd_{0.09}Ce_{0.91}O_{2-\delta}$, 1.5 equiv. methyl acrylate and 2 equiv. of Et_3N in DMF.

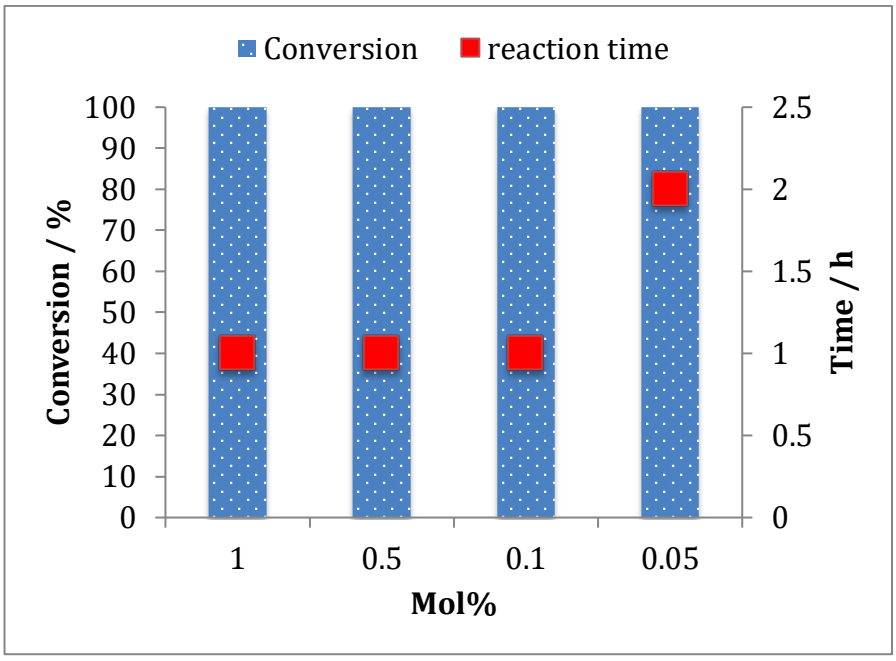

Figure A1.7: Reaction conditions: 2 mmol of iodobenzene, 'X' mol% (based on Pd) of $Pd_{0.09}Ce_{0.91}O_{2-\delta}$, 1.5 equiv. methyl acrylate and 2 equiv. of Et_3N in DMF at 130 °C.

Table A1.5: Ligand effect investigation

	Reaction time/h	%Yield[a]
Ligand free	1	95
Ligand = PPh_3	6	No reaction[b]

[a]Reaction conditions: 2 mmol of iodobenzene, 0.3 mol% (based on Pd) of $Pd_{0.09}Ce_{0.91}O_{2-\delta}$, 1.5 equiv. methyl acrylate and 2 equiv. of Et_3N in DMF at 130 °C. [b]With addition of 2 equiv. of PPh_3.

Supplementary information for Chapter 5

A1.4 Catalyst characterization

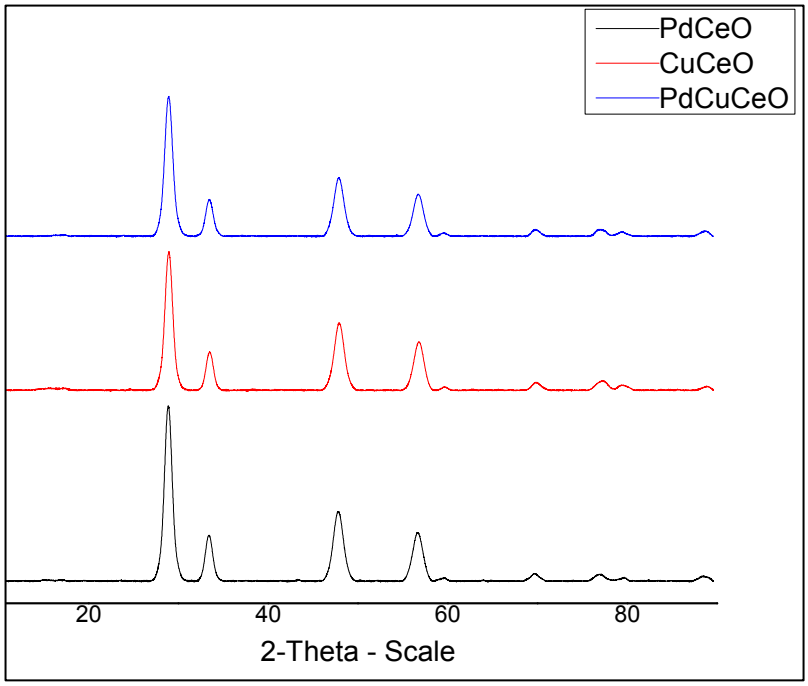

Figure A1.8: XRD patterns of the as-prepared samples

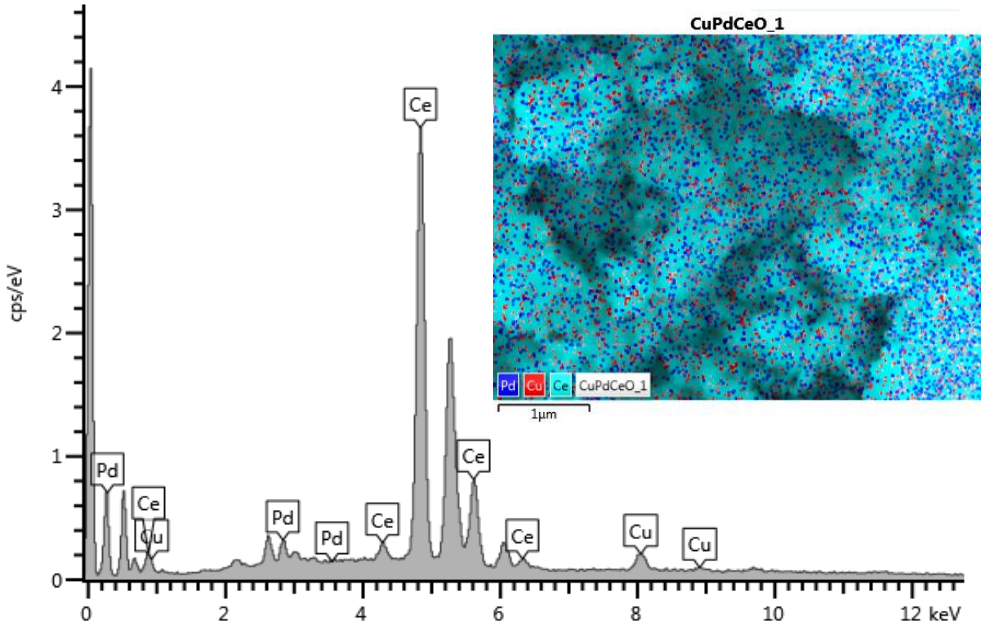

Figure A1.9: SEM-EDX image of PdCuCeO

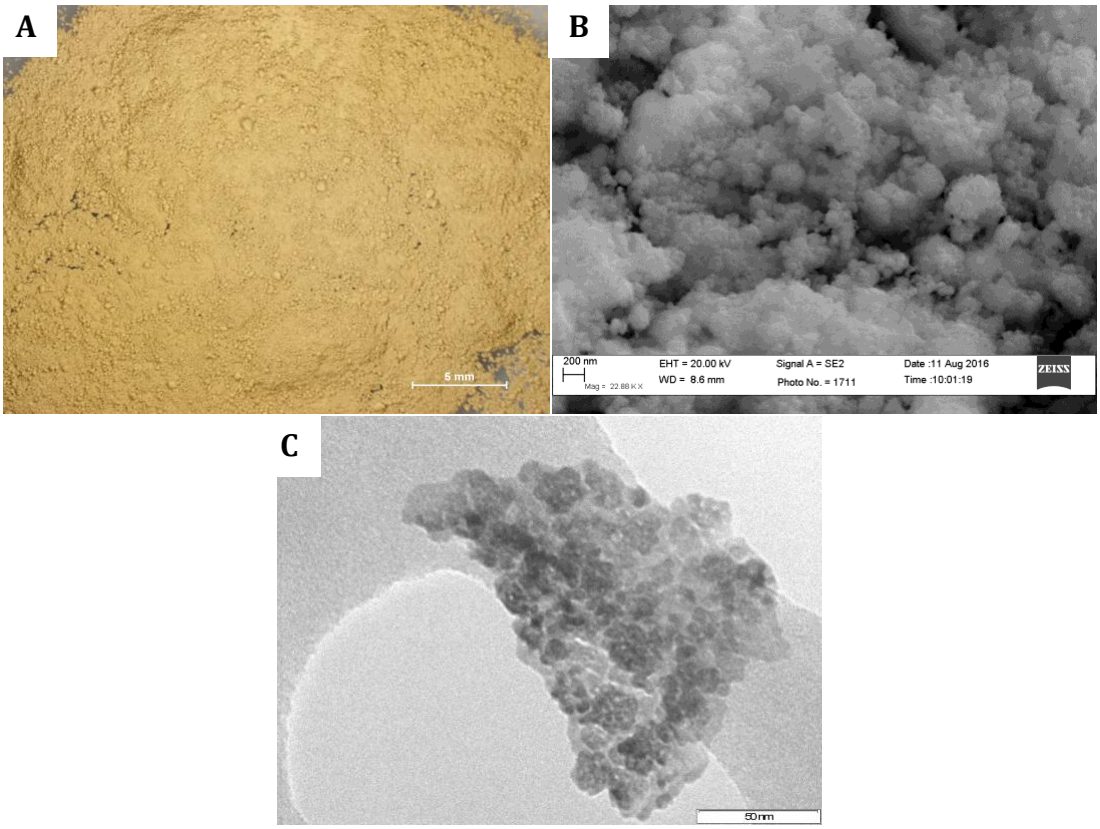

Figure A1.10: Light microscopy (A) SEM (B) and TEM (C) analysis of the PdCuCeO catalyst.

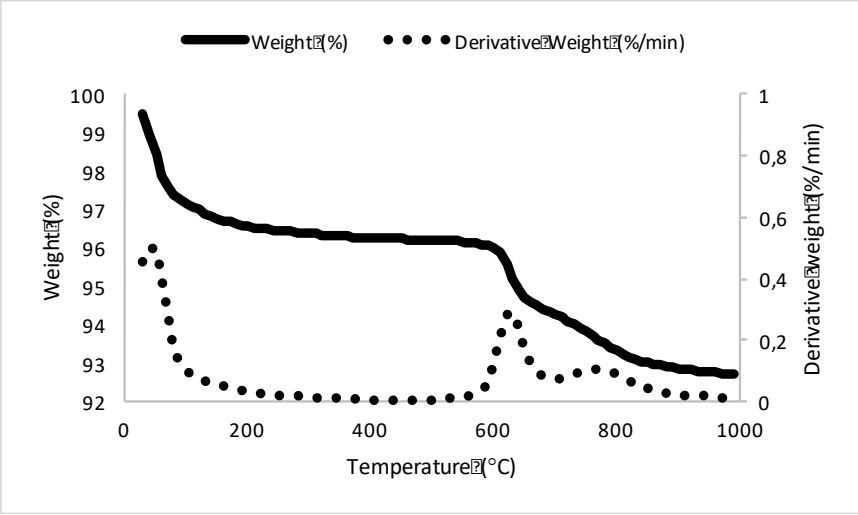

Figure A1.11: TGA analysis of the PdCuCeO catalyst